Martin Marietta Energy Systems

Final Report

ANISOTROPY OF CREEP-FATIGUE DEFORMATION AND DAMAGE UNDER NONPROPORTIONAL LOADING

for the period

January 1, 1985 through February 28, 1986

D. L. McDowell
School of Mechanical Engineering
Georgia Institute of Technology
Atlanta, Georgia 30332
Project No. E25-B01

Attention:

R. L. Huddleston
Martin Marietta Energy Systems
P. O. Box M
Oak Ridge, TN 37831

May 1986

TABLE OF CONTENTS

BASES OF CONTINUUM DAMAGE MECHANICS

The notion of applying continuum mechanics principles to "track" creep damage was first proposed by Kachanov [1-2]. Since creep damage occurs in a number of grains and grain boundaries, it can be treated in a bulk-averaged sense. Creep damage mechanisms are relatively well-understood; voids nucleate, grow and coalesce driven by diffusion processes, viscous creep of surrounding matrix material, or coupled processes [3].

Continuum damage mechanics seeks to reflect the growth of cavities and the mechanical behavior of damaged material by representing physical creep damage (cavitation) by internal mechanical variables. These mechanical variables, then, modify the creep strain rate equations to produce transition from secondary to tertiary creep (void coalesence). The advantage to such an approach is that damage is treated as a path-dependent variable coupled with nonlinear stress analysis.

Isotropic Damage Formulations

If physical creep damage is represented by a scalar, then no directional dependence or variation of damage is assumed. Nonproportional creep tests [4-9] have shown that creep damage does have a directional character; changing the maximum principal stress orientation may result in different subsequent creep damage and strain rates than would be predicted by using a scalar damage variable. We will begin discussion of continuum damage mechanics with a review of isotropic damage models, since much of the rationale for extension to anisotropic damage is derived from these models.

(i) Kachanov's model:

Kachanov [1-2] defined the evolution of a "continuity" variable ψ at a point X by

$$\dot{\psi} = - B\left(\frac{\sigma_{max}}{\psi} \right)^{\nu} \qquad (1)$$

with initial condition $\psi = 1$ in the undamaged state. Here, B and ν are material constants and σ_{max} is the maximum tensile stress at point X in the steady creep field in the perpendicular direction of creep crack growth. Fracture occurs when $\psi = 0$.

Kachanov did not discuss the relationship of ψ to physical damage, nor prediction of strain at rupture. In essence, the creep strain rate was assumed unaffected by the presence of damage.

(ii) Rabotnov's model:

Rabotnov [10-11] generalized Kachanov's model to predict rupture strain in addition to rupture time. He defined a damage parameter ω by

$$\omega = 1 - \psi \qquad (2)$$

which evolves according to

$$\dot{\omega} = G(\sigma,\omega) \qquad (3)$$

For uniaxial loading. Rabotnov also allowed the uniaxial creep strain rate to depend on ω , i.e.

$$\dot{\varepsilon}^{c} = F(\sigma,\omega) \qquad (4)$$

where $\omega = 0$ represents the undamaged state, and $\omega = 1$ the ruptured state. The particular forms of these equations were written as

$$\dot{\omega} = B\sigma^{\nu}/(1 - \omega)^{\mu} \tag{5}$$

$$\dot{\varepsilon}^{c} = A\sigma^{n}/(1 - \omega)^{m} \tag{6}$$

where A, B, m, n, μ and ν are material constants, dependent on temperature.

It should be noted that the term $(1 - \omega)$ is often interpreted in the literature as the reduction in area due to the presence of voids or cracks in the material, i.e.

$$(1 - \omega) = \frac{A_a - A_r}{A_a} \tag{7}$$

where A_r is the reference area (undamaged) and A_a is the reduced (due to damage) area. Rabotnov did not specifically make this interpretation. As a consequence of equation (7), the net stress may be expressed as

$$S = \sigma/(1 - \omega) \tag{8}$$

such that S reflects the increase in stress due to reduced load bearing area. Equation (6) can be identified as Norton's creep law if m = n written in terms of net stress. These equations can be easily integrated for conventional creep tests (constant σ) when the deformation at failure can be considered small.

(iii) Leckie-Hayhurst model:

The model of Rabotnov was derived for unaxial creep behavior. Leckie and Hayhurst [4-6,10,12] generalized the Rabotnov approach to multiaxial loading. The effect of state of stress (for proportional loading) on rupture is normally expressed in terms of isochronous equi-damage surfaces which Hayhurst and Leckie expressed as

$$\sigma^*(\sigma_{ij}) = \alpha\sigma_1 + \beta\bar{\sigma} + (1 - \alpha - \beta)\sigma_{kk} \tag{9}$$

where σ_1 is the maximum principal stress, effective stress $\bar{\sigma} = (3\sigma'_{ij}\,\sigma'_{ij}/2)^{1/2}$, σ'_{ij} is the deviatoric stress tensor, and σ_{kk} is the first invariant of stress. Chaboche [13] suggests that net stress be used in computation of σ_1, $\bar{\sigma}$ and σ_{kk} in equation (9) to reflect damage growth.

Leckie and Hayhurst's multiaxial generalization now takes the form

$$\dot{\varepsilon}^c_{ij} = (3A/2)[\bar{\sigma}/(1 - \omega)]^n(\sigma'_{ij}/\bar{\sigma}) \tag{10}$$

$$\dot{\omega} = B(\sigma^*)^\nu/(1 - \omega)^\mu \tag{11}$$

where α, β, A, B, n, ν and μ are temperature-dependent material constants.

Two comments should be made regarding equations (10) and (11). First, for a creep test with fixed σ'_{ij}, the ratio of creep strain rate components approximately follow a deviatoric flow rule even in the presence of damage. This point was made by Leckie [5-6,10]. Damage growth acts to accelerate the creep strain rate through $\bar{\sigma}/(1 - \omega)$ in equation (1). Secondly, use of σ^* in equation (11) allows for correlation of materials which are maximum principal stress dependent ($\alpha \to 1$) or effective stress dependent ($\beta \to 1$). Increased damage rate due to higher hydrostatic tensile stress is also included.

Though different forms of isochronous surfaces are permitted by variation of α and β, equations (9) - (11) can only apply to proportional loading (i.e. $\sigma'_{ij}/\bar{\sigma}$ fixed for all i and j), or for nonproportional loading for materials which damage isotropically. A material is defined to damage isotropically if rotations of the principal stresses (or deviatoric stresses)

would result in the same rupture time at the same isochronous stress level as for a unaxial test. Hence, for nonproportional loading of materials which damage anisotropically, equations (9) - (11) cannot be used since ω is a scalar parameter. It should also be noted that equation (10) may not be applicable for combined creep-fatigue loading since no measures of work-hardening or backstress are included.

(iv) Chaboche's model:

Chaboche makes the interpretation of $(1 - \omega)$ as reduced area and defines the net stress as

$$S = \sigma/(1 - D) \tag{12}$$

where ω is replaced by D, the scalar damage parameter. He then proceeds to couple static plastic damage D_1, creep damage D_2, and fatigue damage D_3:

$$dD_1 = f_1(\phi, \alpha, D_1, D_2, D_3, \ldots)d\sigma \tag{13}$$

$$dD_2 = f_2(\phi, \alpha, D_1, D_2, D_3, \ldots)dt \tag{14}$$

$$dD_3 = f_3(\phi, \alpha, D_1, D_2, D_3, \ldots)dN \tag{15}$$

where ϕ is the forcing variable, α represents internal variables describing hardening state, and N represents cycles.

Chaboche and Lemaitre [14], assuming creep and fatigue damage to be additive, have defined creep-fatigue damage in the following way:

$$dD_2 = f_2(\sigma, (D_2 + D_3))dt \tag{16}$$

$$dD_3 = f_3(\Delta\sigma, \sigma_m, (D_2 + D_3))dN \tag{17}$$

where $\Delta\sigma$ and σ_m are stress range and mean stress, respectively. Defining $D = D_2 + D_3$ gives

$$dD = f_2(\sigma, D)dt + f_3(\Delta\sigma, \sigma_m, D)dN \tag{18}$$

A Rabotnov-Kachanov approach was taken for both creep and fatigue damage,

$$dD = C\sigma^r(1 - D)^{-k(\sigma)}\, dt + [1 - (1 - D)^{\beta+1}]^{\alpha(\Delta\sigma)}\left[\frac{\Delta\sigma}{M(\sigma_m)(1-D)}\right]^{\beta} dN \tag{19}$$

where the first term is the creep damage increment. $k(\sigma)$, $\alpha(\Delta\sigma)$, $M(\sigma_m)$, r and β are temperature-dependent functions and material constants.

Note the stress dependence of the exponents in the damage rate equation (19). This allows for nonlinear damage accumulation rather than a unique relationship between time fraction and damage.

Chaboche also introduced isotropic and kinematic hardening variables in the uniaxial strain rate equation to model cyclic viscoplasticity in addition to conventional creep strain, i.e.

$$\dot{\varepsilon}^{in} = \left\langle \frac{|S - X^e| - R}{K} \right\rangle^n \text{sign}\,(S - X^e) \tag{20}$$

$$\dot{X}^e = Cf(p)(a\dot{\varepsilon}^{in} - X^e|\dot{\varepsilon}^{in}|) - b|X^e|^m \text{sign}(X^e) \tag{21}$$

where R and X^e are isotropic and kinematic hardening variables, and n, K, C, a, b, and m are temperature-dependent coefficients. Also,

$$f(p) = \ell + (1 - \ell)e^{-\beta p}, \quad p = \int_0^t |\dot{\varepsilon}^{in}(\tau)|d\tau \tag{22}$$

where β and ℓ are temperature-dependent material constants. The inelastic strain rate is given by $\dot{\varepsilon}^{in}$. Note that net stress is used in equations (20) - (22) to introduce coupling of the inelastic strain rate with damage. In equation (20), $\langle Y \rangle = YH(Y)$, H being the unit step function. Note that X^e represents a net backstress for consistency since net stress is used in equations (20) - (21).

Equations for viscoplastic strain rate with an internal variable structure as in equations (20) - (22) can describe effects of unloading and cyclic loading unlike the more restricted creep strain rate equations derived from a dissipative potential (e.g. equations (6) and (10)). These effects include nonlinear hardening, Bauschinger effects, cyclic hardening or softening, and recovery. Additional state variables may be introduced to account for microstructural aging effects or transformation due to temperature changes.

ANISOTROPIC DAMAGE FORMULATION

The Rabotnov-Kachanov scalar damage parameter ω is useful for describing creep damage under uniaxial or proportional loading conditions. Use of an isochronous surface to correlate multiaxial creep rupture is in general valid only for proportional loading; furthermore, the isochronous surface is essentially a description of "initial" creep anisotropy rather than deformation- or damage-induced anisotropy. This distinction is important since it leads to the need to define a damage tensor. Anisotropic deformation of the isochronous surface is equivalent to tensorial damage for loading histories in which principal stress axes rotate.

One is guided in formulation of anisotropic damage by knowledge of dominant cavity growth mechanisms, relevant measures of driving stress, and the general framework of continuum damage mechanics.

Trampczynski, Hayhurst, and Leckie [4-5] conducted experiments on aluminum and copper. Copper cavitates much more easily than the aluminum or austentic stainless steels [15]. They subjected thin-walled tubular specimens to an axial stress of 42.5 MPa and shear stress of 14.2 MPa for nearly the entire steady load lifetime, then reversed the shear stress to -14.2 MPa. For aluminum, the damage was well-distributed along grain boundaries, and the shear stress reversal resulted in no change of creep strain rates, damage rates, or rupture time. In contrast, damage in the form of cavity nucleation and growth occurred in copper on grain boundaries normal to the maximum principal stress. The shear stress reversal resulted in an increase in rupture time by a factor of approximately two for copper. A decrease in creep strain rates was attributed by the authors to deformation-induced anisotropy which is not accounted for in equation (10).

Hence, the anisotropy of damage exhibited by copper cannot be described by the generalized Rabotnov-Kachanov equations with scalar damage parameter ω . The evolution of damage must be computed separately for each of the two planes normal to the maximum principal stress. For aluminum, though, they are satisfactory provided the inelastic strain is predominately viscous or creep strain during and after rotation of principal stress axes. It is interesting to note that the ischronous surfaces for copper and aluminum follow maximum principal stress and effective stress criterion, respectively. The experimental results for nonproportional loading would then imply that the isochronous locus for aluminum is underformed while that for copper is deformed, consistent with the earlier notion of damage-induced anisotropy of the isochronous surface.

At this point, it should be noted that more precise forms of isochronous surfaces have been introduced. Huddleston [16] introduced the form

$$\sigma^*(\sigma_{ij}) = \frac{3}{2} H_1 \left(\frac{2}{3} \frac{\bar{\sigma}}{H_1} \right)^a \exp \left[b \left(\frac{J_1}{S_s} - 1 \right) \right] \tag{23}$$

where

$$H_1 = \sigma_1 - J_1/3, \; J_1 = \sigma_{KK} ,$$

$$S_s = (\sigma_1^2 + \sigma_2^2 + \sigma_3^2)^{1/2} ,$$

and a and b are temperature-dependent material constants. The results for type 304 stainless steel tested at 593°C show much better correlation with equation (23) than with effective stress $\bar{\sigma}$, maximum shear stress, or maximum principal stress. Hence, Huddleston's formulation would be a likely candidate for inclusion in a damage rate equation such as equation (11). Of course, the net stress can be used to compute all stress-related variables in equation (23).

There are several classifications of approaches which will be reviewed for generalization to anisotropic damage:

(i) a scalar damage parameter with a tensor multiplier to apportion damage effects among the various stress components,

(ii) definition of physical creep damage (e.g. cavity or fissure density) in terms of an appropriate rank tensor,

(iii) measure of deterioration of elastic behavior, and

(iv) creep damage potential functions.

(i) Tensor Multiplier Functions

In this approach, damage growth is governed by a scalar, but the growth of damage influences various stress-strain components differently. This representation of damage is implied by the procedure of Leckie et al. [5-6,10] which involved separate calculation of the damage on two non-interacting planes in copper. Defining the scalar damage parameter as ω, the rate of growth of the damage tensor $\underset{\sim}{D}$ is given by

$$\dot{\underset{\sim}{D}} = \underset{\sim}{Q}(\underset{\sim}{S})\dot{\omega} \tag{24}$$

where $\underset{\sim}{Q}(\underset{\sim}{S})$ is an operator of the same rank as $\underset{\sim}{D}$ which defines the preferential orientation of cavity growth and crack formation. Note the dependence of the directionality of damage growth on the net stress tensor $\underset{\sim}{S}$. This is due to the fact that the effective net stress exceeds the effective true stress, and rotation of the net stress tensor relative to the true stress tensor will occur as cavitation proceeds if the principal axes of true stress are rotated (i.e. nonproportional loading).

As stated by Hayhurst [17], it is likely that most metals suffer creep damage of a mixed cavitation/wedge cracking nature along grain boundaries; copper and aluminum offer two "bounds" of mostly cavitation damage and mostly grain boundary sliding-induced wedge cracking, respectively. From an analytical standpoint, this means that if $\underset{\sim}{Q}(\underset{\sim}{S})$ is defined as

$$\underset{\sim}{Q} = \gamma \underset{\sim}{I} + (1 - \gamma)\underset{\sim}{\Gamma} \tag{25}$$

where $\underset{\sim}{I}$ is the identify tensor and $\underset{\sim}{\Gamma}$ apportions damage anisotropy, then $\gamma \simeq 0$ for copper and $\gamma \simeq 1$ for aluminum, at least in the range of stresses tested by Leckie and associates. From consideration of deformation

mechanism maps [18], to be discussed in a later section, it is quite possible that both γ and $\underset{\sim}{\Gamma}$ are net stress and temperature dependent.

Studies which use the form of $\underset{\sim}{\Omega}$ given in equation (25) usually assume damage is represented adequately by a second order tensor, which is only an approximation of physical damage for the general nonproportional loading case. Chaboche [13] extends the stress level dependence of the exponent of damage in the extended Rabotnov-Kachanov damage law to describe scalar damage evolution, i.e.

$$\dot{\omega} = < \frac{\sigma^*(\underset{\sim}{S})}{A} >^r / (1 - \omega)^{k(\sigma^*)}$$

where we again note the use of the isochronous surface concept. Chaboche suggested the use of net stress to compute σ^* within the Macauley bracket in this equation.

Murakami and Ohno, using a second rank symmetric damage tensor, have suggested the general form [9,19]

$$\dot{\underset{\sim}{D}} = \Omega \underset{\sim}{I} + \sum_i M^{(i)} [\underset{\sim}{\nu}^{(i)} \otimes \underset{\sim}{\nu}^{(i)}] + \sum_j \underset{\sim}{N}^{(j)} : [\underset{\sim}{\nu}_D^{(j)} \otimes \underset{\sim}{\nu}_D^{(j)}] \qquad (26)$$

where Ω and $M^{(i)}$ are scalar functions of net stress, temperature and other internal variables, $\underset{\sim}{N}^{(j)}$ is a fourth order tensor, and $\underset{\sim}{\nu}^{(i)}$ and $\underset{\sim}{\nu}_D^{(j)}$ are unit normal vectors in the positive principal value directions of the net stress tensor $\underset{\sim}{S}$ and its deviator, $\underset{\sim}{S}_D = \underset{\sim}{S} - (1/3)S_{kk}\underset{\sim}{I}$. The symbol $\otimes$ stands for outer product. A particular form which seems to encompass the bounding behaviors of copper and aluminum is given by

$$\dot{\underset{\sim}{D}} = B[\sigma^*(\underset{\sim}{S})]^k [n\underset{\sim}{I} + (1-n)\underset{\sim}{\nu}^{(1)} \otimes \underset{\sim}{\nu}^{(1)}] (\underset{\sim}{\phi}:\underset{\sim}{\phi})^{\ell/2} \qquad (27)$$

where

$$\underset{\sim}{\phi} = (\underset{\sim}{I} - \underset{\sim}{D})^{-1} .$$

Here, B, k, η and ℓ are material constants. Note the similarity of equation (27) with Chaboche's approach. The inverse dependence on damage is introduced through $\underset{\sim}{\phi}:\underset{\sim}{\phi}$ in a consistent way in the Murakami-Ohno approach, without recourse to an additional scalar growth law. It should also be noted that ℓ in equation (27) could be made a function of net stress to correspond to Chaboche's modification to achieve a nonlinear damage versus time fraction relationship. Hayhurst and Leckie's generalization of the Rabotnov-Kachanov approach in equation (11) is equivalent to equation (27) if $\eta = 1$, i.e. isotropic damage is assumed.

Murakami and Ohno have also provided a rational definition of the net stress tensor consistent with area reduction due to physical damage. This will be discussed later in the section on anistropic representation of physical damage. It should be emphasized that a second order damage tensor can only approximately reflect the effects of physical damage on the damage rate for general nonproportional loading. The computational simplicity of this approach is desirable, though, provided it is relatively accurate.

One item regarding equation (27) which appears to have been overlooked in the literature is the possibility that the rate of damage growth in a given direction is dependent upon the damage in that direction rather than the equivalent scalar damage, i.e.

$$\dot{\underset{\sim}{D}} = B[\sigma^*(\underset{\sim}{S})]^k \{\eta \underset{\sim}{I}(\underset{\sim}{\phi}:\underset{\sim}{\phi})^{\ell/2} + (1 - \eta)\underset{\sim}{\nu}^{(1)} \otimes \underset{\sim}{\nu}^{(1)} \left[\frac{1}{1 - \underset{\sim}{\nu}^{(1)} \cdot \underset{\sim}{D} \cdot \underset{\sim}{\nu}^{(1)}} \right]^{\ell}\} \quad (28)$$

Of course, this effect could be studied via discrete rotations of maximum principal stress with metallographic examination of otherwise identical specimens at each state to quantify damage extent and direction. The criterion for rupture in this case could be $(\underset{\sim}{\phi}:\underset{\sim}{\phi})^{1/2} \to \infty$ for $\eta \to 1$ or $\underset{\sim}{\nu}^{(1)} \cdot \underset{\sim}{D} \cdot \underset{\sim}{\nu}^{(1)} \to 1$ for $\eta \to 0$.

(ii) Tensorial Description of Physical Damage

The previous section dealt with heuristic descriptions of damage evolution which have evolved primarily out of extension of the Rabotnov-Kachanov continuum damage concepts to multiaxial nonproportional loading. When defining the damage tensor, through, it is necessary that the current state of damage be adequately reflected with regard to direction and sense. Creep damage in the continuum sense is almost universally considered to be quantitatively related to the area density of voids and fissures along grain boundaries in a global mean sense. That is, microscale effects in each grain are not considered. In a materials science approach, heterogeneity of damage from grain to grain can lead to void growth constraint; this would have to be treated as a nonlocal damage growth phenomenon in the continuum approach, i.e. damage in a neighboring grain influences local damage growth. These nonlocal effects are not usually addressed in continuum creep damage mechanics.

Leckie and Onat have proposed a generalized tensorial form for cavitation damage [20]. In their approach, we consider a material element large enough such that deformation and damage may be considered homogeneous within. Then, we consider a unit sphere with unit normal vector $\underset{\sim}{n}$ at each point. The total volume of voids found in grain boundaries in the material element normal to $\underset{\sim}{n}$ is denoted as

$$V(\underset{\sim}{n})dA(\underset{\sim}{n}) \tag{29}$$

where $V(\underset{\sim}{n})$ is the density of the distribution of void volume. Since the physical damage state is invariant with respect to the sign of $\underset{\sim}{n}$,

$$V(\underset{\sim}{n}) = V(-\underset{\sim}{n}) \tag{30}$$

Various order damage tensors can be defined by the moments of the voids of grain boundaries, i.e.

$$V_o = \int_A V(\underset{\sim}{n})dA(\underset{\sim}{n}) \tag{31}$$

$$V_i = \int_A V(\underset{\sim}{n})\, n_i dA(\underset{\sim}{n}) \tag{32}$$

$$V_{ij} = \int_A V(\underset{\sim}{n})\, n_i\, n_j\, dA(\underset{\sim}{n}) \tag{33}$$

.

.

.

and so on, where A is over the unit sphere and n_i are the components of $\underset{\sim}{n}$ in a fixed rectangular coordinate frame (i, j, ... = 1, 2, 3). These damage tensors transform in the usual way and result in invariance of damage with respect to rigid body rotation. From equation (30), all odd rank damage tnsors must vanish. All even rank tensors are symmetric in all indices and

irreducible. We also note that $V_{KK} = V_o$ where V_o is the total volume of voids per unit volume, or the isotropic damage tensor.

Leckie and Onat also define a series of tensors describing the density and direction of void nucleation sites, known to be particularly important in the early stages of creep. These tensors follow the same development as for V_o, V_{ij}, V_{ijkl}, and are defined as N_o, N_{ij}, N_{ijkl}, ..., with the totality of damage tensors defined by a tensor

$$\underset{\sim}{r} = (V_o, V_{ij}, V_{ijk\ell}, \ldots; N_o\ N_{ij}, N_{ijk\ell}, \ldots) \tag{34}$$

with damage evaluation given by

$$\dot{\underset{\sim}{r}} = \underset{\sim}{g}(\underset{\sim}{\sigma},\underset{\sim}{r}) \tag{35}$$

and a rupture criterion

$$R(\underset{\sim}{\sigma}, \underset{\sim}{r}) \leq 0 \tag{36}$$

The creep strain rate equation is assumed to be weakly dependent on $\underset{\sim}{r}$.

Obviously directionality of physical damage could be described with good quantitative accuracy by using fourth and higher order tensors. Yet such an approach is not necessarily economical nor practical. If use of a second order tensor can suitably approximate the directionality of damage, then it is indeed warranted. To this end, Leckie and Onat have suggested the use of second order symmetric tensors $\underset{\sim}{V}$ and $\underset{\sim}{N}$. Again $V_{KK} = V_o$. Applying the mean value theorem to equation (33), we get an estimate of $V(\underset{\sim}{n})$ as

$$V(\underset{\sim}{n}) \simeq \frac{3}{4\pi} V_{ij} n_i n_j \tag{37}$$

which also satisfies equation (31). Likewise,

$$N(\underset{\sim}{n}) \simeq \frac{3}{4\pi} N_{ij} n_i n_j \tag{38}$$

The growth laws are then expressed as

$$\dot{\underset{\sim}{\varepsilon}}^c = \underset{\sim}{f}(\bar{\sigma}, V_o)\underset{\sim}{\sigma}' \tag{39}$$

$$\dot{\underset{\sim}{V}} = \underset{\sim}{g}_V(\underset{\sim}{\sigma}, \underset{\sim}{V}, \underset{\sim}{N}) \tag{40}$$

$$\dot{\underset{\sim}{N}} = \underset{\sim}{g}_N(\underset{\sim}{\sigma}, \underset{\sim}{V}, \underset{\sim}{N}) \tag{41}$$

with the rupture condition

$$R(\underset{\sim}{\sigma}, \underset{\sim}{V}) = 0 \tag{42}$$

Here, $\underset{\sim}{\sigma}'$ is the deviatoric stress tensor. A rupture criterion of the form

$$R(\sigma_{max}, V_o, V_{ij} n_i^* n_j^*) = 0 \tag{43}$$

was suggested, where $\sigma_{max} = n_i^* \sigma_{ij} n_j^*$ is the component of stress in the direction of maximum principal stress, $\underset{\sim}{n}^*$. Thus, a critical combination of maximum stress, total void volume, and void density on grain boundaries normal to the maximum stress dictates rupture. Later work by Leckie resulted in the proposed rupture condition.

$$\max_{\text{all } \underset{\sim}{n}} \left(V_{ij}\, \bar{n}_i \bar{n}_j\, \bar{n}_K \sigma_{K\ell}\, \bar{n}_\ell\right) = \text{constant}$$

It is interesting to note that Leckie and Onat do not use net stress in the constitutive equations for damage and deformation. The effect of area reduction is evidently included via V_o in the creep strain rate equations. Though both void nucleation and growth are included in this formulation, the specific forms for the growth equations are not yet well-developed.

Marakami and Ohno [9,19] have developed a rather complete formulation for creep damage, including finite deformation rotation invariance requirements. In their theory, damage is approximated by a second rank tensor which reflects the change in effective area of the Cauchy tetrahedron due to projected area of cavities on each face. Selecting a material volume element large in comparison to mean void or grain size, but small enough for stress and damage to be uniform, we define the damage tensor as

$$\underset{\sim}{D} = \frac{3}{S_g(V)} \sum_{k=1}^{N} \int_V \left[\underset{\sim}{n}^{(k)} \otimes \underset{\sim}{n}^{(k)} + W^{(k)} \left(\underset{\sim}{I} - \underset{\sim}{n}^{(k)} \otimes \underset{\sim}{n}^{(k)}\right)\right] dS_g^{(k)} \qquad (44)$$

where $dS_g^{(k)}$ and $\underset{\sim}{n}^{(k)}$ denote the area of a grain boundary element occupied by the k-th cavity and the unit vector normal to $dS_g^{(k)}$, respectively, and $S_g(V)$ is the total area of grain boundaries in V. Murakami and Ohno do not distinguish between representation of void nucleation and growth. The definition of cavity can evidently include both wedge-type and r-type cavities as discussed by Raj et al. [15,22]. In equation (44), $W^{(k)}$ denotes the effect of the k-th cavity on the area reduction of planes whose normals are

perpendicular to $\underset{\sim}{n}^{(k)}$, this effect is included since the voids are three-dimensional and cannot be considered just as two-dimensional grain boundary cracks.

The principal values of the damage tensor are bounded by 0 and 1, i.e.

$$0 \leq D_j \leq 1 \quad (j = 1, 2, 3) \tag{45}$$

When $D_j = 1$ for any j, creep rupture occurs on the j-th principal plane. For undamaged material, $\underset{\sim}{D} = \underset{\sim}{0}$. Note the similarity of $\underset{\sim}{D}$ in equation (44) with $\underset{\sim}{V}$ equation (33). Equation (44) is integrated only over the portions of grain boundaries which are cavitated in contrast to the entire unit sphere in equation (33), but the two formulations are substantially equivalent apart from the cavity width correction $W^{(k)}$ in the Murakami-Ohno approach.

The effect of damage accumulation is to decrease the area over which the force is carried on an infinitesimal element, with some directions experiencing more area reduction than others due to preferential cavity growth. Still, equilibrium must be satisfied; for an arbitrary plane in the material, this leads to a definition of a net stress tensor which is not only intensified, but also rotated with respect to the Cauchy stress tensor defined for undamaged material. We define the symmetric part of the stress tensor defined by

$$\underset{\sim}{\sigma} \cdot (\underset{\sim}{I} - \underset{\sim}{D})^{-1} = \underset{\sim}{\sigma} \cdot \underset{\sim}{\phi} \tag{46}$$

as the net stress tensor $\underset{\sim}{S}$, i.e.

$$\underset{\sim}{S} = \frac{1}{2} (\underset{\sim}{\sigma} \cdot (\underset{\sim}{I} - \underset{\sim}{D})^{-1} + (\underset{\sim}{I} - \underset{\sim}{D})^{-1} \cdot \underset{\sim}{\sigma}) \tag{47}$$

where $\underset{\sim}{\sigma}$ is Cauchy stress. $\underset{\sim}{S}$ is essentially the stress acting on a fictitious undamaged material element which is equivalent to application of $\underset{\sim}{\sigma}$ on an element of damaged material. This approach is essentially a generalization of the Kachanov-Rabotnov scalar damage approach. Damage rate equations (27) or (28) could then be employed using $\underset{\sim}{S}$ defined in equation (47), with appropriate specialization to combined isotropic and anisotropic damaging. The Jaumann derivative may be used for damage rate to ensure invariance of the damage rate equation with respect to rigid body rotations.

Again it is recognized that the creep strain rate is less affected by cavity growth than is damage rate or rupture, which are local phenomena. In fact, creep rupture may occur even when the creep strain rate is finite rather than infinite as implied by a Kachanov-Rabotnov scalar damage approach. Recalling the work of Leckie and associates, the creep strain rate is deviatoric with magnitude modified by $1/(1-\omega)$ as in equation (10). Murakami and Ohno point out that the net stress tensor for use in the creep strain rate equation is in general formed by a fourth rank tensor $\underset{\sim}{\xi}$ operating on Cauchy stress, i.e.

$$\overline{\underset{\sim}{S}} = \frac{1}{2} \left(\underset{\sim}{\xi} : \underset{\sim}{\sigma} + \underset{\sim}{\sigma} : \underset{\sim}{\xi} \right) \tag{48}$$

where $\underset{\sim}{\xi} = \underset{\sim}{\xi}(\underset{\sim}{\phi})$. The damage and creep rate equations are then given by

$$\dot{\underset{\sim}{D}} = \underset{\sim}{G} \left(\underset{\sim}{S}, \underset{\sim}{\phi}, \kappa, T \right) \tag{49}$$

$$\dot{\underset{\sim}{\varepsilon}}^{c} = \underset{\sim}{F}\left(\overline{\underset{\sim}{S}}, \underset{\sim}{\phi}, \kappa, T \right) \tag{50}$$

where κ and T denote a matrix work-hardening parameter and absolute temperature, respectively. $\dot{\underset{\sim}{\varepsilon}}^{c}$ may be interpreted here as the rate of deformation tensor for finite creep deformation. Note also that dependence on $\underset{\sim}{S}$ and $\underset{\sim}{\phi}$ in equation (49) is equivalent to dependence on $\underset{\sim}{\sigma}$ and $\underset{\sim}{D}$, as is the pair $\overline{\underset{\sim}{S}}$ and $\underset{\sim}{\phi}$. In earlier work, Murakami and Ohno [9] had written equation (50) as

$$\dot{\underset{\sim}{\varepsilon}}^{c} = \underset{\sim}{F}'(\underset{\sim}{S}, \underset{\sim}{\phi}, \kappa, T) \tag{51}$$

where

$$\underset{\sim}{\phi} = (\underset{\sim}{I} - c\underset{\sim}{D})^{-1} \tag{52}$$

and

$$\overset{\sim}{\underset{\sim}{S}} = \frac{1}{2}(\underset{\sim}{\sigma} \cdot \underset{\sim}{\phi} + \underset{\sim}{\phi} \cdot \underset{\sim}{\sigma}) \tag{53}$$

where c ($0 \leq c \leq 1$) allows variation from a deviatoric or other classical dissipative potential flow rule. The representation for creep strain rate given in equations (48) and (50) may be general, but is very difficult to implement. The approach in equations (51) - (53) is easier to implement, since c can be selected to fit a given data set, but use of $\underset{\sim}{\phi}$ is a rather ad hoc procedure which is not well physically grounded. Fortunately, when the cavity volume fraction is on the order of a few percent or less [19], the effect of damage on creep deformation may be assumed to be isotropic. Hence, the creep strain rate equation may be simplified to

$$\dot{\underset{\sim}{\varepsilon}}^{c} = (3/2)mA^{1/m}\,\kappa^{(m-1)/m}\,\bar{\bar{S}}_{eq}^{(n-m)/m}\,\underset{\sim}{\bar{\bar{S}}}' \tag{54}$$

where the net stress tensor modified by isotropic damage is given by

$$\tilde{\bar{\bar{S}}} = (1 + c\, D_{kk})\tilde{\sigma} \tag{55}$$

where c ($0 \leq c \leq 1$) is a material constant. Furthermore,

$$\bar{\bar{S}}eq = \left(\frac{3}{2}\ \tilde{\bar{\bar{S}}}' : \tilde{\bar{\bar{S}}}'\right)^{1/2} \tag{56}$$

$$\tilde{\bar{\bar{S}}}' = \tilde{\bar{\bar{S}}} - \frac{1}{3}\bar{\bar{S}}_{kk}\tilde{I} \tag{57}$$

The evolution of matrix work-hardening parameter κ is given by

$$\dot{\kappa} = mA^{1/m}\ \kappa^{(m-1)/m}\ \bar{\sigma}^{n/m} \tag{58}$$

In equations (54) - (58), A, m, n, and k are temperature-dependent material constants. Murakami and Ohno have demonstrated the applicability of the second rank damage tensor $\tilde{D}$ for prediction of rupture time for copper subjected to nonproportional loading and for perforated specimens. Their prediction of creep strain under nonproportional reversal of stress using equation (54) is not suitably accurate, however; the introduction of backstress into equation (54) would allow for kinematic hardening (directional dislocation arrangement) and more accurate prediction for nonproportional loading and unloading sequences [22-24]. Hence, use of unified creep-plasticity theories might be warranted [25-30].

It should be noted that Betten [31], employing a tensor representation of area reduction due to damage, also showed that creep damage can be represented

by a second rank symmetric tensor. He derived the creep rate constitutive equations based on generalized tensor function theory. In contrast to Murakami and Ohno, Betten retains a non-symmetric net stress tensor. Furthermore, he introduces initial deformation-induced anisotropy effects into both the creep strain rate and damage rate equations. While it is obvious that initial anisotropy from a rolling or forming process would affect the creep strain rate magnitude and direction, the effect on magnitude and direction of damage rate is inconclusive. As a point of clarification, it should be noted that all previous growth equations in this paper have assumed initial isotropy.

While the work of Betten offers a very rigorous continuum mechanics approach to tensorial damage, its abstract nature and lack of simplification to practical creep constitutive equations limit its usefulness. The work of Murakami and Ohno is of similar nature yet oriented toward the engineering approach.

Baik and Raj [21] have proposed use of a second rank tensor to represent the development of three-dimensional creep damage for the case of wedge-cracking induced by grain boundary sliding for aluminum alloy and austenitic stainless steels subjected to creep-fatigue loading. They showed that wedge-cracking was likely to occur in the aluminum alloy and austenitic stainless steels under conditions of asymmetric load cycle shapes without tension hold, while hole cavitation ("r" type cavitation) was likely to occur under tension hold cycles. This points to the fact that the dominant mechanism of creep damage under creep-fatigue loading is not only sensitive to temperature and loading intensity, but the rate and sequence in which loads are applied. If wedge type creep damage is dominant, then Baik and Raj define damage growth in the principal frame by

$$\frac{d(A_w)_i}{d\bar{\varepsilon}} = \alpha\,\beta[\gamma x_{i1}\,\frac{\sigma_1}{\bar{\sigma}}\,] \tag{59}$$

for i = 1, 2, 3, where β represents the ratio of the grain boundary sliding strain rate to the applied strain rate, α is a proportionality constant, and γ is an adjustable parameter reflecting the extent to which damage produced in tension can be recovered in compression,

$$d\bar{\varepsilon} = (\frac{2}{3}\, d\underset{\sim}{\varepsilon} : d\underset{\sim}{\varepsilon})^{1/2} \tag{60}$$

and the measure of damage is defined by

$$A_w = c/L \tag{61}$$

where c is the wedge crack length, and L is the grain size. As in the earlier approaches, $0 \leq A_w \leq 1$, with $A_w = 0$ indicative of undamaged material, and $A_w = 1$ indicative of fracture. The tensor x_{i1} allows correlation of the stress applied in direction 1, σ_1, with development of damage in directions 2 and 3. Since wedge damage develops at triple junctions of grain boundaries, wedge cracks appear in normal directions along adjacent grain boundaries. It may be the case that when creep damage is dominated by wedge-cracking, the mean damage state (averaged over a number of grains) assumes a more isotropic nature due to random grain orientation than would "r" type cavitation, which is dependent on the maximum principal stress direction. Perhaps these considerations help explain the observed indifference to loading direction of creep strain and damage rates of Leckie and Hayhurst's fixed tension, alternating shear tests on aluminum. It would seem that materials which do

not cavitate easily may experience at least a component of triple junction wedge-cracking in creep-dominated situations with even occasional load reversals present.

Recalling the constructions of damage tensors reported earlier, it is clear that it is not necessary to distinguish between triple junction wedge cracks and well distributed cavities ("r" type) in a continuum damage approach. The three-dimensional character of damage can be described by a tensor with a suitable degree of anisotropy. It is significant, though, that previous continuum damage mechanics analyses have not substantially addressed the possibility of several dominant mechanisms, each with a different damage rate dependence on applied stress, over a range of temperatures and strain rates.

(iii) Measure of Deterioration of Elastic Behavior

It is very common in structural analysis to assume that the presence of damage is manifested by a decrease in stiffness. Usually, the concept of deterioration of stiffness is applied to a structural member rather than at each material point. Chaboche [13] introduced a form for the net stress tensor

$$\underset{\sim}{S} = \underset{\sim}{M}(\underset{\sim}{D}):\underset{\sim}{\sigma} \tag{62}$$

where $\underset{\sim}{M}$ is a fourth order tensor operating on stress. Equation (62) is applicable at each material point. Then $\underset{\sim}{S}$ can be used in lieu of $\underset{\sim}{\sigma}$ in the elastic-viscoplastic constitutive equations with damage-induced anisotropy being included in a natural way through flow rules based on scalar invariants of $\underset{\sim}{S}$. Chaboche suggested that $\underset{\sim}{M}$ could be measured from deterioration of the elastic response by using an equivalence in the elastic strain sense, i.e.

$$\underset{\sim}{\sigma} = \bar{\underset{\sim}{\Lambda}}\ (\underset{\sim}{D}):\underset{\sim}{\varepsilon}^{e} \tag{63}$$

$$\underset{\sim}{S} = \underset{\sim}{\Lambda}(\underset{\sim}{0}):\underset{\sim}{\varepsilon}^{e} \tag{64}$$

where $\underset{\sim}{\varepsilon}^{e}$ is the elastic strain tensor and $\underset{\sim}{\Lambda}(\underset{\sim}{0})$ the fourth rank elasticity tensor for undamaged material. These equations lead to

$$\underset{\sim}{M}(\underset{\sim}{D}) = \underset{\sim}{\Lambda}(\underset{\sim}{0}):\bar{\underset{\sim}{\Lambda}}^{-1}(\underset{\sim}{D}) \tag{65}$$

so that $\underset{\sim}{M}(\underset{\sim}{D})$ could be determined if initial and subsequent elastic responses are known.

As mentioned by Chaboche, this description of damage is consistent with a general thermodynamical framework [13]. However, it is noted from earlier discussion that the dependence of creep deformation on creep damage is not direct as is the rupture condition since rupture may occur in a relatively brittle fashion at low void volume density. In other words the deformation of the matrix is not strongly affected by the presence of grain boundary damage up to tertiary creep, reflected through the applicability of a deviatoric flow rule for creep strain. For these reasons, as pointed out by Murakami and Ohno [19] it seems more appropriate to base the net stress tensor on reduction in projected area due to physical creep damage, and to use this net stress tensor in damage evolution equations but not necessarily in creep strain rate equations.

(iv) Creep Damage Potential Functions

The generalization of uniaxial concepts of creep deformation to the multiaxial case usually involves the assumption of a dissipative potential

function. The creep strain rate is then normal to this dissipative potential surface in stress space. It is tempting to generalize creep damage for the multiaxial case by assuming an appropriate creep damage potential. To this end, both phenomenological and coupled thermo-viscoplastic approaches have been offered.

From a phenomenological standpoint, Bodner and Lindholm [32] have suggested a damage growth law of the form

$$\dot{D} = \alpha(W_s)\beta(\sigma_{kk})\gamma(D) \tag{66}$$

where W_s is the stored energy of cold work, σ_{kk} is the first invariant of stress and D is a scalar damage parameter. The value of D at failure, unlike in the Kachanov-Rabotnov approach, is determined empirically. The mechanistic interpretation of this equation is that α governs nucleation of voids and defects, β controls the rate of growth of voids under applied hydrostatic stress, and γ relates damage growth rate to current damage level. The use of the first invariant of stress as the sole stress parameter in equation (66) is incompatible with the concept of anisotropic creep damage. If $\beta(\sigma_{kk})\gamma(D)$ were to be defined as a surface in stress space, the direction of the damage rate could be defined as the gradient of the damage surface if β depended on σ_{ij} instead of an invariant. The separation of void nucleation and growth processes in equation (66) is similar to the formulation of Leckie and Onat (equations (29)-(44)); the latter formulation, however, assigned directions to void nucleation growth processes in contrast to the Bodner-Lindholm approach. Essentially, then, equation (66) provides very limited capability for modeling nonproportional creep damage and is somewhat difficult to apply.

Krajcinovic [33] has proposed damage evolution laws based on the existence of a potential, suggesting that this approach is ultimately necessary for treatment of cyclic loads. In his approach, the Helmholtz free energy density is composed of elastic and viscous terms

$$\psi = \psi^{(e)}(\underset{\sim}{\varepsilon}^{e}, \underset{\sim}{D}, T) + \psi^{(c)}(\underset{\sim}{\alpha}, p, \underset{\sim}{D}, T) \tag{67}$$

where $\psi^{(e)}$ and $\psi^{(c)}$ are elastic and creep potentials, $\underset{\sim}{\varepsilon}^{e}$ is the elastic strain, and $\underset{\sim}{\alpha}$ and p are kinematic and isotropic hardening variables which affect viscous response. In Krajcinovic's work, damage $\underset{\sim}{D}$ is a vector normal to a plane of cracks or crack-like defects. This definition of the damage tensor is not in agreement with the findings of Onat and Leckie, Murakami and Ohno, Betten, and others that physical damage must be represented by even rank tensors. Minimally, a second rank tensor (or scalar if damage is isotropic) is necessary. Use of a vector attributes a sense to the damage direction which incorrectly implies that the current state of damage is dependent on the sense of the direction; damage growth rate, not the current damage state, is dependent on sense of loading (tension or compression) and this is reflected through the damage evolution equation.

Since the rest of Krajcinovic's development does not hinge on this assertion of vectorial creep damage, we continue the discussion. From the Clausius-Duhem inequality,

$$\rho Q = \underset{\sim}{\sigma} : \overset{\cdot}{\underset{\sim}{\varepsilon}}^{c} - \rho \frac{\partial \psi}{\partial \underset{\sim}{D}} \cdot \overset{\cdot}{\underset{\sim}{D}} - \rho \frac{\partial \psi}{\partial \underset{\sim}{\alpha}} : \overset{\cdot}{\underset{\sim}{\alpha}} - \rho \frac{\partial \psi}{\partial p} \dot{p} - \frac{1}{T} \underset{\sim}{q} \cdot \underset{\sim}{\nabla} T \geq 0 \tag{68}$$

where ρ is mass density, $\dot{\underset{\sim}{\varepsilon}}^{c}$ is the creep strain rate, $\underset{\sim}{q}$ is the heat flux, and T is temperature. Equation (68) states that the energy dissipation power density $\rho Q \geq 0$. The entropy term in the dissipation power density cancels with the term in the total time differential of $\dot{\psi}$ resulting from dependence of ψ on T. Since stress can be derived from ψ by

$$\underset{\sim}{\sigma} = \rho \frac{\partial \psi}{\partial \underset{\sim}{\varepsilon}^{e}} \tag{69}$$

we can write

$$\dot{\underset{\sim}{\sigma}} = \rho \frac{\partial^2 \psi}{\partial \underset{\sim}{\varepsilon}^{e} \partial \underset{\sim}{\varepsilon}^{e}} : \dot{\underset{\sim}{\varepsilon}}^{e} + \rho \frac{\partial^2 \psi}{\partial \underset{\sim}{\varepsilon}^{e} \partial \underset{\sim}{D}} \cdot \dot{\underset{\sim}{D}} \tag{70}$$

and the rates of other generalized forces $-\rho \frac{\partial \psi}{\partial \underset{\sim}{D}}$, $-\rho \frac{\partial \psi}{\partial \underset{\sim}{\alpha}}$, $-\rho \frac{\partial \psi}{\partial p}$ can be similarly found. Next, the rates of change of internal variables $\underset{\sim}{\alpha}$, p, and $\underset{\sim}{D}$ in addition to creep strain $\underset{\sim}{\varepsilon}^{c}$ can be found by assuming the existence of a potential Ω such that

$$\underset{\sim}{j} = \frac{\partial \Omega}{\partial \underset{\sim}{X}} \tag{71}$$

where $\underset{\sim}{j} = \{\dot{\underset{\sim}{\varepsilon}}^{c}, \dot{\underset{\sim}{\alpha}}, \dot{p}, \dot{\underset{\sim}{D}}, \frac{1}{T} \underset{\sim}{\nabla} T\}^{T}$ and $\underset{\sim}{X} = \{\underset{\sim}{\sigma}, -\rho \frac{\partial \psi}{\partial \underset{\sim}{\alpha}}, -\rho \frac{\partial \psi}{\partial p}, -\rho \frac{\partial \psi}{\partial \underset{\sim}{D}}, -\underset{\sim}{q}\}^{T}$. If Ω is quadratic in $\underset{\sim}{X}$, then Ω is equivalent to the energy dissipation power density Q. Krajcinovic suggests a flow potential of the form

$$\Omega = G^{(c)}(\underset{\sim}{X})\, H(G^{(c)}) + G^{(d)}(\underset{\sim}{X})\, H(G^{(d)}) \tag{72}$$

when H is the Heaviside function. For $G^{(c)} < 0$, no viscous deformation occurs, and for $G^{(d)} < 0$, no growth of damage occurs. Hence, the coupling of

damage with creep strain rate and growth of damage would emerge from equations (71) - (72). Possible forms for the viscous flow potential $G^{(c)}$ and damage potential $G^{(d)}$ are

$$G^{(c)} = K \left\| \left(\underset{\sim}{\sigma}' + \rho \frac{\partial \psi}{\partial \underset{\sim}{\alpha}} \right) \right\| - g\left(- \rho \frac{\partial \psi}{\partial p} \right)^{n} \tag{73}$$

$$G^{(d)} = K_1 \left(R_1^2 + a\, D\, R_2^2 \right) - g_1(D)^{m} \tag{74}$$

where K, K_1, a, m, and n are material parameters and $\underset{\sim}{\sigma}'$ is deviatoric stress. R_1 and R_2 are the values of $- \rho \frac{\partial \psi}{\partial \underset{\sim}{D}}$ generalized forces in directions normal and tangential to the "plane of damage" in this formulation and therefore govern the normal and shear components of damage growth, respectively. The damage potential in equation (74) can reflect dominant shear-type damage accumulation, cleavage (normal) - type, or a combination.

The great advantage of using a flow potential is that damage is included as an internal variable. The damage and creep strain rate equations are coupled through the flow potential Ω , providing a rational treatment. The anisotropic character of damage is also defined through Ω . Rigorous application of the flow potential concept, though is difficult. It may be possible to simplify the flow potential or even to express some of the previously mentioned anisotropic theories in term of Ω (e.g. Murakami-Ohno). Certainly, it seems necessary to minimally express $\underset{\sim}{D}$ in equations (68) - (74) as a second order tensor rather than a vector in future work.

As a final comment, it should be noted that considerable work has been done [e.g. 34-37] in characterizing uniaxial cumulative creep damage under varying stress levels. At higher stress levels, damage accumulation more

nearly approaches a linear time fraction accumulation rule than at lower stress levels. Bui-Quoc and associates [35] use a highly phenomenological, normalized damage curve approach to more accurately represent (fit) creep and creep-fatigue damage sequence effects. They suggest that the Chaboche-Lemaitre approach in equation (19) provides a damage parameter which is very small ($D \tilde{=} 0$) even near the end of material life, and suggest that this is not representative of nonlinear damage accumulation processes. It appears to the current author that Chaboche et al, enforce this condition on damage to minimize the influence of damage on the creep strain rate equation until tertiary creep is reached. If the proper dependence of the creep strain rate on damage is prescribed, perhaps theoretical damage growth could more faithfully follow physical creep damage growth. It is strongly felt that the anisotropic damage tensor must accurately reflect physical damage to properly model loading sequence effects and creep-fatigue interaction.

SOME COMMENTS ON THE RELATIONSHIP OF MATERIAL SCIENCE AND CONTINUUM DAMAGE GROWTH LAWS

Naturally, description of creep damage has also been undertaken from the materials science or micromechanical viewpoint. Most of the work has dealt with the nucleation and growth of voids as a function of applied stress and temperature. The primary thrust of these studies has been to identify the regimes of stress and temperature in which voids grow by diffusion, power-law continuum plastic deformation, or by coupled mechanisms. Miller and Langdon [38] point out that three distinct void growth processes may occur:

(a) power-law creep of surrounding matrix at high stress levels,

(b) unconstrained diffusion growth at intermediate stress levels, and

(c) constrained diffusion growth at low stress levels.

Of course, coupling may exist between these mechanisms.

An essential feature of these different cavity growth mechanisms is that void growth rates will differ depending on the dominant mechanisms (highest growth rate). Svensson and Dunlop [39] have produced cavity growth mechanism maps which show the regimes of dominance of constrained diffusion growth, unconstrained diffusion growth, coupled power-law diffusional growth, power law growth, and non-equilibrium diffusional growth. These maps are very similar to the deformation mechanism maps introduced by Ashby and co-workers, but deal specifically with void growth mechanisms rather than creep deformation mechanisms. Other authors [3,15,21,38-44] have offered specific models for the nucleation of voids at grain boundary/slip band intersections, precipitate particles, or triple junctions, and the growth of these voids once nucleated.

Of particular interst to this investigation is the relationship of the cavity growth laws to the evaluation of the damage tensor in Kachanov-Rabotnov continuum damage theories. Obviously, the two must be somewhat compatible or we may extrapolate the continuum growth law into a regime where the damage evolution equation is of inappropriate form.

Cocks and Ashby [3,43] have extensively studied the regimes of diffusion controlled and power-law controlled creep damage growth. They note that growth due to power-law deformation of surrounding matrix material becomes more important as the voids become larger, even if the growth was diffusion controlled when the cavities were small. They also have shown that consideration of both diffusion and power-law controlled damage growth is

necessary for accurate calcuation of rupture times, particularly when variable loading histories are applied which impose diffusion controlled growth over part of the life and power-law growth over the rest. The linear time-fraction damage accumulation rule is not adequate when the mechanisms of cavity growth change due to temperature and/or stress changes. Edward and Ashby [45] have shown that coupled boundary diffusion/power-law growth is the mode of void growth over wide ranges of stress and temperature for structural metals.

Defining the area fraction of voids as

$$f_h = \frac{r_h^2}{l^2} \tag{75}$$

where r_h is the average void radius and $2l$ is the average void spacing, then the growth of damage f_h is described by

$$\dot{f}_h = \frac{\dot{\varepsilon}_o \phi_o}{f_h^{1/2} \ln(\frac{1}{f_h})} \left(\frac{\sigma_1}{\sigma_o}\right) \tag{76}$$

for boundary diffusion alone and

$$\dot{f}_h = \dot{\varepsilon}_o \beta_o \left\{ \frac{1}{(1-f_h)^n} - (1-f_h) \right\} \left(\frac{\sigma}{\sigma_o}\right)^n \tag{77}$$

for power-law creep alone. In equation (76), σ_1 is the stress acting normal to the boundary on which the void(s) lies and σ_o and $\dot{\varepsilon}_o$ are normalizing constants in the uniaxial power-law creep equation

$$\dot{\varepsilon} = \dot{\varepsilon}_o \left(\frac{\sigma}{\sigma_o}\right)^n \tag{78}$$

at a given temperature. Also,

$$\phi_o = \frac{2\Omega D_B \delta}{kT\, l^3} \frac{\sigma_o}{\dot{\varepsilon}_o} \tag{79}$$

where $D_B\delta$ is the boundary diffusivity, Ω the atomic volume, k is Boltzmann's constant, and T is absolute temperature. In equation (77),

$$\beta_o = \sinh\left\{-\frac{2}{3}\left\{\frac{n-\frac{1}{2}}{n+\frac{1}{2}}\right\}\right\} \tag{80}$$

Comparison of the power-law creep equation (77) with the Rabotnov-Kachanov continuum damage theory in equation (5) with $\mu = \nu$ reveals a great deal of similarity. In fact the forms are identical apart from the second term $(1-f_h)$ in equation (77). When f_h is large, the second term may be neglected and the two sets of equations match with f_h being interpreted as the scalar damage parameter ω. A very significant difference is that the continuum damage model gives a finite damage rate when the damage parameter is zero in contrast to the mechanistic approach, where the damage rate is zero for undamaged material. Cocks and Ashby point to this feature as being clearly indicative of the superiority of the mechanistic approach since non-existent holes do not grow. This is strictly true when damage is defined as void density; from the continuum viewpoint, though, a finite rate of damage when the damage parameter is zero could correspond to void nucleation processes or onset of creep damage.

For diffusion controlled growth of voids, as $f_h \to 1$,

$$\dot{f}_h \cong \phi_o \dot{\varepsilon}_o \left(\frac{\sigma_1}{\sigma_o}\right)\left(\frac{1}{1-f_h}\right) \tag{81}$$

which is identical to the Rabotnov-Kachanov relation when $\mu = \nu = 1$. As for power-law creep, for large f_h, the forms of the mechanistic and continuum models are the same, with only the damage power-law exponent differing between mechanisms. The differences between the mechanistic and continuum damage approaches are most pronounced when f_h is small for both diffusion controlled and power-law creep. In fact, the boundary diffusion growth rate in equation (76) exhibits a decrease as f_h increases for $f_h < .1$. Since Ashby et al. use $f_h = 0.25$ as a realistic failure condition, this behavior would be significant over much of life if voids grow by coupled boundary diffusion and power-law creep. Since Rabotnov-Kachanov type continuum damage laws imply that damage rate always increases with damage (for uniaxial creep loading), they cannot conform to boundary diffusion controlled void growth. Life predictions using the continuum damage law of Rabotnov-Kachanov can therefore be more conservative since power-law void growth is at a relatively high rate.

Cocks and Ashby [43] suggest the inclusion of ϕ_o and (σ_1/σ_o) in the continuum damage approach to account for coupled boundary diffusion and power-law creep. Turning to the consideration of anisotropic damage, however, it seems likely that this refinement is not warranted in this initial study. Previous work on coupled diffusion and power-law creep have not involved rotation of the principal stress axes. The materials science studies do tell us, however, that consideration of the creep damage growth regime is very important in determining damage rates. If a transition from the boundary diffusion regime to power-law growth regime is encountered as voids grow and the net stress increases, rotation of the maximum principal stress may result in a significant under-prediction of rupture time using a power-law damage rate. The directionality of damage, though, is another issue; this directionality will depend on propensity to cavitate, grain boundary sliding,

etc. Grain boundary sliding, for example, results in a concentration of normal stress and an increase of hydrostatic stress in each grain due to constraint of surrounding grains. This effect can be suitably described through the dependence of isochronous stress on the first invariant of stress in the anisotropic damage growth law (c.f. equation (26) or (28)).

INCORPORATION OF DAMAGE IN CONSTITUTIVE EQUATIONS FOR DEFORMATION

To this point, the development of rational forms for tensorial damage have concentrated on description of physical damage and its evolution. In reality, the evolution of creep strain rate is not as highly dependent on the anisotropy of the current state of damage (prior to tertiary creep) as is the damage rate. This is due to the fact that creep strain rate in the primary and secondary regimes is primarily affected by matrix work-hardening and recovery processes. The cavitation and sliding processes which occur at grain boundaries do not greatly affect creep strain rate until the voids or grain boundary cracks coalesce. These comments pertain to power-law creep, grain boundary diffusion, surface diffusion, or coupled mechanisms. Hence, it is clear that

(a) the inelastic strain rate magnitude should be affected by a global or averaged measure of physical damage up to the tertiary stage,

(b) the inelastic strain rate direction should be modified by the directional distribution of physical damage, with this effect increasing in importance as damage approaches a critical level in one or more directions,

(c) the anisotropy of damage does not translate into an equivalent anisotropy of inelastic strain rate, since damage may accumulate as cavitation on grain boundaries oriented normal to the maximum principal stress (anisotropic damage) with no concurrent observation of anisotropic deformation [4-6,10,12],

(d) the magnitude of inelastic strain rate may actually be finite in a direction corresponding to a critical (rupture) damage value [5,9], and

(e) the inelastic strain rate is of a power-law form, dependent primarily on the effective stress [10,13,19,25-30].

It should be noted here that the term inelastic strain rate rather than creep strain rate is used in this section, following the unified or state variable theories of creep deformation. In these theories, no distinction is made between the time-independent plastic and time-dependent creep strains. One model structure can exhibit the essential characteristics of monotonic and cyclic, rate-dependent plasticity, and stress and temperature-dependent creep deformation or relaxation [25-30]. Furthermore, inclusion of backstress and drag stress in these unified theories allows for accurate description of inelastic strain rate direction under nonproportional loading [25-26,46] and matrix work-hardening, respectively.

A fairly general statement of the isothermal unified equations, including both backstress and drag stress, is:

$$\dot{\underset{\sim}{\varepsilon}}^{n} = f\left\{\frac{3J_2'}{\kappa^2}\right\}(\underset{\sim}{\sigma}' - \underset{\sim}{\alpha}) \tag{82}$$

$$\dot{\underset{\sim}{\alpha}} = h_\alpha \dot{\underset{\sim}{\varepsilon}}^{n} - d(\underset{\sim}{\alpha}, T)\, \dot{\bar{\varepsilon}}^{n} \underset{\sim}{\alpha} - r_\alpha(\underset{\sim}{\alpha}, T)\, \underset{\sim}{\alpha} \tag{83}$$

$$\dot{\kappa} = h_\kappa \dot{\bar{\varepsilon}}^n - r_\kappa(\kappa,T) \tag{84}$$

where h_α and h_κ are hardening functions, r_α and r_κ are static recovery functions, and d is a dynamic recovery function. $\underset{\sim}{\alpha}$ is backstress, κ is drag stress, $J_2' = \frac{1}{2}(\underset{\sim}{\sigma}' - \underset{\sim}{\alpha}) : (\underset{\sim}{\sigma}' - \underset{\sim}{\alpha})$,and $\dot{\bar{\varepsilon}}^n = (2/3\ \dot{\underset{\sim}{\varepsilon}}^n : \dot{\underset{\sim}{\varepsilon}}^n)^{1/2}$. Terms involving temperature rate are dropped for the isothermal case but can be included if necessary. Common forms of the hardening and recovery functions will now be discussed:

$$h_\alpha = \text{constant} \tag{85}$$

for linear kinematic hardening or

$$h_\alpha = K_1 + K_2 \exp(-d_2\zeta) \tag{86}$$

where K_1, K_2 and d_2 are material constants and $\zeta = \underset{\sim}{\alpha} : \underset{\sim}{\alpha}$, $\zeta = \bar{\varepsilon}^n$, or $\zeta = (\underset{\sim}{\sigma}' - \underset{\sim}{\alpha}) : \underset{\sim}{\alpha}$. Experiments [26] have shown equation (86) to be most accurate. Also,

$$h_\kappa = C_1(\kappa^* - \kappa) \tag{87}$$

or
$$h_\kappa = C_1(\kappa^* - \kappa) + f_1(\bar{\varepsilon}^n, \dot{\bar{\varepsilon}}^n, \underset{\sim}{\alpha}) \tag{88}$$

or
$$h_\kappa = H(I_{\alpha\varepsilon})\left[\left(\frac{3}{2}\underset{\sim}{\alpha}:\underset{\sim}{\alpha}\right)^{1/2} - b_1(b_2\kappa)^{b_3}\right] . \tag{89}$$

where

$$H(I_{\alpha e}) = [a_1 a_2 \exp(a_1(\kappa - \kappa_0))]^{-1} \tag{90}$$

Equations (89) - (90), formulated by Abrahamson, Cescotto, and Leckie [26,47] can accurately model cyclic hardening or softening. Of course, simple forms such as equation (87) may be sufficient for representation of matrix hardening during creep.

The static recovery functions r_α and r_κ are usually of the forms

$$r_\alpha = C_2(\underset{\sim}{\alpha}:\underset{\sim}{\alpha})^{C_3} \tag{91}$$

$$r_\kappa = C_4(\kappa - \kappa_0)^{C_5} \tag{92}$$

where C_2, C_3, C_4, C_5, and κ_0 are material constants.

Common forms of the modulus function $f(3J_2'/\kappa^2)$ are

$$[D_0(3J_2'/\kappa^2)^n/J_2']^{1/2} \tag{93}$$

$$[D_0\exp[-(\kappa^2/3J_2')^n]/J_2']^{1/2} \tag{94}$$

$$[D_0[\sinh(3J_2'/\kappa^2)^m]^n/J_2']^{1/2} \tag{95}$$

where m, n, and D_0 are constants [25].

Temperature dependence of an Arrhenius form may be included in the flow rule and recovery terms [25].

The structure of these equations have been derived from uniaxial experiments. Nonproportional loading, however, can introduce errors in the inelastic strain rate direction and work hardening rate $\dot{\kappa}$ [48]. Since the inelastic strain rate direction is governed by evolution of backstress, it is necessary to include nonproportionality effects in either the backstress evolution law or directly in the flow rule. The latter is the approach taken by Murakami and Ohno [22]; it seems more rational, though, to include this effect in the backstress evolution law, i.e.

$$\dot{\underset{\sim}{\alpha}} = h'_{\alpha}\, \underset{\sim}{\nu}\, \dot{\bar{\varepsilon}}^{n} - d(\underset{\sim}{\alpha},T)\, \dot{\bar{\varepsilon}}^{n}\, \underset{\sim}{\alpha} - r_{\alpha}(\underset{\sim}{\alpha},T)\underset{\sim}{\alpha} \tag{96}$$

where unit vector $\underset{\sim}{\nu}$ is based on a Mroz type hardening rule [23-24,48].

For the evolution of drag stress (isotropic hardening), it has been suggested [25-26] that h_{κ} be modified to account for additional hardening observed [23-24]. Possible forms for inclusion of this effect are

$$h_{\kappa} = C_1(\psi(\phi)\kappa^* - \kappa) \tag{97}$$

or

$$h_{\kappa} = \frac{H(I_{\alpha\varepsilon})}{[\psi(\phi)]^{1/2}} [\psi(\phi)\ (\frac{3}{2}\,\underset{\sim}{\alpha}:\underset{\sim}{\alpha})^{1/2} - b_1(b_2\kappa)^{b_3}] \tag{98}$$

where ϕ $(0 \leq \phi \leq 1)$ represents the additional hardening due to nonproportional loading. Proposed forms of ϕ are

$$\dot{\phi} = \mu^*(1 - \left| \frac{\frac{d}{dt}(\varepsilon_1 - \varepsilon_3)}{(\dot{\underset{\sim}{\varepsilon}})_1 - (\dot{\underset{\sim}{\varepsilon}})_3} \right| - \phi)(\dot{\underset{\sim}{\varepsilon}}^{n}:\dot{\underset{\sim}{\varepsilon}}^{n})^{1/2} \tag{99}$$

due to McDowell [23-24] (ε_1, ε_3 are maximum and minimum principal strains), or

$$\phi = \frac{\dot{\underset{\sim}{\sigma}}'}{\|\dot{\underset{\sim}{\alpha}}'\|} : \frac{\underset{\sim}{\alpha}}{\|\underset{\sim}{\alpha}\|} \tag{100}$$

due to Bodner et al. [25]. It is felt that a history dependent measure of ϕ such as equation (99) is more mechanistically desirable, and fits the data better for cyclic loading. An alternative definition for ϕ might be the quotient of the inelastic strain path projection on the maximum inelastic strain direction with the total inelastic strain path length.

In the deformation is creep-dominated, the work of Oytana et al. [7] indicates that the hardening is primarily kinematic, i.e. backstress

evolution. With the backstress, primary, secondary and anelastic creep strains may be represented by the unified constitutive equations. Ohashi and associates [8], working with type 304 stainless steel, have shown that simple time or strain-hardening theory cannot predict transient softening observed in creep after stress reversals or nonproportional stress field rotations. Furthermore, the modified strain-hardening theory of ORNL is not suitable for nonproportional loading. Pure kinematic hardening theory gives excessive creep strain rate after large rotations of the principal stresses. They found that combined isotropic-kinematic theory (unified theory) incorrectly predicted a cycle-by-cycle decrease in amplitude of creep strain during nonproportional stress reverals. This suggests that the component of isotropic hardening should be weak compared to kinematic hardening in concurrence with the conclusions of Oytana et al. One troubling point in Ohashi's work is the use of a constant apportionment factor between isotropic and kinematic hardening (evidently 1/2), not included in most unified theories; this seems to artifically restrict the kinematic hardening. Regardless, it is clear that prediction of creep strain rate after relatively large, nonproportional stress reversals requires quite accurate constitutive laws more refined than of simple or modified strain-hardening type.

Cho and Findley [49-50] have shown the strong influence of aging at temperature on the subsequent creep deformation of type 304 stainless steel at 593^{o}C (ORNL reference heat 9T2796). They include aging through power-law dependence of plastic, viscoelastic, and viscous strains on aging time. The same sort of manipulation could be accomplished by a power-law dependence of inelastic strain rate on aging time in the unified theories. These aging effects must be represented as Heaviside functions in rate-type constitutive laws and are therefore somewhat difficult to formulate [51]. In principle,

aging effects are not seen to be strongly related to the formulation of anisotropic damage and deformation constitutive laws and will not be considered at the present time. The nonproportional test program in this study does not investigate these effects, with the exception of aging which may occur continuously during the tests.

As mentioned earlier, experimental evidence suggests that the creep strain rate equations is relatively insensitive to damage anisotropy until tertiary creep. It follows that directional internal stresses and isotropic hardening in the matrix should develop with weak dependence on anisotropy of damage through the secondary creep stage. There seems to be two alternative methods to achieve this weak dependence. First the components of the damage tensor can remain small until the onset of tertiary creep. In this case, following a Kachanov-Rabotnov approach as in equation (6) (e.g. Chaboche),

$$\dot{\underset{\sim}{\varepsilon}}^{c} = \underset{\sim}{F}\,(\underset{\sim}{\phi}\colon \underset{\sim}{\phi},\ \kappa,\ \underset{\sim}{\bar{S}}' - \underset{\sim}{\bar{\alpha}},\ T) \tag{101}$$

where $\underset{\sim}{\phi} = (\underset{\sim}{I}-\underset{\sim}{D})^{-1}$ as in the Murakami-Ohno approach, and $\underset{\sim}{\bar{S}}'$ and $\underset{\sim}{\bar{\alpha}}$ are the deviatoric modified net stress and backstress tensors. Such an expression would account for continuity of creep strain rate with respect to damage if damage is isotropic, or anisotropy of creep strain rate (reflected through net stress $\underset{\sim}{\bar{S}}' - \underset{\sim}{\bar{\alpha}}$) if damage is anisotropic or mixed. These results are compatible with the experimental findings of Trampczynski and Hayhurst [4] for copper, aluminum, and Nimonic 80A.

The other method to include damage in the inelastic strain rate is provide isotropic dependence on the first invariant of damage. This approach, stated in equations (54) - (58) for strain-hardening theory, seems adequate up to the tertiary creep stage since the cavity volume fraction is low for most

metals up to this stage, and anisotropy in the primary creep deformation subsequent to stress reversals can be accounted for through backstress in the unified theories [25-30]. Of course, the transition from secondary to tertiary creep is accompanied by an attendant increase in dependence of the inelastic strain rate on damage anisotropy.

Based on the current experimental evidence and state-of-the-art, a suggested initial form of the unified equations with inclusion of anisotropic damage is

$$\dot{\underset{\sim}{\varepsilon}}^{n} = f\left\{ \frac{3\bar{\bar{J}}_2'}{\kappa^2} \right\} \left(\bar{\bar{\underset{\sim}{S}}}' - \bar{\bar{\underset{\sim}{\alpha}}} \right) \tag{102}$$

$$\dot{\bar{\bar{\underset{\sim}{\alpha}}}} = h_\alpha \dot{\underset{\sim}{\varepsilon}}^{n} - d(\bar{\bar{\underset{\sim}{\alpha}}}, T)\dot{\bar{\varepsilon}}^{n}\bar{\bar{\underset{\sim}{\alpha}}} - r_\alpha(\bar{\bar{\underset{\sim}{\alpha}}}, T)\bar{\bar{\underset{\sim}{\alpha}}} \tag{103}$$

$$\dot{\kappa} = h_\kappa \dot{\bar{\varepsilon}}^{n} - r_\kappa(\kappa, T) \tag{104}$$

where $$\bar{\bar{\underset{\sim}{S}}} = \gamma(D_{kk})(1 + C_1 D_{kk})\underset{\sim}{\sigma} + (1 - \gamma(D_{kk}))\underset{\sim}{S} \tag{105}$$

and $\bar{\bar{\underset{\sim}{\alpha}}}$ is similarly defined. The function $\gamma(D_{kk})$ introduces a smooth transition from isotropic dependence on damage ($\gamma(D_{kk}) = 1$) to complete anisotropic dependence on net stress $\underset{\sim}{S}$ ($\gamma(D_{kk}) = 0$) which is highly dependent on the tensorial character of damage. It is anticipated that $\gamma(D_{kk}) \cong 1$ based on previous results, at least if the cavity volume fraction at rupture is relatively low. Otherwise, results of Murakami [19] indicate that a power-law dependence on D_{kk} may be appropriate.

In equation (102), $\bar{\bar{\underset{\sim}{S}}}'$ is the deviatoric modified net section stress, and

$$\bar{\bar{J}}_2' = \frac{1}{2}\left(\bar{\bar{\underset{\sim}{S}}}' - \bar{\bar{\underset{\sim}{\alpha}}}\right) : \left(\bar{\bar{\underset{\sim}{S}}}' - \bar{\bar{\underset{\sim}{\alpha}}}\right)$$

CORRELATION WITH EXPERIMENTS

The motivation for the suggested anisotropic damage formulation was presented earlier. Here, the full equations will again be presented and appropriate simplifications will be introduced for purposes of demonstration and correlation with experiments completed to date at ORNL.

The proposed general framework for the isothermal coupled damage and creep strain rate equations is:

Damage Rate Equation:

$$\dot{\underset{\sim}{D}} = B\left[\sigma^*(\underset{\sim}{S})\right]^k \left[\eta \underset{\sim}{I}\left(\underset{\sim}{\phi}:\underset{\sim}{\phi}\right)^{\ell/2} + (1 - \eta) \sum_{j=1}^{3} \underset{\sim}{\nu}^{(j)} \otimes \underset{\sim}{\nu}^{(j)} M\left(\underset{\sim}{\nu}^{(j)}, \underset{\sim}{\phi}\right)\right], \tag{106}$$

where η, B, k, and ℓ are material constants, and

$$M(\underset{\sim}{\nu}^{(j)}, \underset{\sim}{\phi}) = (\underset{\sim}{\phi}:\underset{\sim}{\phi})^{\ell/2} M_j^*(\sigma_j)$$

or

$$M\left(\underset{\sim}{\nu}^{(j)}, \underset{\sim}{\phi}\right) = \left[\frac{1}{1 - \underset{\sim}{\nu}^{(j)} \cdot \underset{\sim}{D} \cdot \underset{\sim}{\nu}^{(j)}}\right]^{\ell} M_j^*\left(\sigma_j\right)$$

where $M_j^*(\sigma_j)$ admits anisotropic contribution of non-maximal principal net stresses, and $\sigma^*(\underset{\sim}{S})$ is the isochronous stress given by

$$\overset{*}{\sigma}(\underset{\sim}{S}) = \frac{3}{2} H_1 \left(\frac{2}{3} \frac{S_{eq}}{H_1}\right)^a \exp\left[b\left[\frac{S_{kk}}{S_s} - 1\right]\right] \tag{107}$$

due to Huddleston [16], where

$S_{eq} = ((3/2)\underset{\sim}{S}':\underset{\sim}{S}')^{1/2}$

$H_1 = S_1 - S_{kk}/3$

$\underset{\sim}{S}' = \underset{\sim}{S} - (1/3)S_{kk}\underset{\sim}{I}$

$S_s = (S_1^2 + S_2^2 + S_3^2)^{1/2}$

$\underset{\sim}{S}$ = net stress tensor = $(1/2)(\underset{\sim}{\sigma}\cdot\underset{\sim}{\phi} + \underset{\sim}{\phi}\cdot\underset{\sim}{\sigma})$

$\underset{\sim}{\phi} = (\underset{\sim}{I} - \underset{\sim}{D})^{-1}$

$\underset{\sim}{D}$ = 2^{nd} order damage tensor

$\underset{\sim}{\nu}^{(j)}$ = unit vector in principal net stress direction, S_j

and a and b are material constants. $\underset{\sim}{\sigma}$ is the Cauchy stress.

Rupture Criterion:

Possible rupture criteria include

$$D_j = D_{cr} \text{ for } j = 1, 2, \text{ or } 3 \tag{108}$$

where D_j are the principal values of $\underset{\sim}{D}$, and D_{cr} is a critical damage level, or

$$R(\sigma_{max}, D_{kk}, n_i^* D_{ij} n_j^*) = 0 \tag{109}$$

where $\sigma_{max} = n_i^* \sigma_{ij} n_j^*$ is the component of stress in the maximum principal stress direction, $\underset{\sim}{n}^*$. Here, a critical combination of maximum principal

stress, total void or cavity fraction, and void density on grain boundaries normal to the maximum principal stress dictates rupture. Leckie has also proposed the criterion

$$\max_{\text{all } \bar{n}} \left(\bar{n}_i D_{ij} \bar{n}_j \cdot \bar{n}_k \bar{\sigma}_{kl} \bar{n}_l\right) = \text{constant} \tag{110}$$

where $\underset{\sim}{\bar{n}}$ is an arbitrary unit vector.

Coupled Creep Strain Rate Equation:

Suggested coupling with a rate-dependent unified creep plasticity theory is given by:

$$\dot{\underset{\sim}{\epsilon}}^{n} = f(\|\underset{\sim}{\bar{S}}' - \underset{\sim}{\bar{\alpha}}\|/\kappa)(\underset{\sim}{\bar{S}} - \underset{\sim}{\bar{\alpha}}) \tag{111}$$

$$\dot{\underset{\sim}{\bar{\alpha}}} = h_{\alpha}(\dot{\underset{\sim}{\epsilon}}^{n} : \underset{\sim}{\bar{\nu}})\underset{\sim}{\bar{\nu}} - r_{\alpha}\underset{\sim}{\bar{\alpha}} \tag{112}$$

$$\dot{\kappa} = h_{\kappa}\dot{\bar{\epsilon}}^{n} - r_{\kappa} \tag{113}$$

where $\underset{\sim}{\bar{\nu}}$ is a selected directional index, and

$$\underset{\sim}{\bar{S}} = f_1(D_{kk})\underset{\sim}{\sigma} + f_2(D_{kk})\underset{\sim}{S} \tag{114}$$

$$\underset{\sim}{\bar{\alpha}} = f_1(D_{kk})\underset{\sim}{\alpha} + f_2(D_{kk})\underset{\sim}{\bar{\alpha}} \tag{115}$$

$$\underset{\sim}{\bar{\alpha}} = (1/2)(\underset{\sim}{\alpha}\cdot\underset{\sim}{\phi} + \underset{\sim}{\phi}\cdot\underset{\sim}{\alpha}) \tag{116}$$

$$\underset{\sim}{\bar{S}}' = \underset{\sim}{\bar{S}} - (1/3)\bar{S}_{kk}\underset{\sim}{I} \tag{117}$$

Here, h_α, h_κ and r_α, r_κ are hardening and recovery functions, respectively. It is important to note that the strain rate is assumed to depend on the first invariant of damage in keeping with the findings of Leckie et al. [20] and Murakami et al. [9].

Application to Type 304 Stainless Steel at 593°C

The proposed theory in equations (106)-(117) is quite general in applicability. There exists various levels of complexity or sophistication at which one can choose to apply this theory. Compatible with the goals of the first year of this program, the equations were simplified to a form involving engineering stress in the isochronous stress equation, a simple multiaxial creep strain rate equation, and a simple rupture criterion. Lack of a sufficiently exhaustive base of multiaxial rupture tests warrants this level of sophistication. Actually, the limiting assumptions made in this section are also those made by other investigators of the creep continuum damage approach and should not be viewed as unusually restrictive. Future research in this program should increase the model accuracy and sophistication.

Briefly, the pertinent equations are:

$$\dot{\underset{\sim}{D}} = B[\sigma^*(\underset{\sim}{\sigma}^{pk})]^k(\underset{\sim}{\phi}:\underset{\sim}{\phi})^{\ell/2}[\eta \underset{\sim}{I} + (1-\eta)\sum_{k=1}^{3} \underset{\sim}{\nu}^{(k)} \otimes \underset{\sim}{\nu}^{(k)} M^{(k)}] \qquad (118)$$

where

$$M^{(k)} = \langle \underset{\sim}{\nu}^{(k)} \cdot \frac{\underset{\sim}{\sigma}^{pk}}{\sigma_1} \cdot \underset{\sim}{\nu}^{(k)} \rangle$$

and $\langle F \rangle = F$ if $F \geq 0$; $\langle F \rangle = 0$ if $F < 0$. $\underset{\sim}{\sigma}^{pk}$ is the 2nd Piola-Kirchoff stress tensor. For purposes of brevity, it will be understood that $\underset{\sim}{\sigma}$ will be taken to represent $\underset{\sim}{\sigma}^{pk}$ in all that follows.

The isochronous stress is defined by

$$\sigma^* = \frac{3}{2} S_1 \left(\frac{2}{3} \frac{\bar{\sigma}}{S_1}\right)^a \exp\left[b\left(\frac{J_1}{S_s} - 1\right)\right] \tag{119}$$

where

$$J_1 = \sigma_1 + \sigma_2 + \sigma_3$$

$$\bar{\sigma} = [\{(\sigma_1 - \sigma_2)^2 + (\sigma_2 - \sigma_3)^2 + (\sigma_1 - \sigma_3)^2\}/2]^{1/2}$$

$$S_1 = \sigma_1 - J_1/3$$

$$S_s = (\sigma_1^2 + \sigma_2^2 + \sigma_3^2)^{1/2}$$

and B, k, ℓ, a and b are material constants. Note that only positive principal stresses are permitted to contribute to damage evolution. Also,

$\underset{\sim}{\nu}^{(k)}$ = unit vector in k^{th} principal stress direction

$\underset{\sim}{\phi} = (\underset{\sim}{I} - \underset{\sim}{D})^{-1}$

η = isotropic damage weighting factor $(0 \leq \eta \leq 1)$

A simple form of the creep strain rate equation was used to obtain an estimate of the evolution of in-plane creep strain components in the axial-torsional tests. State variables $\underset{\sim}{\alpha}$ and κ (e.g. backstress and dragstress) were not included due to lack of characterization of the hardening and recovery functions; the initial scope of this investigation does not require their inclusion. Prediction of creep strain accumulation for alternating nonproportional loading would, in general, require their inclusion to reflect deformation-induced anisotropy effects.

Also, compatible with the goals of the initial analysis, predictions and results are compared on the basis of nominal or engineering strain. The further assumption is made that creep strain rate is coupled to damage through the first invariant of damage only, i.e.

$$\overset{\bullet}{\underset{\sim}{e}}^{n} = \frac{3}{2}\left[\frac{\bar{\sigma}}{A}\right]^{n}\frac{\underset{\sim}{\sigma}'}{\bar{\sigma}}\left[1+\left[cD_{kk}\right]^{m}\right] \tag{120}$$

where c and m are constants determined by fitting the secondary and tertiary creep regimes of a uniaxial creep test at fixed stress.

Determination of Material Constants

All material constants were determined from uniaxial creep tests found in the literature and by examination of ruptured uniaxial specimens. Constants a and b were given by Huddleston [16] for type 304 stainless steel at 593°C as

$$a = 1.086 \qquad b = 0.289$$

The exponent n was determined from uniaxial creep tests on annealed specimens as seen in Figure 1.

$$n = 10.74 \tag{121}$$

From the same tests,

$$A = 60.0 \tag{122}$$

where units of stress are ksi and strain rate in hr^{-1}.

Integrating equations (118) for a uniaxial constant load creep test with axial stress σ_{11} leads to a rupture time t_R of

$$t_R = \frac{1}{B(\sigma^*)^k} \int_0^{D_c} \left[\left[\frac{1}{1-D_{11}} \right]^2 + 2 \left[\frac{1}{1-\eta D_{11}} \right]^2 \right]^{-\ell/2} dD_{11} \qquad (123)$$

where D_{11} is the damage component in the axial direction.

If D_{11} = critical value = D_{cr} at rupture, then rupture time depends explicitly on stress level and equation (123) can be expressed as

$$\log t_R = A_1 - k \log \sigma_{11} \qquad (124)$$

where A_1 is a constant. From Huddleston's data for uniaxial tests [16], k = 8.5551.

From analysis of the damaged microstructure of two uniaxial creep specimens (to be discussed later), an average value of $\eta = 0.61$ was selected as representative of the degree of anisotropy of damage since wedge cracking is the dominant failure mode at the temperature and stress levels of this study. Precise determination of the nonlinearity of damage evolution, reflected by the exponent ℓ, requires the interruption of tests at various points in the creep history along with sectioning and examination. Since interrupted test specimens are not available at this time, it was thought that values of B and ℓ should be selected in the range typical of other stainless steels reported in the literature [13-14]. Hence,

$$B = 1.539 \times 10^{-17}$$

$$\ell = 4.80$$

As will be discussed shortly, the values for B and ℓ were adjusted in an iteration process which involved fitting the tertiary portion of a uniaxial engineering creep strain curve.

In order to determine the coupling of strain rate with damage, a uniaxial creep curve shown in Figure 2 was digitized and a computer program was written to integrate the coupled equations (120) and (123) for the uniaxial case, i.e.

$$\dot{D}_{11} = B\left(\sigma^*\right)^k \left[\left[\frac{1}{1-D_{11}}\right]^2 + 2\left[\frac{1}{1-\eta D_{11}}\right]^2\right]^{\ell/2} \tag{125}$$

$$\dot{e}^n_{11} = \left[\frac{\sigma_{11}}{A}\right]^n \left[1 + \left[cD_{kk}\right]^m\right] \tag{126}$$

A flowchart of the computer program used to fit the uniaxial creep curve appears in Figure 3. In the first iterative loop, constants B and ℓ are adjusted until the value of the axial damage component D_{11} at rupture is approximately unity. Then, the values of c and m in equation (126) are determined iteratively by plotting the resulting predicted tertiary creep response as an overlay on the digitized experimental data. The values of B and ℓ can be adjusted slightly to best match the tertiary region, with the stipulation that the axial damage component at rupture should essentially be unity. It is important to realize that the area fraction of damaged grain boundaries at rupture perpendicular to the loading axis in a uniaxial creep test is usually significantly less than one [43], but the current formulation does not require that the area fraction be identically equal to the damage parameter. It is required, however, that the predicted damage components are of the same ratio as those experimentally determined. For the purpose of comparing tests conducted at the same isochronous stress level, specifying

that $D_{11} = 1$ at rupture is sufficient. For variable stress histories, though, one would like to employ the full capability of the model by relating area fractions identically to components of damage.

A plot of the predicted versus experimental creep curve for the values of the "best-fit" parameters is shown in Figure 4. Note that c = 1.35 and m = 2.25 provided the most accurate fit of the creep response for the assumed values of B and ℓ. It must again be emphasized that a more rigorous determination of B and ℓ would require interrupted testing; however, the stress-independent rupture criterion and damage-independent isochronous stress of this initial formulation should provide rupture times consistent with the isochronous stress concept regardless of the B and ℓ values for constant load, proportionally loaded creep tests. Accurate values of B and ℓ are particularly important for step stress tests or for nonproportional loading.

The rupture criterion employed in this demonstration was

$$\underset{\sim}{\nu}^{(i)} \cdot \underset{\sim}{D} \cdot \underset{\sim}{\nu}^{(i)} = 1 \tag{127}$$

where i = 1, 2, 3. This is equivalent to the criterion stated in equation (108) with $D_{cr} = 1$. Though the area fraction of grain boundaries in the continuum sense in any direction is generally not unity at rupture, the high nonlinearity of terms involving damage in the damage rate equation results in very little difference in predicted rupture time for critical maximum principal damage values between about 0.5 and 1.

Microstructural Damage Evaluation

In order to determine the appropriate value of η for type 304 stainless steel at 593°C and to compare analytical predictions with observed physical damage, biaxial creep specimens were sectioned, polished, and etched. Then,

micrographs were taken at various locations to obtain a sample distribution rather than a single micrograph. Since the rupture surface is viewed primarily as a fracture phenomenon resulting from linkage of voids and wedge cracks into an unstably propagating crack, all samples were taken from points away from the rupture crack but still in the zone of uniform temperature and deformation. A discolored region was observed in the middle third of the 2.43 inch gage section, evidently associated with localization of deformation; all micrographs were taken in this region.

Since both wedge cracking and cavitation contribute to grain boundary damage, it was initially desired to include both in constructing the damage tensor from micrographs. Due to the different nature of each type of damage, however, the wedge cracking and cavitation components of the damage tensor were initially computed separately, i.e.

$$\underset{\sim}{D}_{exp} = \underset{\sim}{D}_{w} + \underset{\sim}{D}_{c} \tag{128}$$

where $\underset{\sim}{D}_{exp}$ represents the total damage tensor measured experimentally. In general, the cavitation damage is more difficult to quantify than the wedge cracking. Lack of resolution in the micrographs, even at 1000X, made it difficult to assign an area fraction value quantitatively to a cavitated grain boundary. Also, grain boundary carbides were so prevalent that small cavities were indiscernable. Furthermore, due to the relatively large deformations encountered at rupture in type 304 stainless steel, cavities are smeared due to grain boundary sliding and elongation. This elongation of grains in the primary stretch direction also created a preferred orientation for grain boundary segments which skewed the calculation of the cavitation damage tensor from micrographs, since cavitation was observed almost uniformly on all grain boundaries. In contrast, wedge cracking was much more readily quantifiable.

The argument can be made, of course, that the damage tensor should only be computed based on grain boundary microcracks, since they represent coalesced voids in addition to triple point cracks.

It is desirable to obtain a representative sample of grains for quantitative damage measurement to ensure reliable results. To include a sufficient sample size of grain boundaries, a magnification of 200X was used for determining the wedge crack or microcrack damage tensor. A magnification of 1000X was used to determine the cavitation damage tensor to improve the resolution of grain boundaries. As previously mentioned, determination of the cavitation damage tensor was frought with problems; perhaps the most serious reservation is that the cavitation observed or measured in the ruptured specimen is not representative of the evolution of cavitation and eventual linkage of cavities due to the smearing effects. It is our current thinking that quantification of the wedge cracking will most successfully describe the rupture state and its link to damage history, as mentioned above.

Sections were taken at two locations each at the inside and outside specimen diameters. At each section, five different locations were photographed to provide a suitable sample lot. For the uniaxial specimens, the damage was evaluated at the specimen centerline at five locations. Typical micrographs for the wedge crack and cavity distributions appear in Figure 5 for biaxial Specimen GT-1, a proportionally loaded specimen. It is interesting to note that a radial gradient of damage is clearly observed in micrographs of the entire specimen wall with a heavier distribution of wedge cracking at the specimen outer diameter. This effect is possibly due in part to the higher shear strain accumulated at the outer diameter than at the inner. Figure 6 illustrates the radial damage gradient.

Computer programs were written for a Weiss Videoplan (available in Dr. Underwood's quantitative metallography laboratory) to allow the user to

move the cursor along grain boundaries and to mark wedge cracks or cavitated segments. The results were immediately digitized on floppy disk. Post-processing programs were written to convert the raw data in the wedge crack or cavity files to print to any output file the grain boundary segment length, fraction wedge cracked or cavitated, and the normal vector to the segment. All grain boundary segments in a given micrograph were digitized, regardless of whether or not any damage was present. Hence, total grain boundary length for each micrograph is available.

The processed data files were stored on floppy disks formatted with MSDOS. BASIC computer programs were written to perform the computation of wedge crack and cavitation damage tensors on an IBM PC based on the numerical integration implied by the equations

$$\underset{\sim}{D}_w \doteq \frac{1}{L_T} \sum_{k=1}^{N} \underset{\sim}{n}^{(k)} \otimes \underset{\sim}{n}^{(k)} \Delta S_{gw}^{(k)} \tag{129}$$

$$\underset{\sim}{D}_c \doteq \frac{1}{L_T} \sum_{k=1}^{M} \underset{\sim}{n}^{(k)} \otimes \underset{\sim}{n}^{(k)} \Delta S_{gc}^{(k)} \tag{130}$$

where L_T is the total grain boundary length in the micrograph $\underset{\sim}{n}^{(k)}$ is the unit normal vector to the k^{th} grain boundary segment, and $\Delta S_{gw}{}^{(k)}$ and $\Delta S_{gc}{}^{(k)}$ are, respectively, the length of the wedge crack or cavitated segment associated with the k^{th} grain boundary segment. Copies of the two computer programs written to compute the damage tensors appear in the APPENDIX.

Prediction of Damage Evolution and Comparisons with Data

In the present theoretical continuum damage approach, no distinction is made between cavitation damage or wedge crack damage. A computer program was

written to integrate the coupled equations (118)-(120). The numerical integration technique used was a Runge-Kutta with fixed time step size. This method was found to result in very efficient, accurate integration of unified creep-plasticity theory in an earlier study [46] for nonproportional cyclic loading. A flowchart of the computer program appears in Figure 7.

Since the damage evolution depends on η, it was necessary to establish a value of η from micrographs of uniaxial creep tests. Two specimens were provided by ORNL for this purpose. The value of η was based on quantification of wedge type damage only; this should not be too restrictive since this type of damage most likely dominates the rupture process in the stress and temperature regimes of the tests. Referring to equation (118) it is clear that the transverse damage D_{22} is related to the axial damage D_{11} by $D_{22} = \eta D_{11}$. Hence, η is the ratio of the transverse to axial components of damage in a uniaxial creep test. A value of $\eta = 0.61$ was determined as the average value of η computed from ten micrographs, five from each specimen. It should be noted that this value of η indicates that the isotropic component of the damage tensor is "larger" than the anisotropic component. Hence, we would not expect a change in loading direction at the same isochronous stress level to result in a factor of two difference in rupture life as in pure copper.

The computer program was written to allow any nominal stress history to be input. Output includes rupture time and plots of damage components D_{11} and D_{12} in addition to engineering strain components e_{11} and e_{12}.

It should be noted that the experimental values of e_{11} and e_{12} were computed using the equations

$$e_{11} = \delta L/L_o \tag{131}$$

$$e_{12} = \frac{1}{2}\,\bar{r}\delta\Psi/L_o \tag{132}$$

where L_o is the gage length, $\bar{r}$ is the average radius, and $\delta\Psi$ is the relative rotation of the gage section in radians. Obviously, engineering strain is not indicative of the true strains occurring at large deformations. It is not entirely unreasonable, though, to compare the engineering strains predicted by the model with those obtained experimentally; the difference between true strains and nominal strains in the experiments of this study are less than ten percent.

Discussion of Results

The biaxial loading histories of Specimens GT-1,2,3,4 appear in Figure 8. The applied axial and shear stresses plotted in theses histories are nominal values, i.e. based on initial dimensions. The shear stress (moment) was applied at the bottom of each specimen in either a clockwise or counter-clockwise sense viewing down the specimen longitudinal axis. It should be noted that the isochronous stress for Specimens GT-1,2,3 is constant (based on nominal stresses) at $\sigma^*(\underset{\sim}{\sigma}^{pk})$ = 25.54 ksi. Hence, differences in rupture time should be attributable to nonproportionality of loading, neglecting the possibility of reversal of plastic strain. Specimens GT-1 and GT-2 were subjected to identical loading histories apart from the sign of shear stress. The loading history of Specimen GT-3 involved a reversal in sign of the shear stress at 456 hours.

Predicted and experimental results for the biaxial loading histories appear in Table 1. Note that a counter-clockwise applied moment corresponds to a positive shear stress in the X_1,X_2 coordinate system shown in Table 1. The predicted damage and creep strain components correspond to the time step immediately preceding satisfaction of the rupture criterion in equation (108) with D_{cr} = 1. It is observed in Table 1 that a rupture time of 1020 hours is predicted for Specimens GT-1 and GT-2; the actual values are 892 hours and

1173 hours, respectively. Good estimates of rupture time and accumulated creep strain components are achieved by the model, including the tertiary regime. Note that the actual creep strain components in Table 1 include only secondary and tertiary components as measured from plots of gage length extension and angle of twist versus time.

Plots of predicted damage and strain rate evolution appear in Figures 9-10 for Specimens GT-1 and GT-2. For reference, plots of relative angle of twist and gage length elongation versus time appear in Figures 11-12. Note the excellent agreement of the onset of tertiary creep and magnitude of creep strain at rupture between theory and experiment. Also note that the slope of the predicted creep strain rate is not infinite at rupture, which is confirmed by the experiments. The actual grain boundary microcrack damage at rupture is significantly less than unity for Specimens GT-1 and GT-2, with an average maximum principal damage of $D_1 = 0.28$. It is quite interesting to note that this value is very close to the rupture criterion used by Ashby et al. [43], i.e. $f_h = 0.25$ $(=D_1)$. This result provides confirmation that the rupture event is a process of unstable linkage and propagation of grain boundary cracks after a critical level of grain boundary damage is reached. It is important to note that the rupture criterion used in these calculations, $D_j = D_{cr} = 1$, may be replaced by any other, more realistic, criterion such as $D_{cr} = 0.25$ or equation (109), provided that the coupling constants c and m in the creep strain rate equation are determined in conjunction with this criterion.

It is concluded that the second rank damage tensor approach of this study offers an improvement on prior isotropic damage models with regard to assigning magnitude and direction of creep damage for proportional loading. Note in Table 1 that the average orientation of the measured maximum principal damage values (among 42 digitized micrographs) were in relatively good agreement with the maximum principal stress directions. The relatively large standard

deviations for the principal values of damage and orientation, given in Table 2, are reflective of the heterogeneity of damage and the relatively large isotropic components. A highly anisotropically damaging material would obviously display less scatter.

The purpose of experiments GT-3 and GT-4 was to evaluate the capability of the second order tensor damage model to predict direction and magnitude of accumulated creep damage in addition to rupture time for nonproportional loading histories. As seen in Figure 13, Specimen GT-3 was subjected first to a counter-clockwise shear stress and an axial stress at the same isochronous stress level as Specimens GT-1 and GT-2; after 456 hours, however, the shear stress was reversed while maintaining the same isochronous stress level. A maximum principal stress rotation of 34° resulted from this shear stress reversal. Evolution of damage components and creep strain components are shown in Figure 14. The measured gage length extension and relative angle of twist versus time is shown in Figure 15 for comparison.

It is noted first that the predicted rupture time of 1030 hours listed in Table 1 is significantly lower than the observed 1398 hours. Also, the measured orientation of maximum principal damage is 13° from the predicted orientation. This result indicates that the actual rotation of the damage tensor was not as great as that predicted by the theory. Also, note that the magnitude of damage at rupture is less than in proportionally loaded Specimens GT-1 and GT-2. There are several likely reasons for these discrepancies.

Firstly, it is noted that there is a significantly higher creep shear strain observed experimentally than would be predicted using a simple deviatoric flow rule. This can be attributed to creep-plasticity interaction. In particular, memory of plastic deformation incurred in the initial loading direction was retained upon reversal of applied shear stress. Hence, power law creep does not occur radially after load reversal, but with respect to a

backstress imposed by the initial loading and slightly altered by plasticity during the shear stress reversal. Another consequence of this memory of the initial loading direction is that secondary creep rate is reduced (by ~10%) after reversal of shear stress. A simple creep strain rate equation without backstress cannot reflect this memory. Since grain boundary damage in these particular experiments is driven by matrix power law creep, the isochronous stress dependence of the coefficient in the damage rate equation implies a unique relationship between applied stress and time to rupture. It is felt that dependence on isochronous overstress $(\sigma - \alpha)^*$ may be more appropriate for the damage rate equation under power law creep conditions. In this case $(\sigma - \alpha)^*$ is based on the backstress from an appropriate unified creep-plasticity constitutive law (e.g. equations (111) - (113)) and is computed in identical fashion to σ^*. This modification would more appropriately reflect the driving force for creep damage growth.

Secondly, regarding the measured damage distribution, it is noted that the maximum principal value of damage is nearly collinear with the specimen longitudinal axis. This is quite possibly an artifact of the assumed second order tensor distribution of damage. For proportional loading, a second order tensor distribution for the anisotropic component of damage appears appropriate as evidenced by the correlations achieved for Specimens GT-1 and GT-2. However, a second rank damage tensor simply rotates its three eigenvectors in response to change in principal stress orientations. This rotation amounts to an "averaging effect" on the damage distribution. As pointed out by the work of Leckie and Onat (equations (29)-(43)), it may be necessary to represent the anisotropic component of the damage distribution by higher, even-ordered tensors. For example, Specimen GT-3 may require a fourth order distribution to properly model the physical damage incurred by the two loading directions. The required distribution must be determined by further examination of the

wedge crack damage without the constraint of a second order damage tensor assumption. It is fully intended to pursue this determination.

Thirdly, the experimental result that the effective damage at rupture in nonproportionally loaded Specimen GT-3 is less than that for the proportionally loaded Specimens GT-1 and GT-2 is of concern. There is, of course, the question of statistical significance of this single result which tempers any mechanistic interpretation. However, this result possibly reflects influence of the first invariant of damage (or mean value of damage) on the rupture event since it is likely a higher fraction of the maximum value of damage in a nonproportional test than in a proportional test. This assertion can also be evaluated by considering the higher order damage distribution in the plane of the specimen. Such an evaluation will be pursued.

As seen in Figure 16, Specimen GT-4 was subjected to a relatively complex loading history. The experiment was originally intended to be a repeat of GT-3, but experimental difficulties related to an initial zero offset of torque of approximately 44% of the intended torque resulted in an initial overload which was later realized and corrected to produce an appropriate rupture time.

The problems involving creep-plasticity interaction and assumption of a second order anisotropic damage distribution are exacerbated by the nature of this history. Conclusions of model performance are somewhat difficult to draw regarding damage at rupture and creep strain at rupture due to the variable isochronous stress loading history and greater number (four) of principal stress orientations. It may be concluded, however, that the model refinements suggested by history GT-3 are also germane in this case. In particular, the inelastic strain rate equation should be modified to include backstress, the isochronous stress should be referenced to backstress, and the physical damage distribution should be studied to evaluate the necessity of a higher order

damage distribution. It is the author's judgment that these refinements will provide much more accurate modeling of both of histories GT-3 and GT-4.

There is a noteworthy aspect of GT-4 which deserves comment. The initial overload resulted in a model prediction of a rupture time of 440 hours, significantly shorter than the observed 1230 hours. This discrepancy is not attributable to the anisotropic form of the damage model, but to the dependence of rupture time on isochronous stress since the loading is proportional. The value of k has been properly determined from uniaxial rupture tests. However, the values of B and ℓ have been assumed and require further determination from experiments. To see that B and ℓ can influence rupture time, a function of stress, it is necessary only to express the integrated damage model at rupture, assuming D=constant at rupture and uniaxial loading, as:

$$\log t_R = \log \frac{1}{B} \int_0^{D_c} \left[\left(\frac{1}{1-D_{11}} \right)^2 + 2 \left(\frac{1}{1-\eta D_{11}} \right)^2 \right]^{-\ell/2} dD_{11} - k \log \sigma \qquad (133)$$

Hence, having selected ℓ, B is constrained by this equation. Such a constraint was not, however, imposed on B in the first year of this work (although the values used are relatively close to the constrained values) since all experiments were to be conducted at the same isochronous stress level. By imposing the constraint, rupture would probably not be predicted until approximately 1100 hours which agrees more readily with the experiment.

In summary, history GT-4 has emphasized the refinements necessary in the creep strain rate equation, the order of the anisotropic damage representation, and determination of B and ℓ values.

One additional result of the experimental program regards the analysis of the two uniaxial specimens mentioned earlier. It is quite interesting to note

that the angle θ determined for wedge cracking in the uniaxial case is only - 8.3°, indicating that that maximum principal damage value is more nearly collinear with the loading axis than for the proportionally loaded biaxial Specimen GT-1. Since only two uniaxial specimens were sectioned and examined, it is likely that the angle of 8.3° is not of high confidence level. Accuracy of the angle is more highly dependent on sample size than is accuracy of η since orientation is particularly important for calculation of the shear component of damage.

Discussion of Practical Implementation of Simple Second Order Tensor Approach

In this section, matrix forms of the damage rate equations will be written for those more familiar with matrix structural analysis. In the full nine dimensional damage space, we may write equation (106) as

$$\begin{bmatrix} \dot{D}_{11} & \dot{D}_{12} & \dot{D}_{13} \\ & \dot{D}_{22} & \dot{D}_{23} \\ \text{sym} & & \dot{D}_{33} \end{bmatrix} = B[\sigma^*(\underset{\sim}{\sigma})]^{k_\Psi \ell/2} \left\{ \eta \begin{bmatrix} 1 & 0 & 0 \\ 0 & 1 & 0 \\ 0 & 0 & 1 \end{bmatrix} + \right.$$

$$\left. \sum_{k=1}^{3} (1 - \eta) \begin{bmatrix} [\nu_1^{(k)} \ \nu_1^{(k)}][\nu_1^{(k)} \ \nu_2^{(k)}][\nu_1^{(k)} \ \nu_3^{(k)}] \\ [\nu_2^{(k)} \ \nu_2^{(k)}][\nu_2^{(k)} \ \nu_3^{(k)}] \\ \text{sym} \quad [\nu_3^{(k)} \ \nu_3^{(k)}] \end{bmatrix} < \frac{[\nu_1^{(k)} \nu_2^{(k)} \nu_3^{(k)}]}{\sigma_1} \begin{bmatrix} \sigma_{11} & \sigma_{12} & \sigma_{13} \\ & \sigma_{22} & \sigma_{23} \\ \text{sym} & & \sigma_{33} \end{bmatrix} \right\} \quad x$$

$$\left\{ \begin{Bmatrix} \nu_1^{(k)} \\ \nu_2^{(k)} \\ \nu_3^{(k)} \end{Bmatrix} > \right\} \tag{134}$$

where $\nu_i^{(k)}$ are the i^{th} components of the unit vector in the direction of the k^{th} principal stress (k^{th} eigenvector), $\underset{\sim}{\sigma}$ is the engineering stress, and

$$\Psi = (\underset{\sim}{\phi}:\underset{\sim}{\phi}) = \mathrm{tr}\{[\phi]^T[\phi]\} \tag{135}$$

$$\text{where } [\phi] = \begin{bmatrix} (1-D_{11}) & -D_{12} & -D_{13} \\ & (1-D_{22}) & -D_{23} \\ \text{sym} & & (1-D_{33}) \end{bmatrix}^{-1} \tag{136}$$

In equation (134), $\langle F\rangle = F$ if $F \geq 0$; $\langle F\rangle = 0$ if $F < 0$.

The simple deviatoric form of the creep strain rate may be written

$$\begin{bmatrix} \dot{\epsilon}_{11}^{c} & \dot{\epsilon}_{12}^{c} & \dot{\epsilon}_{13}^{c} \\ & \dot{\epsilon}_{22}^{c} & \dot{\epsilon}_{23}^{c} \\ \text{sym} & & \dot{\epsilon}_{33}^{c} \end{bmatrix} = \frac{3}{2}\left(\frac{\bar{\sigma}}{A}\right)^{n} \frac{\left[1+(c(D_{11}+D_{22}+D_{33}))^{m}\right]}{\bar{\sigma}} \quad * \tag{137}$$

$$\begin{bmatrix} \left(\sigma_{11} - \frac{1}{3}\sigma_{kk}\right) & \sigma_{12} & \sigma_{13} \\ & \left(\sigma_{22} - \frac{1}{3}\sigma_{kk}\right) & \sigma_{23} \\ \text{sym} & & \left(\sigma_{33} - \frac{1}{3}\sigma_{kk}\right) \end{bmatrix}$$

Determination of Constants B, k, ℓ, η, A, n, c, m:

Constants A and n may be determined from uniaxial tests at multiple levels since

$$\dot{\epsilon}^c = \left(\frac{\sigma_{11}}{A}\right)^n \tag{138}$$

in uniaxial secondary creep.

Exponent k may be identified as the magnitude of the slope of a log t_R versus log σ_{11} plot at the desired temperature obtained from uniaxial creep tests.

Isotropic damage weighting factor η may be determined from a uniaxial creep test by

$$\eta = \frac{D_{22}}{D_{11}} \tag{139}$$

where D_{11} is the longitudinal damage and D_{22} is the transverse damage. These damage components can be determined from micrographs as

$$D_{11} = \frac{1}{L_T} \sum_{k=1}^{N} n_1(k) n_1(k) \Delta S_g(k) \tag{140}$$

$$D_{22} = \frac{1}{L_T} \sum_{k=1}^{N} n_2^{(k)} n_2^{(k)} \Delta S_g^{(k)} \tag{141}$$

where $n_1^{(k)}$ and $n_2^{(k)}$ are the components of the unit vector normal to the k^{th} damaged grain boundary segment in the specimen longitudinal and transverse directions, respectively; L_T is the total grain boundary length and $\Delta S_g^{(k)}$ is the length of the k^{th} grain boundary micro-discontinuity (e.g. wedge crack, cavity, coalesced cavities).

Constants B and ℓ are properly determined from interrupted uniaxial tests in addition to ruptured specimens at the same stress level. Consider a test interrupted at a known (t/t_R) value; ℓ may be found by

$$\left[\frac{t}{t_R}\right] = \frac{\int_0^{D_t} \left[\left(\frac{1}{1-D_{11}}\right)^2 + 2\left(\frac{1}{1-\eta D_{11}}\right)^2\right]^{-\ell/2} dD_{11}}{\int_0^{D_c} \left[\left(\frac{1}{1-D_{11}}\right)^2 + 2\left(\frac{1}{1-\eta D_{11}}\right)^2\right]^{-\ell/2} dD_{11}} \tag{142}$$

where D_c is the measured longitudinal damage at rupture, D_t is the measured longitudinal damage at time t of interruption. All quantities in equation (142) are known except for ℓ. Then, having solved for ℓ, B can be determined, i.e.

$$B = \frac{1}{t_R \left(\sigma_{11}\right)^k} \int_0^{D_c} \left[\left(\frac{1}{1-D_{11}}\right)^2 + 2\left(\frac{1}{1-\eta D_{11}}\right)^2\right]^{-\ell/2} dD_{11} \tag{143}$$

Constants c and m can then be adjusted to fit the secondary-tertiary uniaxial response by simultaneous integration of the damage rate equation and creep strain rate equation.

It should be noted that the damage at rupture, D_c, is in general a function of stress level as expressed in equation (109). A reasonable choice for the rupture criterion is

$$\max_{\text{all } \underset{\sim}{n}} \left[(n_i D_{ij} n_j)^r (n_k \sigma_{k\ell} n_\ell) \right] = \text{constant} \tag{144}$$

which can be written for the uniaxial case as

$$\sigma_{11} D_c^{\ r} = \text{constant} \tag{145}$$

where r is a constant determined by measuring axial damage in uniaxial tests at multiple stress levels.

Comparison With Linear Time Fraction Rule:

The linear time fraction rule may be stated as

$$\sum_{j=1}^{M} \left[t_j / t_{R_j} \right] = 1 \tag{146}$$

Clearly, this rule implies that damage is isotropic. Rotation of the principal stresses, for example, at a constant isochronous stress results in a predicted rupture time from the linear rule equal to the uniaxial rupture time. The continuum damage rule will produce the same result only if $\eta = 1$. However, for $\eta < 1$ the predicted rupture time increases nonlinearly in the continuum damage approach during rotation of principal stresses.

Two features of the continuum damage model play a key role in relating damage fraction to time fraction for multiple stress level tests (variable loading histories). These features are the rupture criterion and exponent ℓ.

Assuming damage is isotropic (i.e. $\eta = 1$), the damage rate equation may be integrated for uniaxial loading to give uniaxial damage as a function of time fraction:

$$D_{11} = 1 - \left[1 - \left\{1 - \left[1 - D_c\right]^{(1+\ell)}\right\}\left[\frac{t}{t_R}\right]\right]^{\left(\frac{1}{1+\ell}\right)} \tag{147}$$

It is very important to note that if damage is assumed constant at rupture, i.e. D_c = constant, and if ℓ = constant then D_{11} is a unique function of time fraction independent of stress level. The linear time fraction rule may then be stated in terms of the damage parameter as

$$\sum_{j=1}^{M} \frac{\left\{1 - (1 - D_j)^{(1+\ell)}\right\}}{\left\{1 - (1 - D_c)^{(1+\ell)}\right\}} = 1 \tag{148}$$

where D_j is the value of D_{11} at time t_j. No stress level sequence effects are described by this approach. Note, though, that the damage ratio (D_j/D_c) is not summed to one.

Stress level sequence effects can, in general, be very important in creep. It is well-documented [34] that the grain boundary damage accumulated at low stress levels can be significantly larger than at higher stress levels. Hence, low-high sequences can be more damaging than high-low sequences at a given temperature [34]. In contrast to the current work, Chaboche introduced sequence effects by making exponent ℓ [14] a function of applied stress while maintaining the rupture criterion $D_c = 1$. However, the stress level dependence may be more rationally introduced through a rupture criterion such as equation (144) which recognizes the contribution of applied stress to the rupture process. In fact, if an inverse relationship exists between applied

stress and damage, as in equation (144), then the ratio of damage at any selected time fraction of a lower stress level test to that of a higher stress level test will be greater than unity; this result, of course, is equivalent to that of the $\ell = \ell(\sigma)$ approach taken by Chaboche. This result is easily obtained from equation (147). In this case, however, coefficient B must be made a function of applied stress to ensure that a Monkman-Grant (or other applicable) relationship is maintained between applied stress and rupture time.

The importance of the rupture criterion in a mechanistically accurate formulation of creep damage is now established. It should be noted that all aforementioned statements regarding sequence effects apply as well to the anisotropic damage case. For clarity of presentation, the isotropic damage case is discussed since closed form solutions exists for the integrals.

It is interesting to note that in the current formulation with ℓ = constant, materials which obey a linear time fraction criterion are defined by D_C = constant at rupture; i.e. a stress-level independent rupture criterion. Other rupture criterion lead to nonlinear time fraction rules. It is reasonable to expect, if the damage parameter is based on physical damage, that proper correlation of the growth of this damage and the rupture event will result in a mechanistically based damage accumulation rule, whether expressed in terms of the damage parameter or time fraction.

Suggested Further Developments

The results of this study have suggested several important areas which require further attention. These areas are briefly listed as follows:

(A) Interrupted tests need to be run to determine damage growth exponent ℓ accurately.

(B) Damage must be measured for both uniaxial and biaxial tests at different effective stress levels and stress states to investigate appropriate stress-level and damage-dependent rupture criteria.

(C) The measured directional distribution of damage should be examined for biaxial proportional and nonproportional tests to determine if second order tensor representation is accurate. More general anisotropic (higher even rank tensor) damage framework should be developed for materials which exhibit a high degree of damage anisotropy (i.e. low η). Current framework may be sufficient for medium to high degrees of isotropy of damage (i.e. $\sim .4 \leq \eta \leq 1$). Also, coupling of creep and plastic deformation may lead to necessity of introducing the effects of plastic deformation during a load reversal or rotation on subsequent creep, particularly since the damage rate after such a reversal depends on matrix power law creep.

(D) A stress-level-dependent creep damage rate equation based on void growth and coalescence should recognize the relative roles of grain boundary diffusion and power law creep, including regimes of coupling between these two mechanisms. This coupling could be expressed through the appropriate modified form of the current damage state in the isothermal damage rate equation, e.g.

$$\dot{\underset{\sim}{D}} = [B_1(\sigma^*)^k\{(\underset{\sim}{\phi}:\underset{\sim}{\phi})^{\ell/2} - (\underset{\sim}{\phi}:\underset{\sim}{\phi})^{-1/2}\} +$$

$$+B_2\{(D_{kk})^{-1/2}/\ln(1/D_{kk})\}\sigma_1]\{\eta\underset{\sim}{I} + (1-\eta)\sum_{j=1}^{3} \underset{\sim}{\nu}^{(j)} \otimes \underset{\sim}{\nu}^{(j)}{}_M{}^{(j)}\} \qquad (149)$$

where B_1 and B_2 are functions of effective stress. Of course, other micro-mechanical formulations can be appropriate, depending on

whether diffusion is constrained or unconstrained, grain boundary or matrix, etc. The problem is exacerbated by the fact that actual components may be loaded at low stress levels conducive to diffusion dominated damage growth, while experiments are conducted at higher stress levels, due to time constraints, where power law void growth occurs.

It is also necessary to acknowledge the presence of unstable microstructures when such exist. Precipitated carbides on grain boundaries can serve as void initiation sites; a high area fraction of carbides may actually retard void growth. Such microstructural "aging" effects may require the addition of a scalar state variable and associated evolution equation representative of area fraction of grain boundary void initiation sites. Obviously, this state variable would couple with the damage rate (void growth) equation. This approach would seemingly be necessary only for unstable microstructures.

(E) Solution of general coupled thermo-viscoplastic problems admitting damage requires a proper constitutive equation for growth of all internal variables including damage. Proper growth equations should satisfy the Clausius-Duhem inequality with the generalized thermodynamic forces related to the rate of conjugate internal variables through a viscous/damage potential function. This function can be constructed in an inverse manner, proceeding from the phenomenological growth laws to the potential function, invoking normality as a heuristic postulate. The anisotropy of damage rate would therefore be embedded in the damage potential.

Conclusions

The major achievement of this study has been the physical linkage of the continuum creep damage approach to grain boundary damage. It is the first study known to the author which compares predicted tensorial damage with measured values. The following is a list of key results of this investigation.

1. A generalization of isochronous stress and continuum damage concepts has been made to include multiaxial nonproportional loading.
2. Material tests necessary to determine isothermal model constants and parameters have been identified.
3. Good agreement has been obtained for both rupture time and physical damage between predicted and measured results on two proportionally loaded biaxial specimens.
4. The second rank tensor-based definition of damage is an approximation of the physical damage distribution when the principal axes of stress rotate. Further work must address the accuracy of this approximation.
5. Wedge crack damage in the proportionally loaded type 304 stainless steel specimens of this study was comprised of nearly equal contribution of isotropic and anisotropic components, with an orientation of the principal values of damage coincident with those of the stress tensor. Investigation of cavitation damage was inconclusive due to the great extent of cavitation and grain boundary sliding at rupture. It is apparent that a definition of damage based on area fraction of coalesced voids or wedge cracks results in a value of damage much less than unity at rupture (~ 0.2), in agreement with prior micromechanical studies. Hence, the rupture criterion is most aptly expressed in a "psuedo-fracture" manner as a function of both accumulated grain boundary damage and stress level.

6. Further required refinements include use of a unified creep-plasticity theory to properly model creep-plasticity interaction, use of an isochronous overstress when power law creep drives void growth, and more precise experimental determination of B and ℓ.

Implementation of these refinements should substantially improve the capability to model cumulation of damage under nonproportional loading. Future work will address this implementation.

TABLE 1

Predicted and Measured Quantities
for Specimens GT-1,2,3,4

	Specimen Identification							
	GT-1		GT-2		GT-3		GT-4	
	Pred.	Act.	Pred.	Act.	Pred.	Act.	Pred.	Act.
D_{11}	0.63	0.31	0.63	0.24	0.67	0.15	0.57	0.20
D_{12}	0.071	0.037	-0.071	-0.016	-0.048	0.0014	0.082	0.0035
D_{22}	0.42	0.24	0.42	0.15	0.44	0.096	0.40	0.13
D_1	0.65	0.326	0.65	0.24	0.68	0.15	0.60	0.20
D_2	0.40	0.224	0.40	0.15	0.43	0.096	0.37	0.13
$\eta=D_2/D_1$	0.61	0.69	0.61	0.62	0.63	0.64	0.61	0.65
$\theta(+_{ccw})$	17.0°	23.0°	-17.0°	-9.9°	-11.5°	1.5°	22.0°	2.9°
e_{11}^c	0.18	0.155	0.18	0.146	0.19	0.119	0.24	0.181
e_{12}^c	0.091	0.097	-0.091	-0.080	-0.036	-0.126	0.175	-0.009
t_R(hrs)	1020	892	1020	1173	1030	1398	440	1230

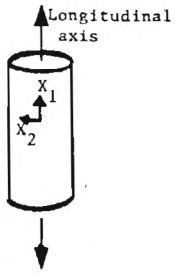

Definitions:

D_1, D_2 = maximum and minimum in-plane principal damage values, respectively.

θ = angle, measured positive counter-clockwise at the specimen outer surface, from the longitudinal axis to the direction of D_1.

TABLE 2

Standard Deviations of Wedge Crack Damage Components
Using each Micrograph as "Sample"

Standard Deviation	Specimen Identification		
	GT-2	GT-3	GT-4
$SD(D_1)$	0.17	0.088	0.11
$SD(D_2)$	0.12	0.074	0.081
$SD(\theta)$	44.1°	48.3°	51.9°
# Micrographs	42	42	36

Note: Number of grains per micrograph $\cong$ 30-60.

REFERENCES

1. Kachanov, L., Fundamental of Fracture Mechanics, Nauka, Moscow, 1974.

2. Kachanov, L., "Crack Growth Under Conditions of Creep and Damage," Creep in Structures, IUTAM, 1980, pp. 520-524 (Eds. Ponter and Hayhurst).

3. Cocks, A.C.F., and Ashby, M. F., "Creep Fracture by Void Growth," Creep in Structures, IUTAM, 1980, pp. 368-387 (Eds. Ponter and Hayhurst).

4. Trampczynski, W. A., and Hayhurst, D. R., "Creep Deformation and Rupture Under Non-Proportional Loading," Creep in Structures, IUTAM, 1980, pp. 388-405 (Eds. Ponter and Hayhurst).

5. Trampczynski, W. A., Hayhurst, D. R., and Leckie, F. A., "Creep Rupture of Copper and an Aluminum Alloy under Non-Proportional Loading," Univ. of Leicester, Dept. of Engr., Report No. 80-8, 1980.

6. Hayhurst, D. R., Leckie, F. A., and McDowell, D. L., "Damage Growth Under Nonproportional Loading," ASTM STP 853, 1985.

7. Oytana, C., Delobelle, P., and Mermet, A., "Constitutive Equations Study in Biaxial Stress Experiments," ASME J. Engr. Materials and Technology, Vol. 104, Jan. 1982, pp. 1-11.

8. Ohashi, Y., Ohno, N., and Kawai, M., "Evaluation of Creep Constitutive Equations for Type 304 Stainless Steel Under Repeated Multiaxial Loading," ASME J. Engr. Materials and Technology, Vol. 104, July 1982, pp. 159-164.

9. Murakami, S., and Ohno, N., "A Continuum Theory of Creep and Creep Damage," Creep in Structures, IUTAM, 1980, pp. 422-444 (Eds. Ponter and Hayhurst).

10. Leckie, F. A., "The Constitutive Equations for High Temperatures and Their Relationship to Design," Proc. Int. Conf. on Constitutive Laws for Engineering Materials, Eds. Desai and Gallagher, Univ. of Arizona, Tucson, Jan. 1983, p. 93.

11. Rabotnov, Y. N., Creep Problems in Structural Members, Amsterdam, North Holland Publishing Co., 1969.

12. Hayhurst, D. R., and Storakers, B., "Creep Rupture of the Andrade Shear Disk," Proc. Roy. Soc. London, A. 349, 1976, pp. 369-382.

13. Chaboche, J. -L., "Continuous Damage Mechanics - A Tool to Describe Phenomena Before Crack Initiation," Nuclear Engr. and Design, Vol. 64, 1981, pp. 233-247.

14. Lemaitre, J., and Chaboche, J. -L., "A Non-Linear Model of Creep-Fatigue Damage Cumulation and Interaction," Mechanics of Visco-Plastic Media and Bodies, Ed. Jan Hult, Springer, Berlin, 1975, pp. 297-301.

15. Baik, S. and Raj, R., "Mechanisms of Creep-Fatigue Interaction," Metallurgical Trans. A, Vol. 13A, July 1982, pp. 1215-1221.

16. Huddleston, R. L., "An Improved Multiaxial Creep-Rupture Strength Criterion," ASME J. Pressure Vessels and Piping, Paper 84-PVP-106, 1984.

17. Hayhurst, D. R., "Creep Rupture Under Multiaxial States of Stress," J. Mech. Phys. Solids, Vol. 20, 1972, pp. 381-390.

18. Frost, H. J., and Ashby, M. F., Deformation-Mechanism Maps, Pergamon Press, 1982.

19. Murakami, S., "Notion of Continuum Damage Mechanics and its Application to Anisotropic Creep Damage Theory," ASME J. of Engineering Materials and Technology, Vol. 105, April 1983, pp. 99-105.

20. Leckie, F. A., and Onat, E. T., "Tensorial Nature of Damage Measuring Internal Variables," Physical Non-Linearities in Structural Analysis, IUTAM, 1980, pp. 140-155 (Eds. Hult and Lemaitre).

21. Baik, S., and Raj, R., "Wedge Type Creep Damage in Low Cycle Fatigue," Metallurgical Trans. A, Vol. 13A, July 1982, pp. 1207-1214.

22. Murakami, S., and Ohno, N., "A Constitutive Equation of Creep Based on the Concept of a Creep-Hardening Surface," Int. J. Solids Structures, Vol. 18, No. 7, 1982, pp. 597-609.

23. McDowell, D. L., "A Two Surface Model for Transient Nonproportional Cyclic Plasticity: Part 1," ASME J. Applied Mechanics paper No. 85-APM-9, 1985.

24. McDowell, D. L., "A Two Surface Model for Transient Nonproportional Cyclie Plasticity: Part 2," ASME J. Applied Mechanics Paper No. 85-APM-10, 1985.

25. Lindholm, U. S., Chan, K. S., Bodner, S. R., Weber, R. M., Walker, K. P., and Cassenti, B. N., Constitutive Modeling for Isotropic Materials, NASA CR-174718, 1985.

26. Abrahamson, T. E., "Modeling the Behavior of Type 304 Stainless Steel with a Unified Creep-Plasticity Theory," Ph.D. Thesis, University of Illinois at Urbana-Champaign, 1983.

27. Pugh, C. E., and Robinson, D. N., "Some Trends in Constitutive Equation Model Development for High-Temperature Behavior Model Development for High-Temperature Behavior of Fast-Reactor Structural Alloys," Nuc. Engr. and Design, Vol. 48, 1978, pp. 269-276.

28. Krieg, R. D., Swearengen, J. C., and Rohde, R. W., "A Physically-Based Internal Variable Model for Rate-Dependent Plasticity," Inelastic Behavior of Pressure Vessel and Piping Components (Eds. Chang and Krempl), PVP-PB-028, ASME, 1978, pp. 15-28.

29. Miller, A., "An Inelastic Constitutive Model for Monotonic, Cyclic, and Creep Deformation," ASME J. of Engineering Materials and Technology, Vol. 98, 1976, pp. 97-113.

30. Lagneborg, R., "A Modified Recovery-Creep Model and its Evaluation," Metal Science Journal, Vol. 6, 1972, pp. 127-133.

31. Betten, J., "Net-Stress Analysis in Creep Mechanics," Ingenieur-Archiv, Vol. 52, 1982, pp. 405-419.

32. Bodner, S. R., and Lindholm, U. S., "An Incremental Criterion for Time-Dependent Failure of Materials," ASME J. Engr. Materials and Technology, April 1976, pp. 140-145.

33. Krajcinovic, D., "Creep of Structures - A Continuous Damage Mechanics Approach," J. Structural Mechanics, 11(1), 1983, pp. 1-11.

34. Woodford, D. A., "Creep Damage and the Remaining Life Concept," ASME J. Engr. Materials and Technology, Vol. 101, Oct. 1979, pp. 311-316.

35. Bui-Quoc, T., "An Engineering Approach for Cumulative Damage in Metals Under Creep Loading," ASME J. Engr. Materials and Technology, Vol. 101, Oct. 1979, pp. 337-343.

36. Ostergnen, W . J., and Krempl, E., "A Uniaxial Damage Accumulation Law for Time-Varying Loading Including Creep-Fatigue Interaction," ASME J. Pressure Vessel Technology, Vol. 101, May 1979, pp. 118-124.

37. Lemaitre, J., and Plumtree, A., "Application of Damage Concepts to Predict Creep-Fatigue Failures," ASME J. Engr. Materials and Technology, Vol. 101, 1979, pp. 284-292.

38. Miller, D. A., and Langdon, T. G., "Independent and Sequential Cavity Growth Mechanisms," Scripta Metallurgica, Vol. 14, 1980, pp. 143-148.

39. Svensson, L. E., and Dunlop, G. L., "Mechanisms for the Growth of Intergranular Creep Cavities," Creep in Structures, IUTAM, 1980, pp. 445-462 (Eds. Ponter and Hayhurst).

40. Dyson, B. F., and McLean, D., Metal Science, Vol. 11, 1977, pp. 37-45.

41. Lagneborg, R., "Creep Fracture Mechanisms," Creep of Engr. Materials and Structures, Applied Science Publ., London, 1979, pp. 35-46 (Eds. Bernasconi and Piatti).

42. Yoo, M. H., and Trinkaus, H., "Crack and Cavity Nucleation at Interfaces during Creep," Metallurgical Trans. A, Vol. 14A, April 1983, pp. 547-561.

43. Cocks, A.C.F., and Ashby, M. F., "On Creep Fracture by Void Growth," J. Progress in Materials Science, Vol. 27, 1981, pp. 189-245.

44. Hull, D., and Rimmer, D. E., "The Growth of Grain-Boundary Voids Under Stress," Phil. Mag., Vol. 4, 1979, pp. 673-687.

45. Edward, G. H., and Ashby, M. F., "Intergranular Fracture During Power-Law Creep," Acta Metallurgica, Vol. 27, 1979, pp. 1505-1518.

46. Sotolongo, W., and McDowell, D. L., "An Evaluation of Several Constitutive Model Structures for Transient Nonproportional Cyclic Plasticity," under review by ASME J. Pressure Vessel Technology, 1985.

47. Cescotto, S., and Leckie, F. A., "Determination of Unified Constitutive Equations for Metals at High Temperature," Proc. Int. Conf. on Constitutive Laws for Engr. Materials (Eds Desai and Gallagher), Tucson, AZ, Jan. 1983, pp. 105-111.

48. McDowell, D. L., "The Significance of Nonproportional Loading Tests for Characterization of Cyclic Response of Metals," Proc. 1985, SEM(SESA) Spring Conf. on Experimental Mechanics, Las Vegas, 1985.

49. Cho, U. W., and Findley, W. N., "Creep and Plastic Strains of 304 Stainless Steel at 593^{o}C Under Step Stress Changes, Considering Aging," ASME J. Applied Mechanics, Vol. 49, June 1982, pp. 297-304.

50. Cho, U. W., and Findley, W. N., "Creep and Creep Recovery of 304 Stainless Steel at Low Stresses with Effects of Aging on Creep and Plastic Strains," ASME J. Applied Mechanics, Vol. 48, Dec. 1981, pp. 785-790.

51. Krempl, E., Cernocky, E. P., and Liu, M. C. M., "The Representation of Viscoplastic Phenomena in Constitutive Equations," Constitutive Equations in Viscoplasticity: Computational and Engineering Aspects (Eds. Stricklin and Saczalski), AMD Vol. 20, 1976, ASME, pp. 95-114.

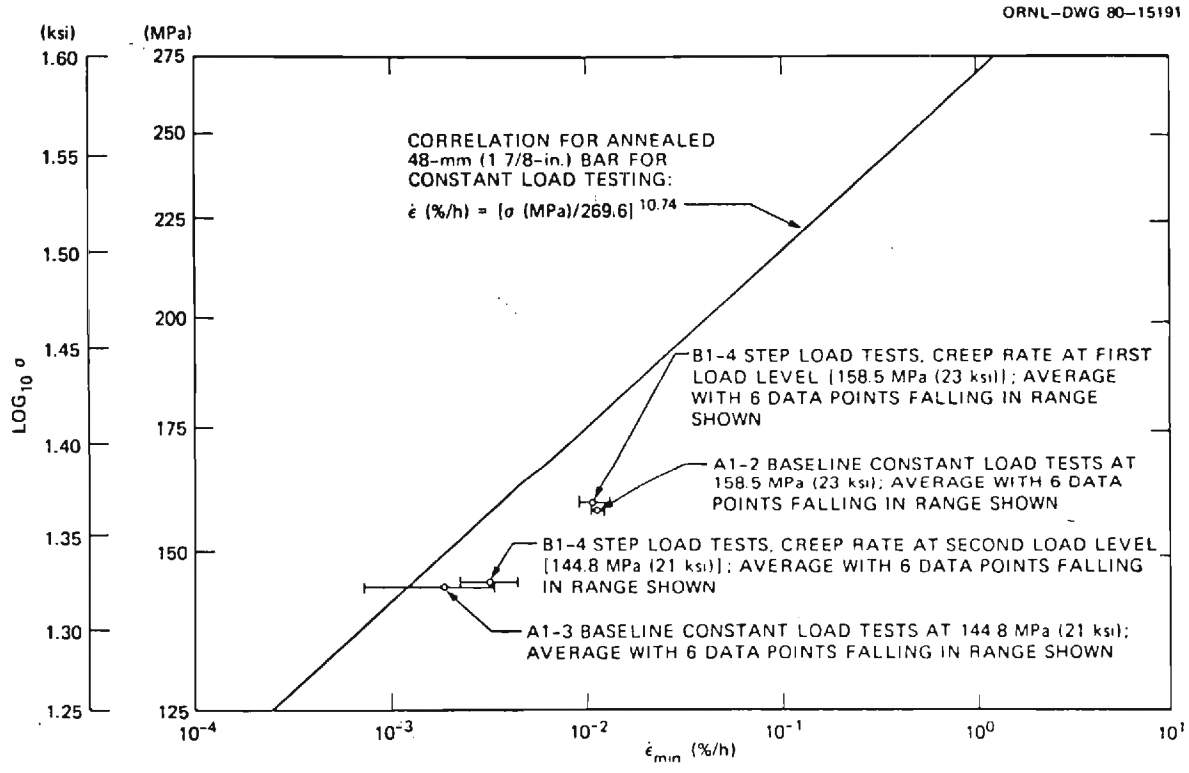

Fig. 1 Comparison of minimum creep rates at 593°C for several types of uniaxial tests.

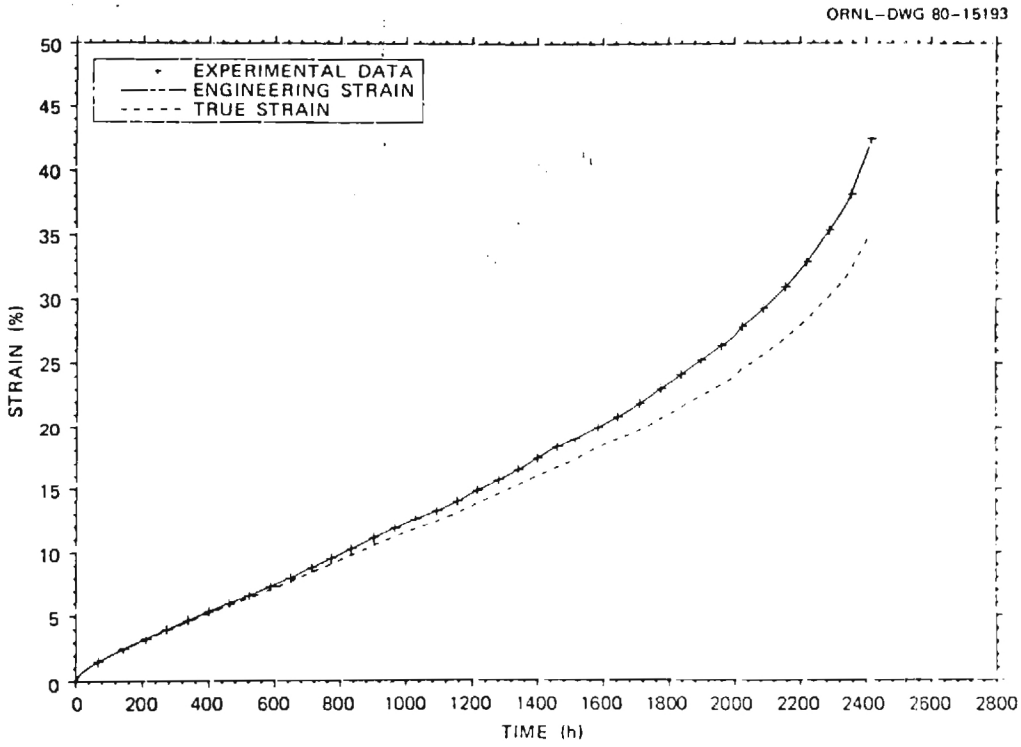

Fig. 2 Constant load uniaxial creep curve at 593°C and 23.0 ksi.

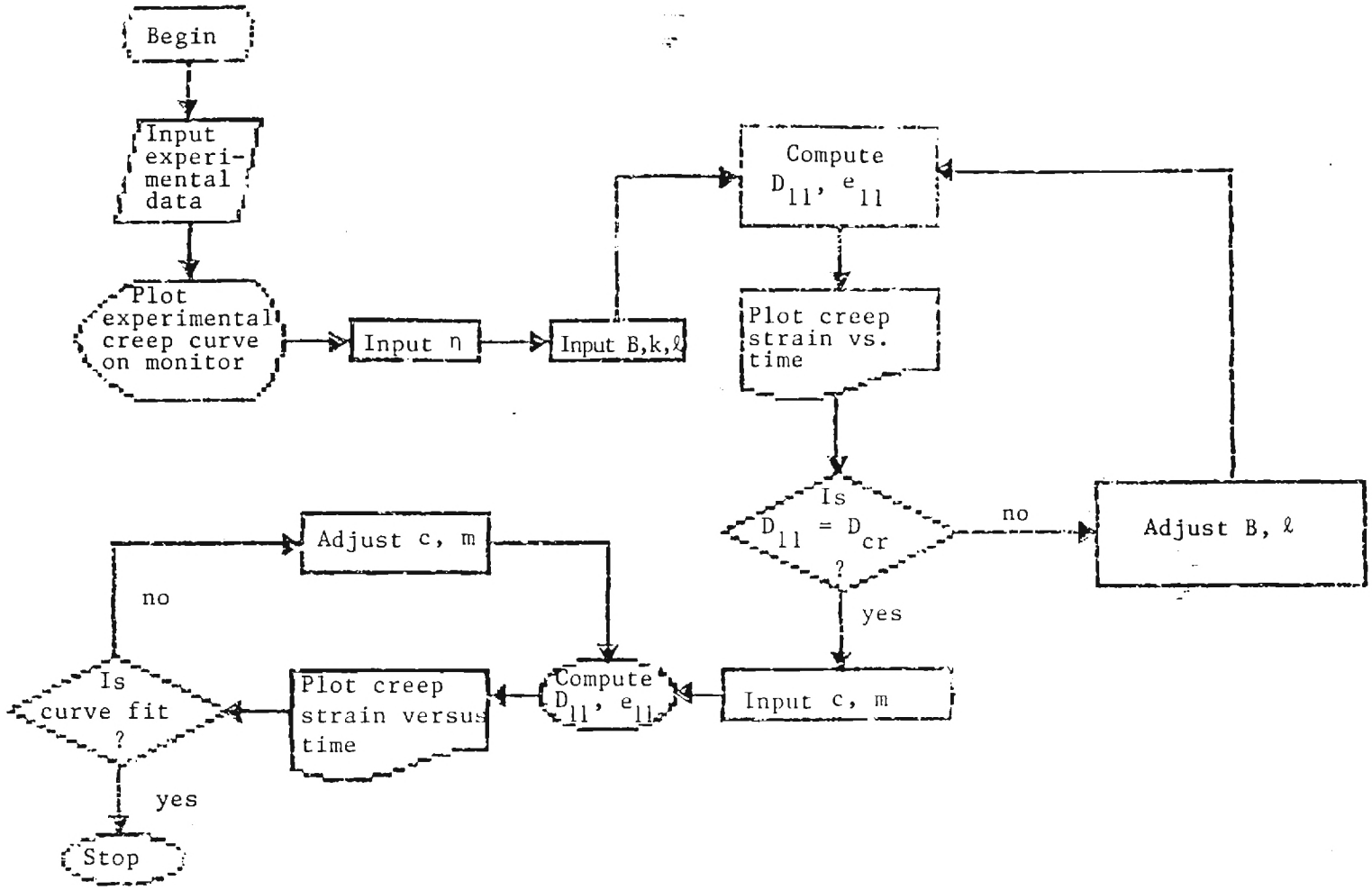

Fig. 3 Flowchart of computer program used to iteratively fit the uniaxial creep curve.

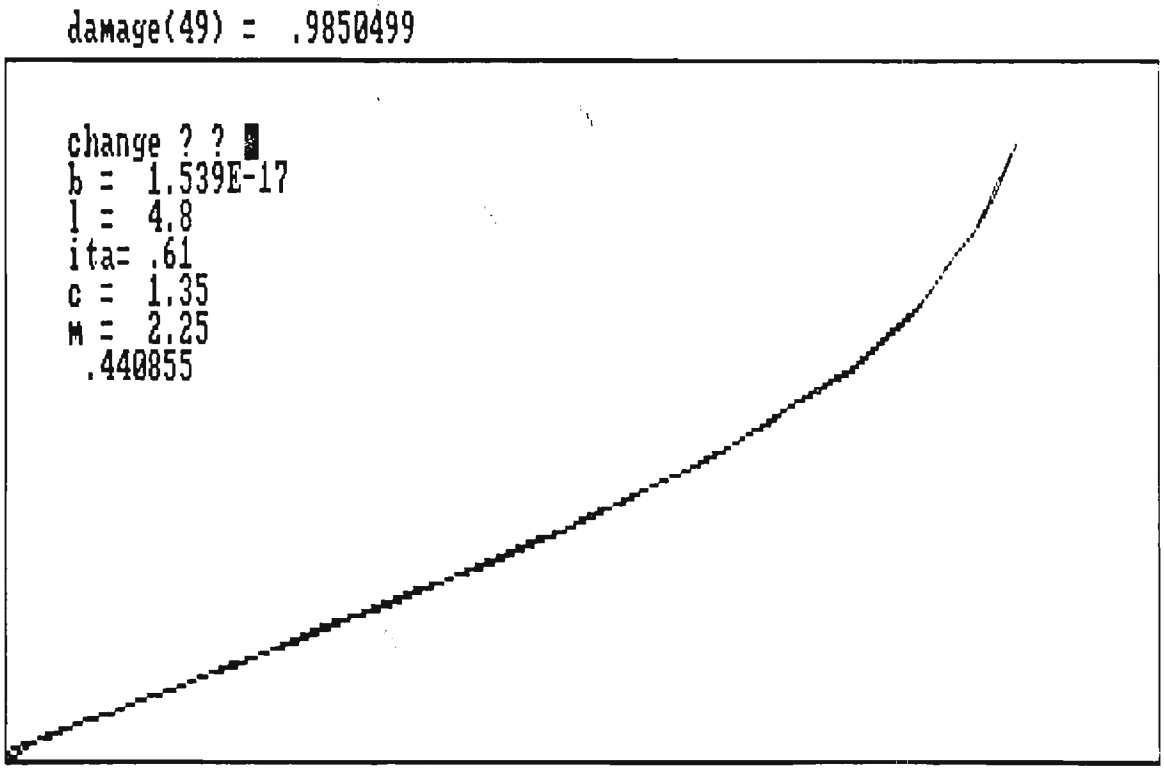

Fig. 4 Overlay of experimental creep curve and output of model.

Long. Axis

200X

Long. Axis

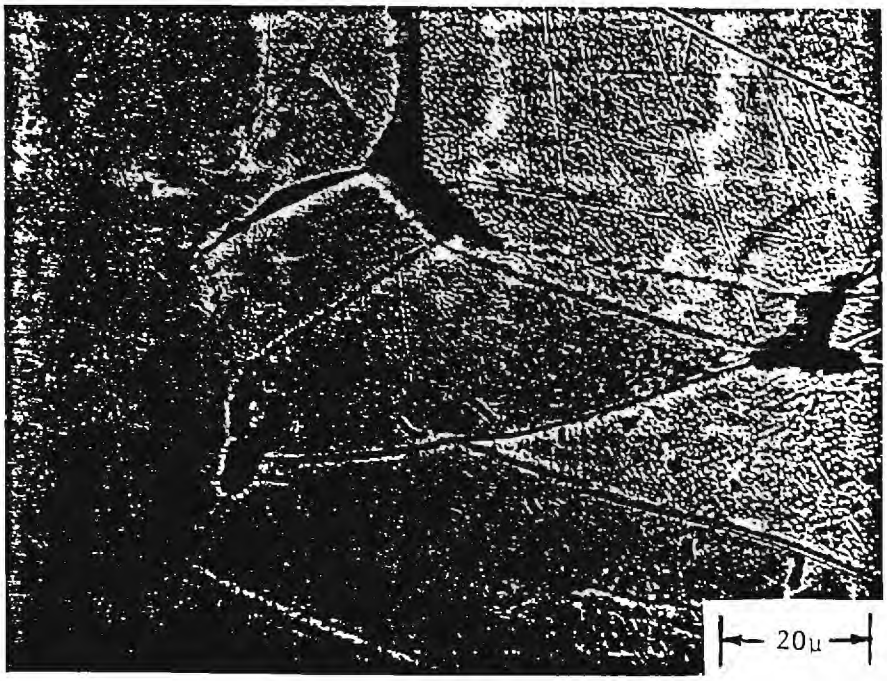

1000X

Fig. 5 Typical micrographs for determination of wedge crack (top) and cavitation (bottom) damage tensors.

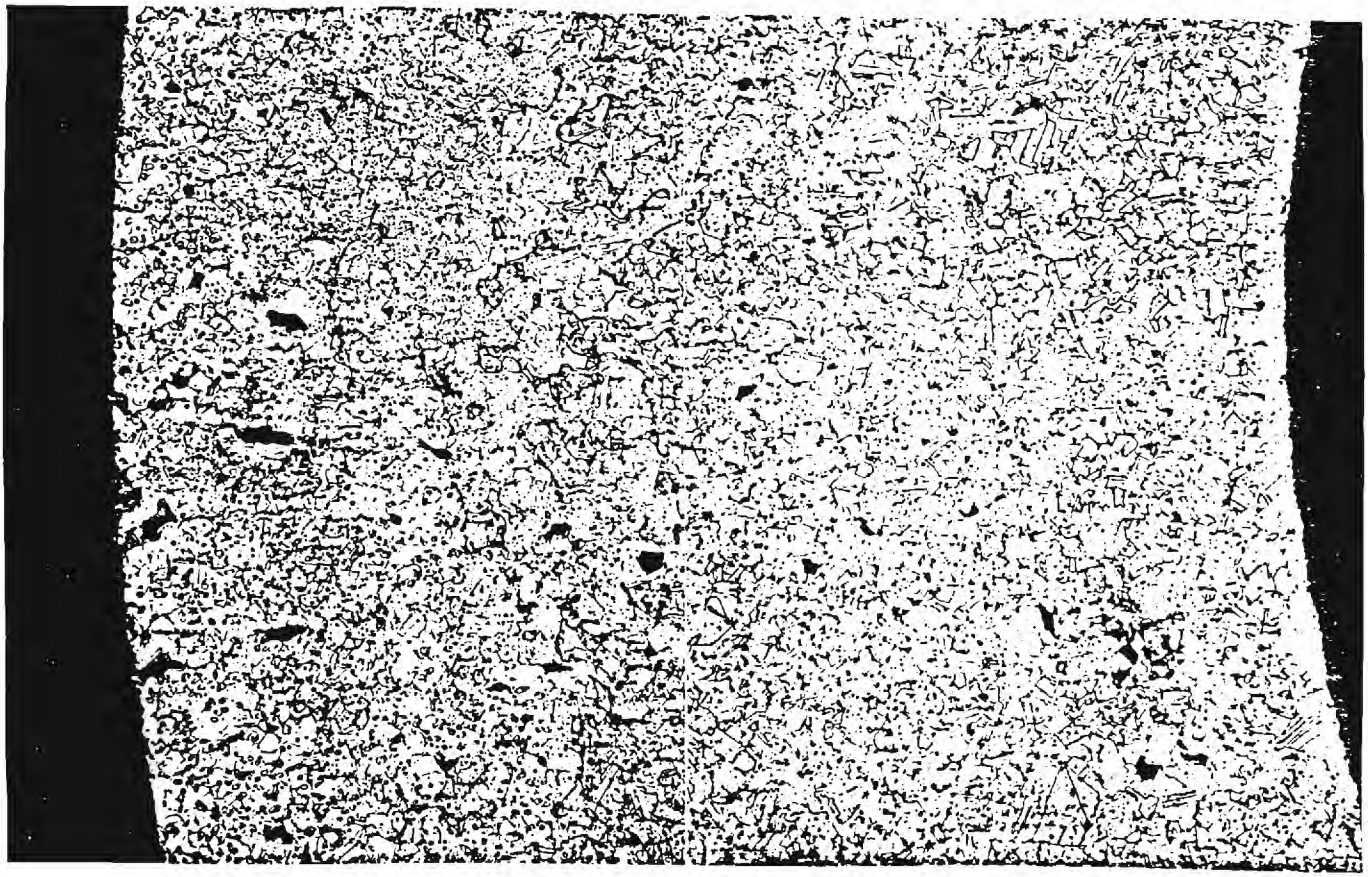

32X

Fig. 6 Specimen transverse cross-section, illustrating radial damage gradient.

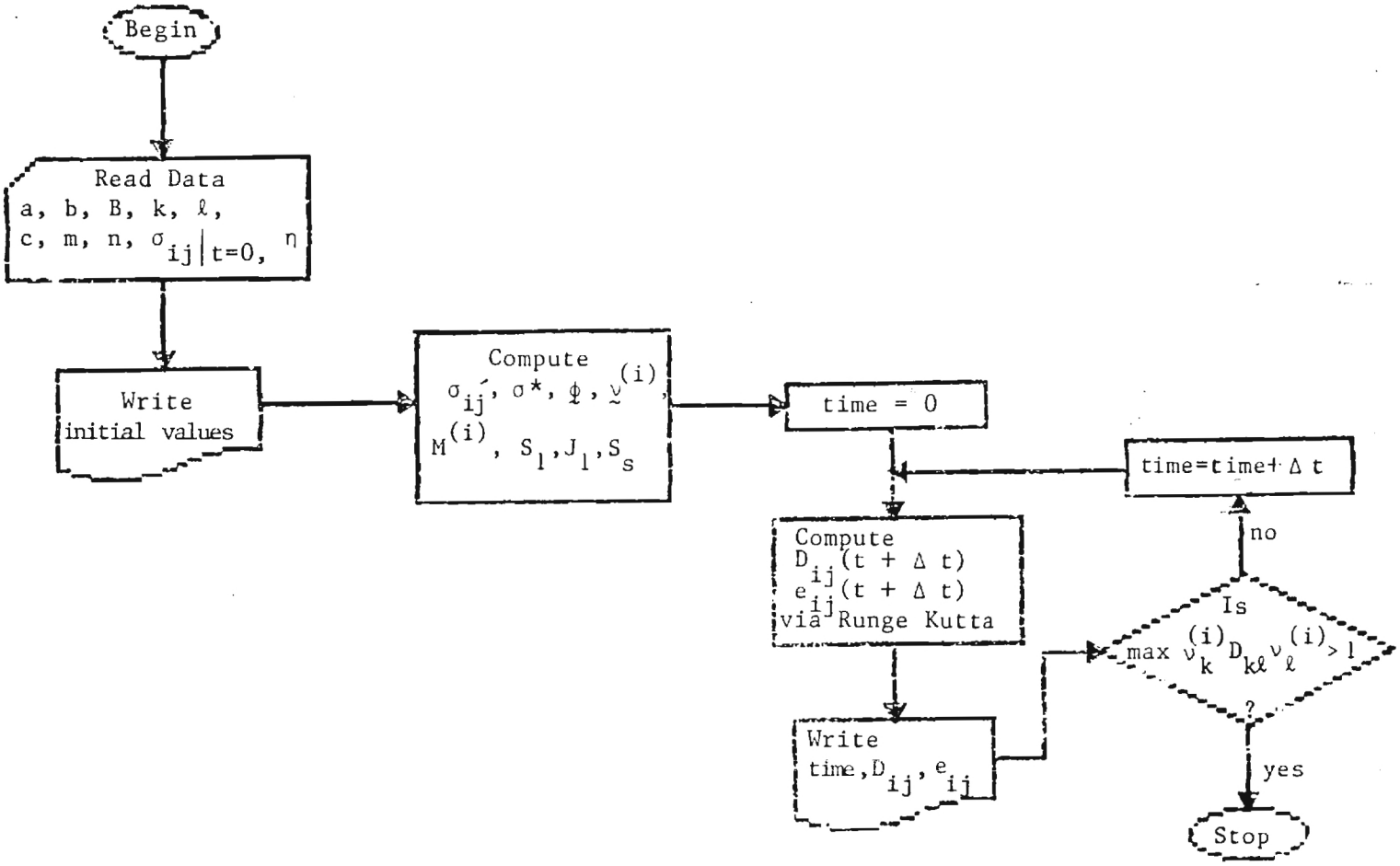

Fig. 7 Flowchart of computer program used to integrate coupled deformation-damage equatins for the biaxial histories of this study.

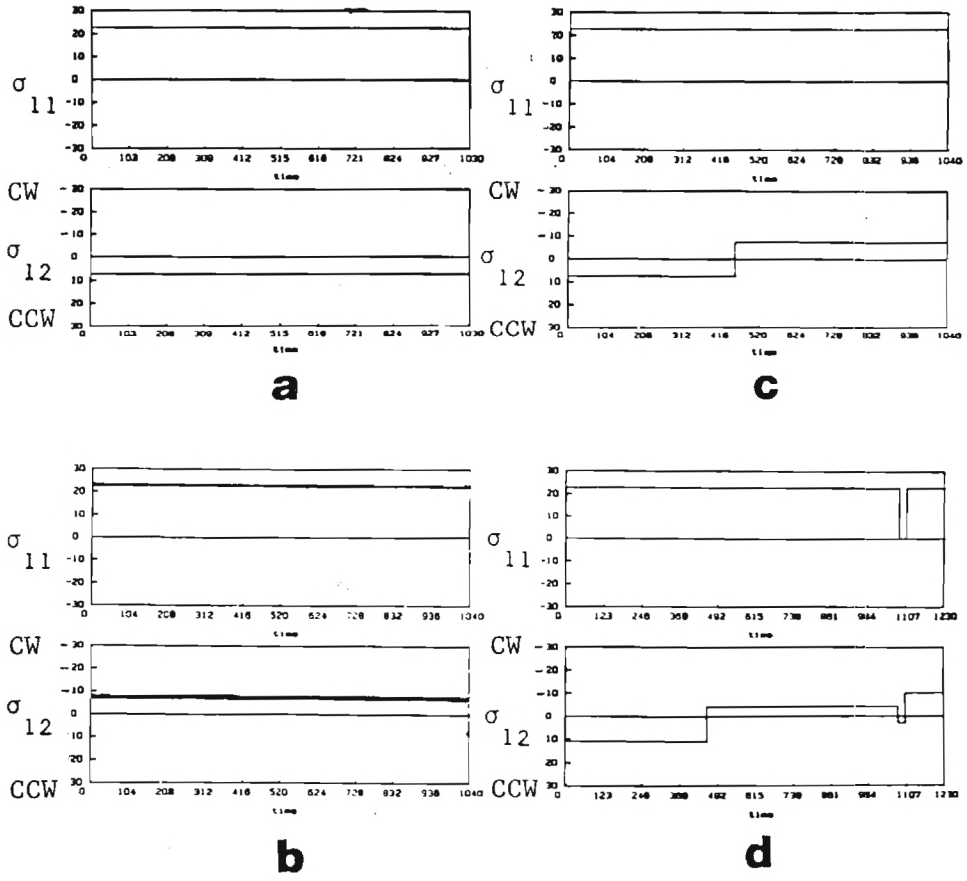

Note: All stresses in ksi

Fig. 8 Axial-torsional nominal stress loading histories for (a) Specimen GT-1, (b) Specimen GT-2, (c) Specimen GT-3, and (d) Specimen GT-4. Axial and shear stress magnitudes for specimens GT-1,2,3 are 22.73 ksi and 7.58 ksi, respectively, which results in an isochronous stress of 25.54 ksi.

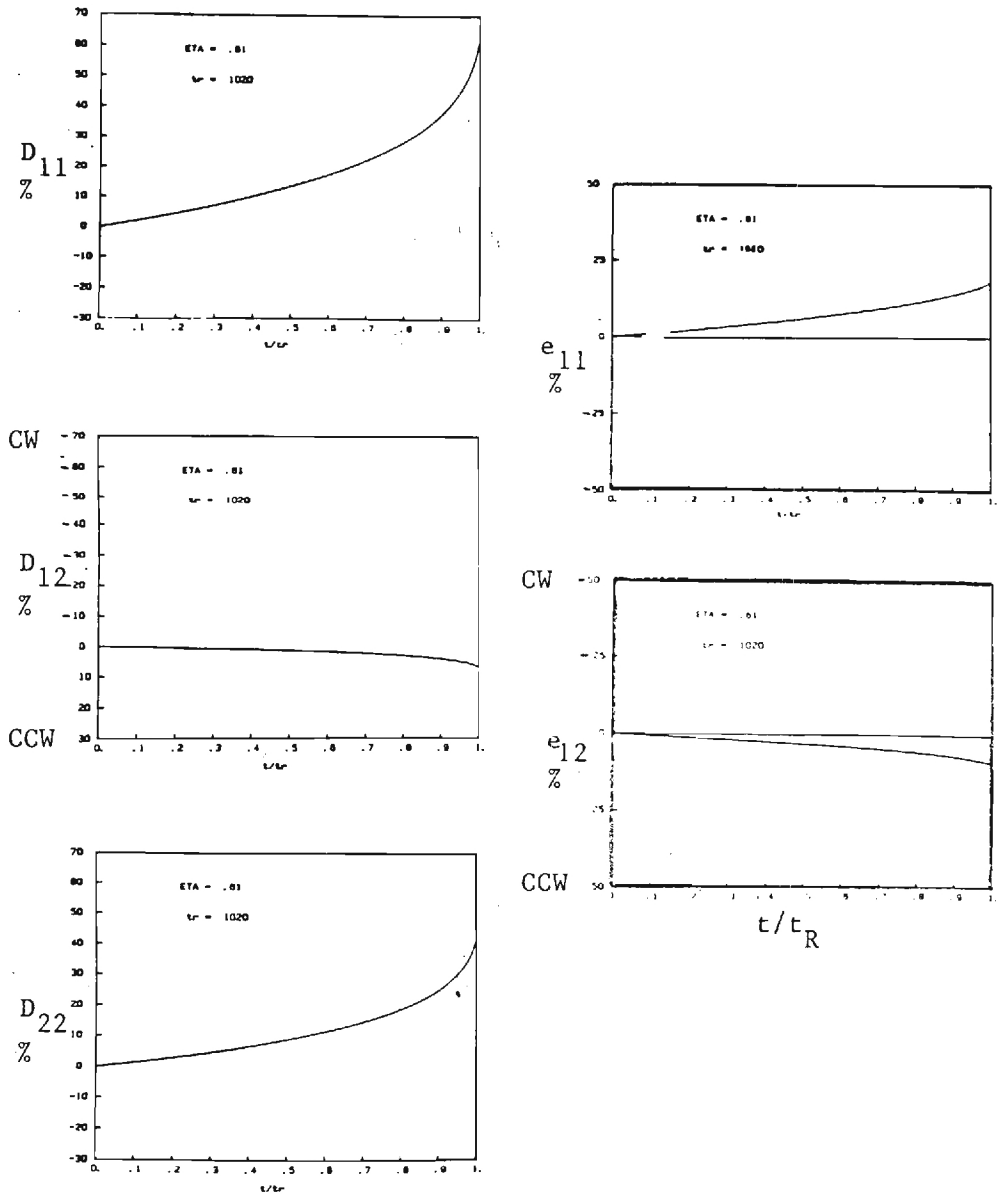

Fig. 9 Evolution of predicted damage and creep strain components versus t/t_R for Specimen GT-1.

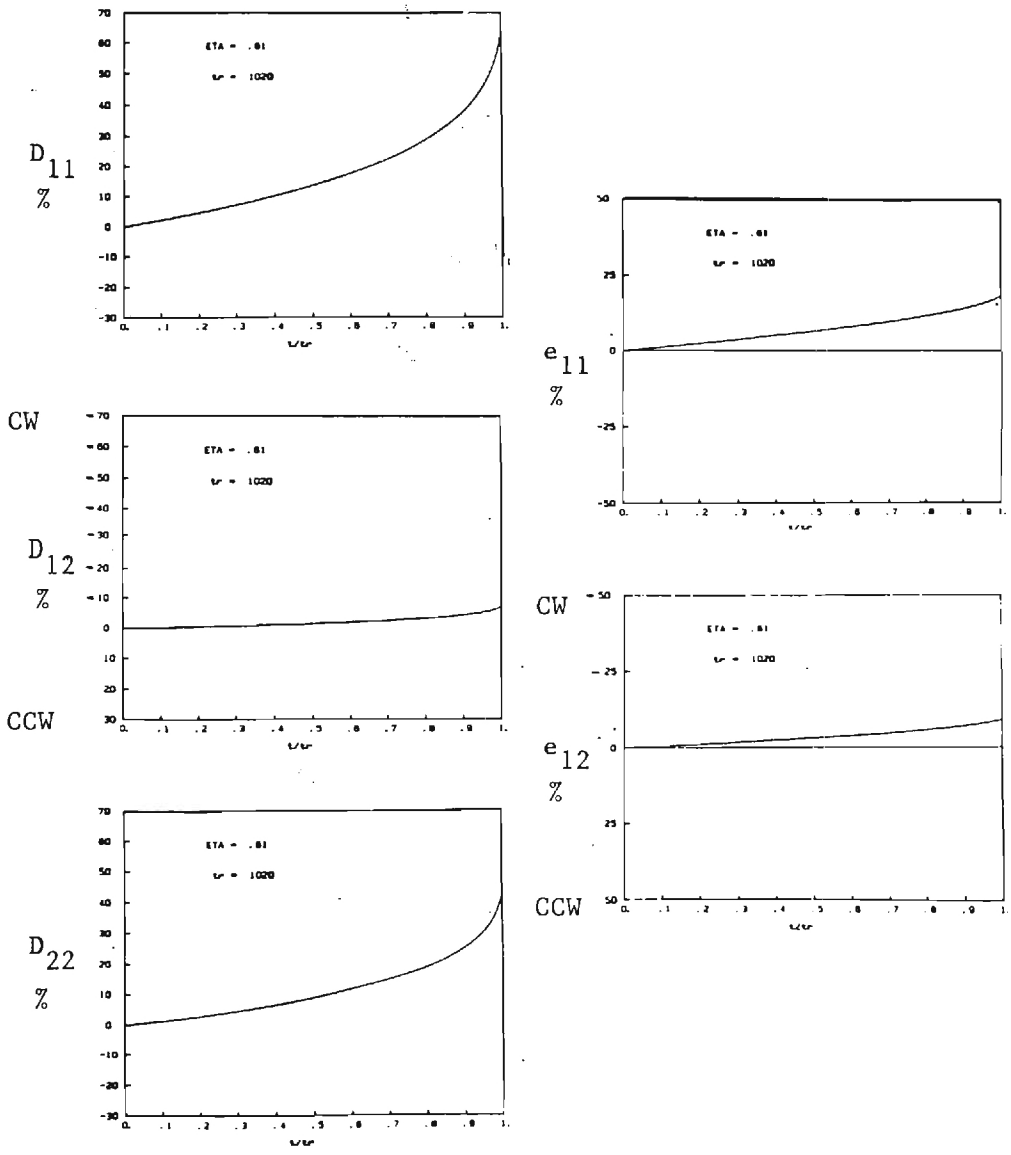

Fig. 10 Evolution of predicted damage and creep strain components versus t/t_R for Specimen GT-2.

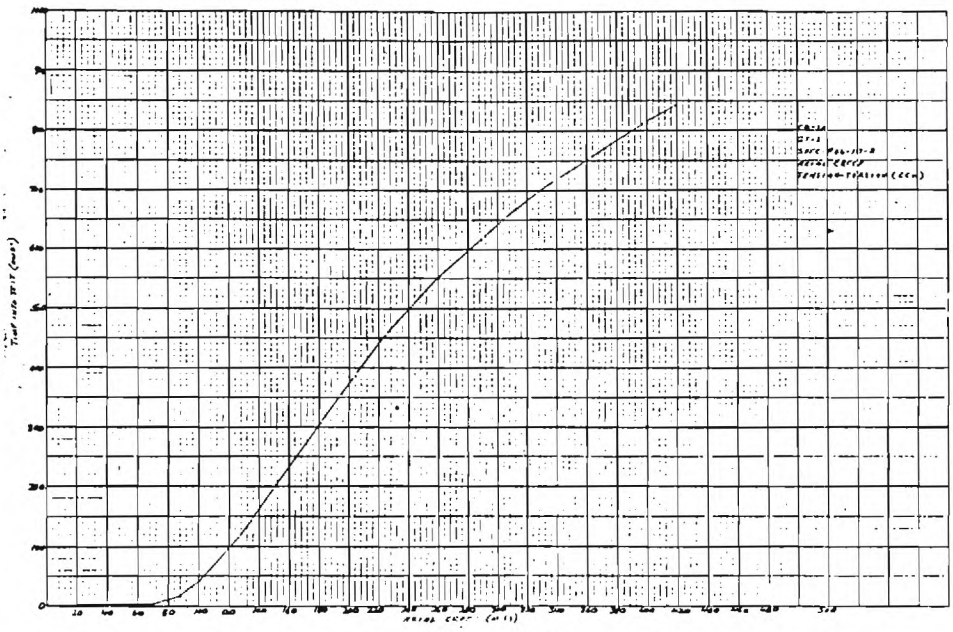

t

δL

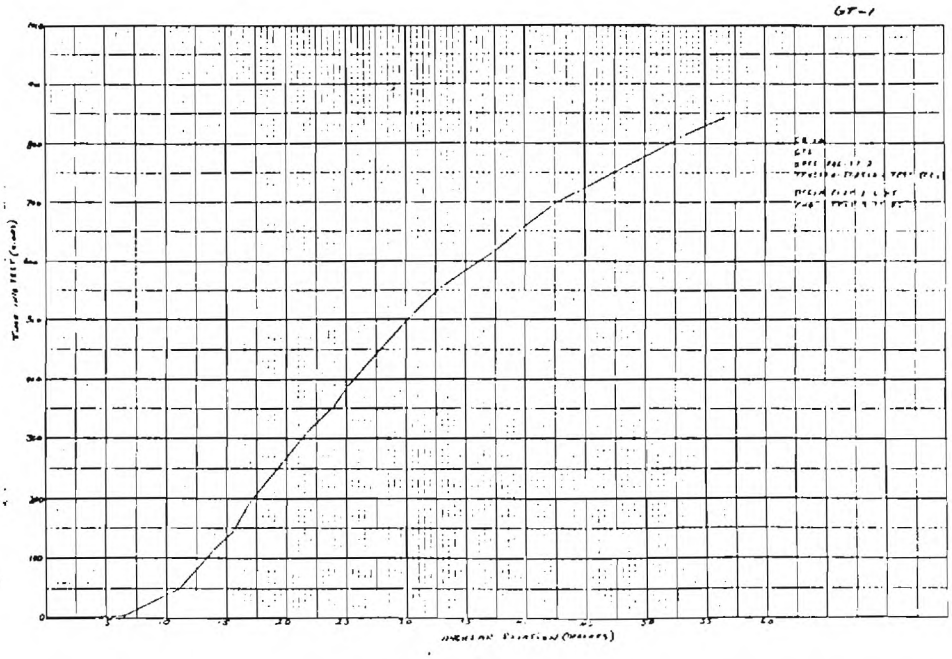

t

δΨ

Fig. 11 Experimental curves for axial displacement (top) and relative angular rotation (bottom) versus time for the gage length of Specimen GT-1.

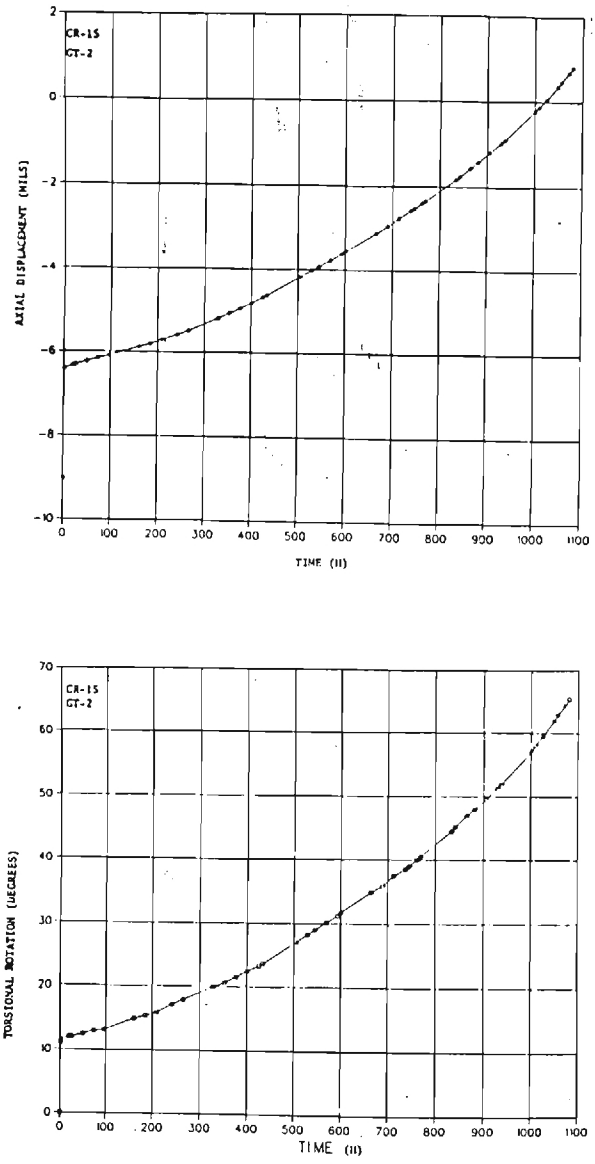

Fig. 12 Experimental curves for axial displacement (top) and relative angular rotation (bottom) versus time for the gage length of Specimen GT-2.

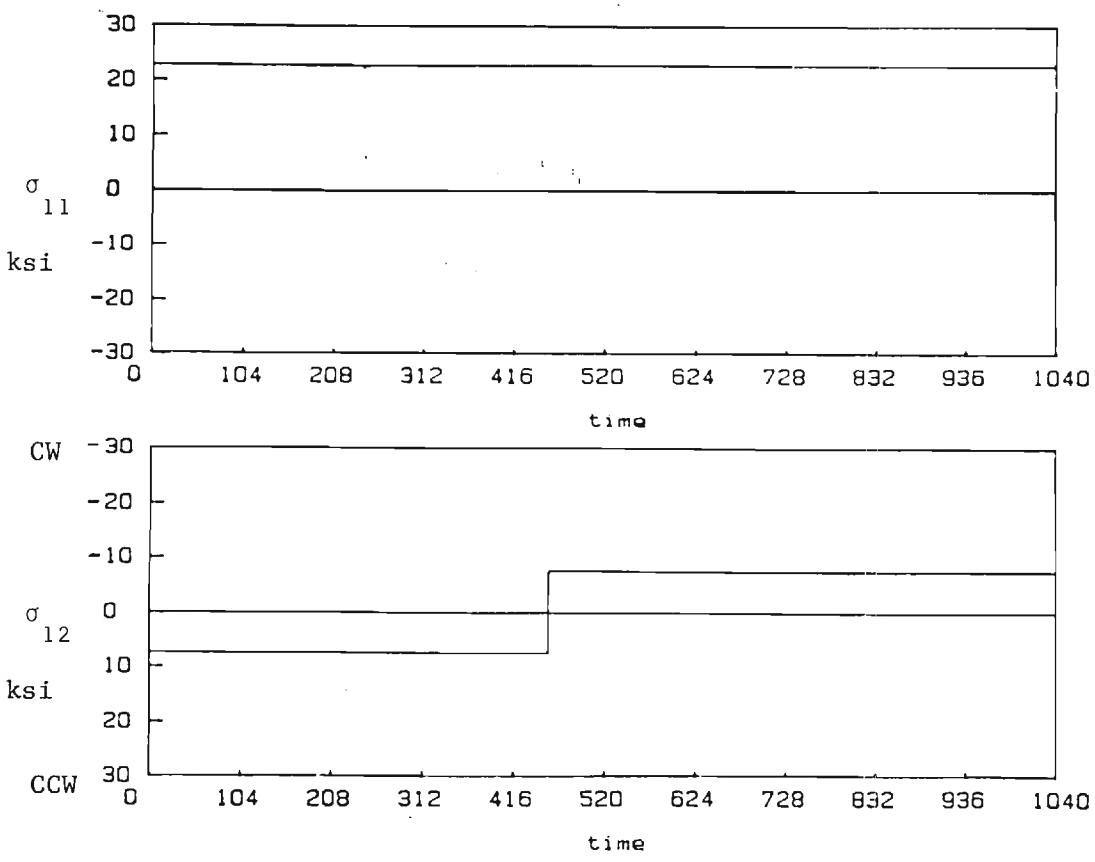

Fig. 13 Axial-torsional nominal stress loading history of Specimen GT-3.

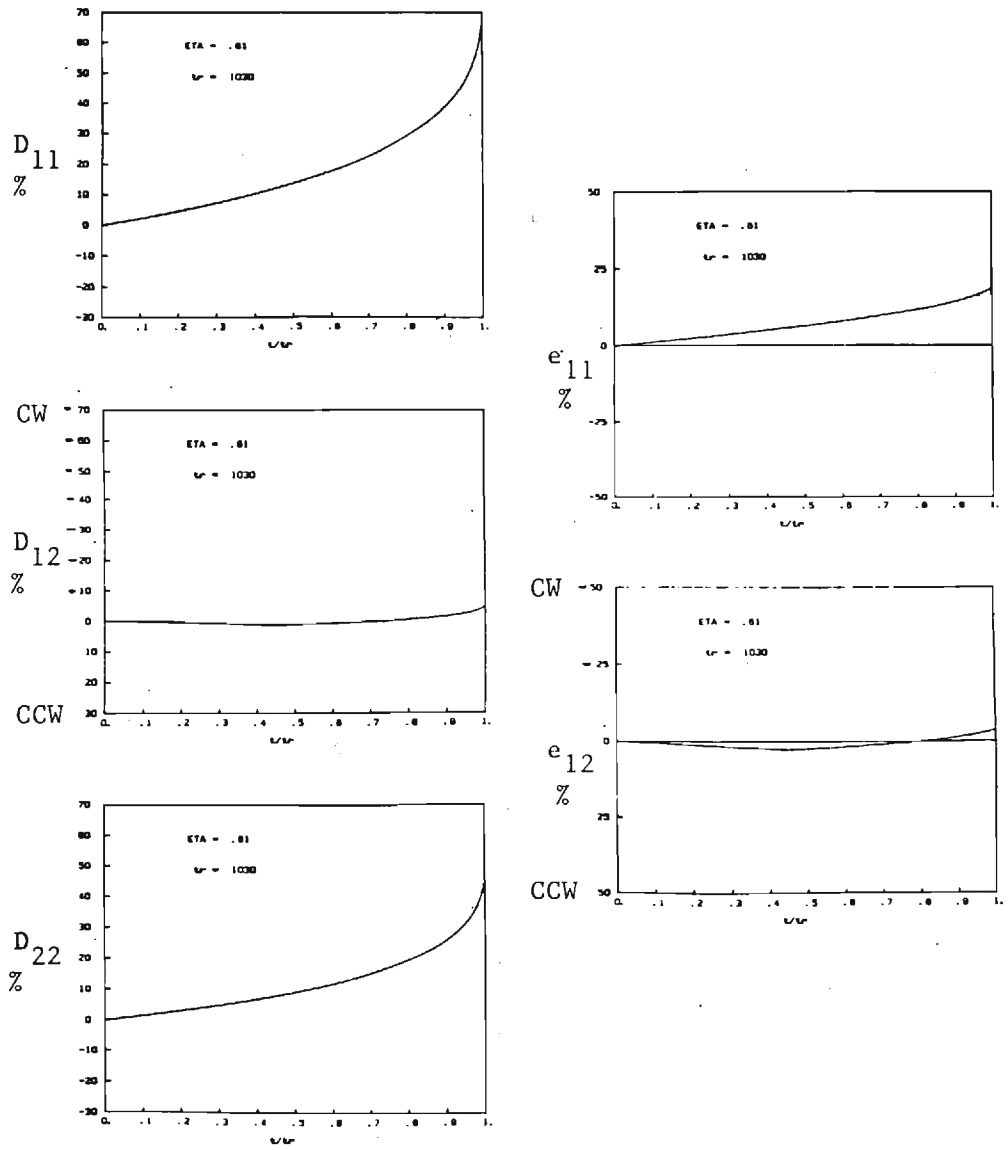

Fig. 14 Evolution of predicted damage and creep strain components versus t/t_R for Specimen GT-3.

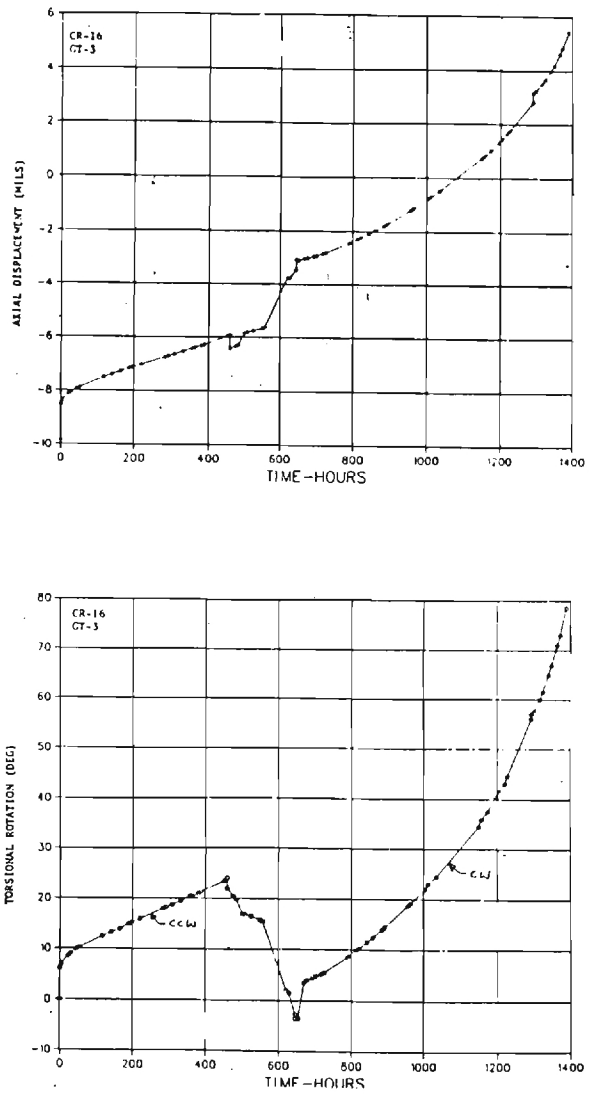

Fig. 15 Experimental curves for axial displacement (top) and relative angular rotation (bottom) versus time for the gage length of Specimen GT-3.

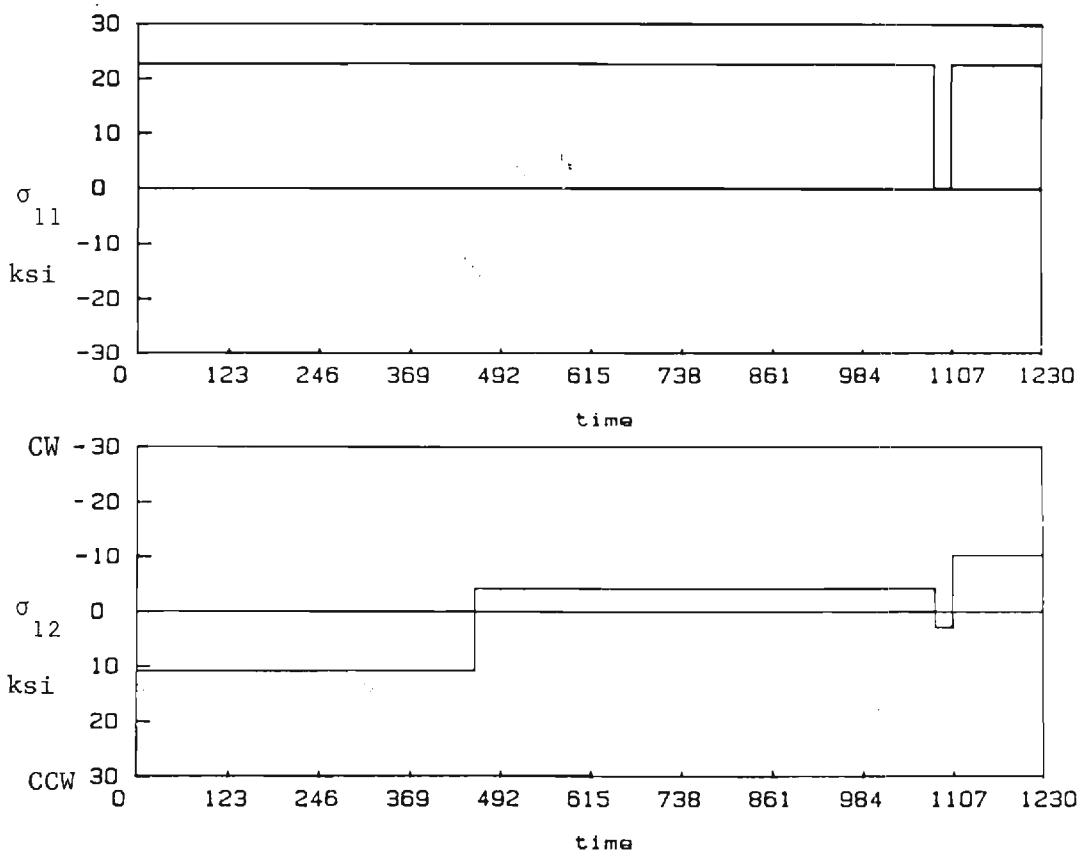

Fig. 16 Axial-torsional nominal stress loading history of Specimen GT-4.

APPENDIX

LISTING OF COMPUTER PROGRAMS

I. Wedge crack damage tensor analysis program.

II. Cavitation damage tensor analysis program.

III. Coupled deformation-damage integration program.

WEDGE.BAS

```
' this program computes the 2nd order wedge crack damage tensor.
' input file is generated by program wedge.for.
 PRINT "input name of wedge crack data file:": INPUT A$
'***** definitions *****
'gblen = total grain boundary length
'bl = segment boundary length
'bn1 = x dir. normal vector comp. to segment boundary
'bn2 = y dir. normal vector comp. to segment boundary
OPEN A$ FOR INPUT AS #1
GBLEN=0 : ' initialize grain boundary length = 0
 INPUT #1,BL
PRINT BL
IF BL=0 THEN 72
 GBLEN=GBLEN+BL
INPUT #1,BN1,BN2
PRINT BN1,BN2
TNORM=SQR(BN1^2+BN2^2):BN1=BN1/TNORM:BN2=BN2/TNORM
GOTO 50
PRINT "grain boundary length =";GBLEN
PRINT "press any key to continue:":INPUT H$
INPUT #1,BL:PRINT BL
D11=0!: D22=0! : D12=0!
'input wedge crack information
'and compute wedge crack damage tensor.
'    wlen = wedge crack length
'    wn1= x dir. normal vector comp. to wedge crack
'    wn2= y dir. normal vector comp. to wedge crack
'    dw11 = damage component 11
'    dw22 = damage component 22
'    dw12 = damage component 12
INPUT #1,WLEN
0 INPUT #1,WN1,WN2
5 TNORM=SQR(WN1^2+WN2^2):WN1=WN1/TNORM:WN2=WN2/TNORM
0 T11=WN1^2 : T22=WN2^2 : T12=WN1*WN2
0 T11=T11*WLEN : T22=T22*WLEN : T12=T12*WLEN
0 D11=D11+T11 : D22=D22+T22 : D12=D12+T12
0 DW11=(1!/GBLEN)*D11 : DW22=(1!/GBLEN)*D22 : DW12=(1!/GBLEN)*D12
0 PRINT DW11,DW22,DW12
0 IF WLEN <> -9999 THEN 90
0 D1=(DW11+DW22)/2!+SQR((DW11-DW22)^2/4+DW12^2/4)
0 D3=(DW11+DW22)/2!-SQR((DW11-DW22)^2/4+DW12^2/4)
0 PRINT "d1=";D1,"d3=";D3
5 ' d1=max. principal damage value
6 ' d3=min. principal damage value
7 CLOSE #1
0 END
```

CAVITY.BAS

```
' this program computes the 2nd order cavitation damage tensor.
' input file is generated by program cavity.for.
 PRINT "input name of cavitation data file:": INPUT A$
'***** definitions *****
'gblen = total grain boundary length
'bl = cavitated segment boundary length
'bn1 = x dir. normal vector comp. to segment boundary
'bn2 = y dir. normal vector comp. to segment boundary
'fcav = fraction of segment boundary cavitated.
'nseg = total number of cavitated segments
GBLEN=0
OPEN A$ FOR INPUT AS #1
D11=0 : D12=0: D22=0!
 INPUT #1,NSEG
'    input cavity information and compute
'    cavity damage tensor.
 FOR I=1 TO NSEG
INPUT #1,BL
GBLEN=GBLEN+BL
INPUT #1,BN1,BN2
TNORM=SQR(BN1^2+BN2^2) : BN1=BN1/TNORM : BN2=BN2/TNORM
INPUT #1,FCAV
D11=D11+FCAV*BL*BN1^2 : D22=D22+FCAV*BL*BN2^2 : D12=D12+FCAV*BL*BN1*BN2
DC11=(1/GBLEN)*D11 : DC22=(1/GBLEN)*D22 : DC12=(1/GBLEN)*D12
PRINT DC11,DC22,DC12
'    dc11 = damage component 11
'    dc22 = damage component 22
'    dc12 = damage component 12
NEXT I
END
```

COPY

```
      PROGRAM START(INPUT,OUTPUT,TAPE5=INPUT,TAPE6=OUTPUT)
      REAL KAPPA,LAMBDA,M,NU,INEDAM
      COMMON /HOKY1/ALPHA,BETA,B,KAPPA,LAMBDA,ETA,SIGMA(3,3)
      COMMON /HOKY2/DAMAGE(3,3),DAMRATE(3,3),NU(3,3,3),SSTAR
      COMMON /HOKY3/INEDAM(3,3),FI(3,3)
      COMMON /HOKY4/SEI(3),SP(3),SIGBAR,SIFRIM(3,3)
      COMMON /HOKY5/EIVEC(3,3),TEN(3,3),VEC(3),M(3)
      COMMON /HOKY6/ERROR,MITER
      COMMON /HOKY7/STRAIN(3,3),STRATE(3,3),DKK
      COMMON /HOKY8/ACONST,CTIMES,POWERM,POWERN
      DATA ALPHA,BETA/1.0859,0.2893/
      DATA B,KAPPA,LAMBDA/1.44021E-17,8.5551,4.8/
      DATA ACONST,CTIMES,POWERM,POWERN/47.66,1.49,2.9,12.5/
      SIGMA(1,1)=0.0
      SIGMA(1,2)=-19.45
      SIGMA(1,3)=0.0
      SIGMA(2,1)=-19.45
      SIGMA(2,2)=0.0
      SIGMA(2,3)=0.0
      SIGMA(3,1)=0.0
      SIGMA(3,2)=0.0
      SIGMA(3,3)=0.0
      SIGM=(SIGMA(1,1)+SIGMA(2,2)+SIGMA(3,3))/3.
      DO 243 IU=1,3
      DO 243 IL=1,3
    SIFRIM(IU,IL)=SIGMA(IU,IL)-SIGM
       IF(IU.NE.IL) SIFRIM(IU,IL)=SIGMA(IU,IL)
243      CONTINUE
      ETA=.65
       INTEVAL=49
      ERROR=1.E-5
      MITER=20
      DELTIME=10
C     . H E A D I N G - I N P U T - D A T A
      WRITE(6,30)
30    FORMAT(10X,"SIGMA")
        DO 50 I=1,3
50      WRITE(6,100) (SIGMA(I,J),J=1,3)
100          FORMAT(3(2X,E15.7,5X))
        WRITE(6,110) ALPHA,BETA
110          FORMAT(2X,"ALPHA = ",F14.7,2X,"BETA = ",F14.7)
        WRITE(6,120) B,KAPPA,LAMBDA
120          FORMAT(5X,E15.7,5X,F14.7,5X,F14.7)
        WRITE(6,205) ETA
205          FORMAT(2X," ETA = ",F5.2)
C       I N I T I A L I Z E
666     DO 10 I=1,3
        DO 10 J=1,3
      STRAIN(I,J)=0.0
10      DAMAGE(I,J)=0.0000
      CALL STPNU
C
C
      I=1
      TIME=(I-1)*DELTIME
467   WRITE(6,200) TIME
200          FORMAT(5X,"TIME = ",F10.5)
      DO 40 LLLL=1,3
40    WRITE(6,210) (DAMAGE(LLLL,JJ),JJ=1,3)
```

```
      DO 42 IN=1,3
42      WRITE(6,210) (STRAIN(IN,IM),IM=1,3)
210          FORMAT(3(3X,E15.7))
      IF(MOD(I-1,INTEVAL).EQ.0) GO TO 700
750   DKK=DAMAGE(1,1)+DAMAGE(2,2)+DAMAGE(3,3)
      CALL RUNGE(1,DELTIME)
        CALL BIJAIAJ(EIVEC,DAMAGE,VALUE)
      CALL RUNGE2(1,DELTIME,I)
      IF(VALUE.GE.1.) GO TO 999
      I=I+1
      TIME=(I-1)*DELTIME
      GO TO 467
700     SIGMA(1,2)=-SIGMA(1,2)
        SIGMA(2,1)=-SIGMA(2,1)
        SIGM=(SIGMA(1,1)+SIGMA(2,2)+SIGMA(3,3))/3.
        DO 710 IU=1,3
        DO 710 IL=1,3
     SIFRIM(IU,IL)=SIGMA(IU,IL)-SIGM
      IF(IU.NE.IL) SIFRIM(IU,IL)=SIGMA(IU,IL)
710      CONTINUE
        CALL STPNU
        GO TO 750
999     CONTINUE
333     CONTINUE
      STOP
        END
C     S U B R O U T I N E   R U N G E - K U T T A
      SUBROUTINE RUNGE(IN,H)
      REAL KAPPA,LAMBDA,NU,INEDAM,M
      DIMENSION ERRY(3,3)
      DIMENSION A(4),B(4),C(4),D(4),CDX(4)
      COMMON /HOKY1/ALPHA,BETA,BI,KAPPA,LAMBDA,ETA,SIGMA(3,3)
      COMMON /HOKY2/Y(3,3),YPRIME(3,3),NU(3,3,3),SSTAR
      COMMON /HOKY3/INEDAM(3,3),FI(3,3)
      COMMON /HOKY4/SEI(3),SP(3),SIGBAR,SIFRIM(3,3)
      COMMON /HOKY5/EIVEC(3,3),TEN(3,3),VEC(3),M(3)
      COMMON /HOKY6/ERROR,MITER
      COMMON /HOKY7/STRAIN(3,3),STRATE(3,3),DKK
      COMMON /HOKY8/ACONST,CTIMES,POWERM,POWERN
      IF(IN.NE.1) GO TO 2100
      IN=0
      CDX(1)=0.0
      A(1)=0.5
      B(1)=2.0
      C(1)=1.5
      D(1)=0.5
      CDX(2)=0.5
      A(2)=1.-SQRT(0.5)
      B(2)=1.0
      C(2)=3*(1.-SQRT(0.5))
      D(2)=1.-SQRT(0.5)
      CDX(3)=0.0
      A(3)=1.+SQRT(0.5)
      B(3)=1.0
      C(3)=3*(1.+SQRT(0.5))
      D(3)=1.+SQRT(0.5)
      CDX(4)=0.5
      A(4)=1./6
      B(4)=2.0
      C(4)=0.5
```

```
      D(4)=0.5
              DO 2000 I=1,3
              DO 2000 II=1,3
2000          ERRY(I,II)=0.0
2100  CONTINUE
      DO 2300 I=1,4
      CALL DDOT2
              DO 2200 J=1,3
              DO 2200 JJ=1,3
              ERRTJY=H*YPRIME(J,JJ)-B(I)*ERRY(J,JJ)
              Y(J,JJ)=Y(J,JJ)+A(I)*ERRTJY
              ERRY(J,JJ)=ERRY(J,JJ)+C(I)*ERRTJY-D(I)*H*YPRIME(J,JJ)
2200          CONTINUE
2300  CONTINUE
      RETURN
      END
C     S U B R O U T I N E   R U N G E - 2
      SUBROUTINE RUNGE2(IN,H,IJ)
      REAL KAPPA,LAMBDA,NU,INEDAM,M
      DIMENSION ERRY(3,3)
      DIMENSION A(4),B(4),C(4),D(4),CDX(4)
      COMMON /HOKY1/ALPHA,BETA,BI,KAPPA,LAMBDA,ETA,SIGMA(3,3)
      COMMON /HOKY2/DAMAGE(3,3),DAMRATE(3,3),NU(3,3,3),SSTAR
      COMMON /HOKY3/INEDAM(3,3),FI(3,3)
      COMMON /HOKY4/SEI(3),SP(3),SIGBAR,SIFRIM(3,3)
      COMMON /HOKY5/EIVEC(3,3),TEN(3,3),VEC(3),M(3)
      COMMON /HOKY6/ERROR,MITER
      COMMON /HOKY7/Y(3,3),YPRIME(3,3),DKK
      COMMON /HOKY8/ACONST,CTIMES,POWERM,POWERN
      CDX(1)=0.0
      A(1)=0.5
      B(1)=2.0
      C(1)=1.5
      D(1)=0.5
      CDX(2)=0.5
      A(2)=1.-SQRT(0.5)
      B(2)=1.0
      C(2)=3*(1.-SQRT(0.5))
      D(2)=1.-SQRT(0.5)
      CDX(3)=0.0
      A(3)=1.+SQRT(0.5)
      B(3)=1.0
      C(3)=3*(1.+SQRT(0.5))
      D(3)=1.+SQRT(0.5)
      CDX(4)=0.5
      A(4)=1./6
      B(4)=2.0
      C(4)=0.5
      D(4)=0.5
              DO 2000 I=1,3
              DO 2000 II=1,3
2000          ERRY(I,II)=0.0
2100  CONTINUE
      DO 2300 I=1,4
      CALL EDOT2(IJ)
              DO 2200 J=1,3
              DO 2200 JJ=1,3
              ERRTJY=H*YPRIME(J,JJ)-B(I)*ERRY(J,JJ)
              Y(J,JJ)=Y(J,JJ)+A(I)*ERRTJY
              ERRY(J,JJ)=ERRY(J,JJ)+C(I)*ERRTJY-D(I)*H*YPRIME(J,JJ)
```

```
2200          CONTINUE
2300      CONTINUE
          RETURN
          END
C          S U B R O U T I N E   S T R A I N - R A T E
          SUBROUTINE EDOT2(IJ)
          REAL KAPPA,LAMBDA,M,NU,INEDAM
          COMMON /HOKY1/ALPHA,BETA,B,KAPPA,LAMBDA,ETA,SIGMA(3,3)
          COMMON /HOKY2/DAMAGE(3,3),DAMRATE(3,3),NU(3,3,3),SSTAR
          COMMON /HOKY3/INEDAM(3,3),FI(3,3)
          COMMON /HOKY4/SEI(3),SP(3),SIGBAR,SIFRIM(3,3)
          COMMON /HOKY5/EIVEC(3,3),TEN(3,3),VEC(3),M(3)
          COMMON /HOKY6/ERROR,MITER
          COMMON /HOKY7/STRAIN(3,3),STRATE(3,3),DKK
          COMMON /HOKY8/ACONST,CTIMES,POWERM,POWERN
          DUM1=(SIGBAR/ACONST)**POWERN
          DUM2=(1.+(CTIMES*DKK)**POWERM)
          DO 10 I=1,3
          DO  10 J=1,3
          STRATE(I,J)=1.5*DUM1*DUM2*(SIFRIM(I,J)/SIGBAR)
10        CONTINUE
          RETURN
          END
C         S U B R O U T I N E   F I F I - (FI:FI) L/2)
          SUBROUTINE FIFI(A,B,C)
          DIMENSION A(3,3)
C                 VARIABLES
C                         A   INVERSE DAMAGE TENSOR (3,3)
C                         B   SCALAR VALUE
C                         C   MATERIAL CONSTANT
          BT=0.
                  DO 10 I=1,3
                  DO 10 J=1,3
10                BT=BT+A(I,J)*A(I,J)
          B=BT**(C/2)
          RETURN
          END
C         S U B R O U T I N E   S U B S T I T U T I O N
          SUBROUTINE SUBN(A,B,N)
          DIMENSION A(3,3),B(3,3)
C                 VARIABLES
C                         A   ORIGINAL MATRIX (N,N)
C                         B   DUPLICATING MATRIX (N,N)
C                         N   DIMENSION OF MATRIX
                  DO 10 I=1,N
                  DO 10 J=1,N
10                B(I,J)=A(I,J)
          RETURN
          END
C         S U B R O U T I N E   M U L T I P L I C A T I O N
          SUBROUTINE MPLY(A,B,C,N)
          DIMENSION A(3,3),B(3,3),C(3,3)
C                 VARIABLES
C                         A   PREMULTIPLYING MATRIX (N,N)
C                         B   POSTMULTIPLYING MATRIX (N,N)
C                         C   A X B  (N,N)
C                         N   DIMENSION
                  DO 10 I=1,N
                  DO 10 J=1,N
                          C(I,J)=0.
```

```
                    DO 10 K=1,N
10                  C(I,J)=C(I,J)+A(I,K)*B(K,J)
      RETURN
      END
C     S U B R O U T I N E   I D E N T I T Y - B
      SUBROUTINE INEGAB(B,IMB)
      REAL IMB(3,3)
      DIMENSION B(3,3)
C           VARIABLES
C                   B   DAMAGE TENSOR (3,3)
C                 IMB   I - B (3,3)
            DO 10 I=1,3
            DO 10 J=1,3
            IF(J.EQ.I) THEN
                    IMB(I,J)=1.-B(I,J)
            ELSE
                    IMB(I,J)=-B(I,J)
            ENDIF
10          CONTINUE
      RETURN
      END
C     S U B R O U T I N E   I N V E R S E
      SUBROUTINE INVS(H,HINVS,N)
      DIMENSION H(3,3),HINVS(3,3),A(3,3),B(3,3)
C           VARIABLES
C                   H   ORIGINAL MATRIX (N,N)
C               HINVS   INVERSED MATRIX (N,N)
C                   N   DIMENSION
C           REQUIRED SUBROUTINES
C                   1) SUBN
C                   2) MPLY
C     CHECK IDENTITY MATRIX
         IF(N.EQ.3) GO TO 300
            IF(H(1,1).NE.H(2,2)) GO TO 450
            IF(H(1,2).NE.H(2,1)) GO TO 450
            IF(H(1,2).NE.0.0   ) GO TO 450
               DO 210 I=1,N
               DO 210 J=1,N
210            HINVS(I,J)=H(I,J)/(H(1,1)*H(2,2))
            GO TO 999
300      IF(H(1,1).NE.H(2,2)) GO TO 450
         IF(H(1,1).NE.H(3,3)) GO TO 450
         IF(H(1,2).NE.H(1,3)) GO TO 450
         IF(H(2,1).NE.H(2,3)) GO TO 450
         IF(H(3,1).NE.H(3,2)) GO TO 450
         IF(H(1,2).NE.H(2,1)) GO TO 450
         IF(H(1,2).NE.H(3,1)) GO TO 450
         IF(H(1,2).NE.0.0   ) GO TO 450
               DO 310 I=1,N
               DO 310 J=1,N
310            HINVS(I,J)=H(I,J)/(H(1,1)*H(2,2)*H(3,3))
         GO TO 999
450        CALL SUBN(H,A,N)
      NM1=N-1
               DO 10 I=1,NM1
               SUM=0.
                       DO 11 K=1,N
11                     SUM=SUM+A(K,K)
               SUM=SUM/I
                       DO 12 J=1,N
```

```
12                    A(J,J)=A(J,J)-SUM
                IF(I.EQ.NM1) CALL SUBN(A,HINVS,N)
                CALL MPLY(H,A,B,N)
10              CALL SUBN(B,A,N)
        DO 13 I=1,N
        DO 13 J=1,N
13      HINVS(I,J)=HINVS(I,J)/A(1,1)
          RETURN
999       CONTINUE
        RETURN
        END
C       S U B R O U T I N E   E I G E N - V A L U E
        SUBROUTINE EIGEN(H,EIGENS,ERROR,MITER,N)
        DIMENSION B(4),C(5),DBDA(4),H(3,3),EIGENS(3)
        DATA B(1),DBDA(1)/1.0,0.0/
C               VARIABLES
C                       H   ORIGINAL MATRIX (N,N)
C                  EIGENS   EIGENVALUES OF ORIGINAL MATRIX (N)
C                   ERROR   MAXIMUM ERROR-RANGE OF EIGENVALUES
C                   MITER   MAXIMUM ITERATION COUNTS
C                       N   DIMENSION
C               REQUIRED SUBROUTINES
C                       1) COEFF
      DUM01=H(1,1)*(H(2,3)**2 - H(2,2)*H(3,3))
      DUM02=H(1,2)*(H(1,2)*H(3,3) - H(1,3)*H(2,3))
      DUM03=H(1,3)*(H(1,3)*H(2,2) - H(1,2)*H(2,3))
    DUM0 = DUM01 + DUM02 + DUM03
      DUM11=H(1,1)*H(2,2) + H(2,2)*H(3,3) + H(3,3)*H(1,1)
      DUM12=H(1,2)**2 + H(2,3)**2 + H(3,1)**2
    DUM1 = DUM11 - DUM12
    DUM2 = - (H(1,1) + H(2,2) + H(3,3))
C         C O N D I T I O N S
       IF(ABS(DUM0) .LT.1.E-40) THEN
           IF(ABS(DUM1).LT.1.E-40) THEN
             EIGENS(1)=0.0
             EIGENS(2)=0.0
             EIGENS(3)= - DUM2
           ELSE
             EIGENS(1)=0.0
             EIGENS(2)=(-DUM2-SQRT(DUM2**2-4.*DUM1))/2.
             EIGENS(3)=(-DUM2+SQRT(DUM2**2-4.*DUM1))/2.
           ENDIF
        ELSE
          C(1)=0.
          C(2)=1.
          C(3)=C(3)/C(2)
          C(4)=C(4)/C(2)
          C(5)=C(5)/C(2)
        I=N+1
10      A=0.
        IM1=I-1
                DO 40 LI=1,MITER
                        DO 41 J=2,I
                        B(J)=C(J+1)-A*B(J-1)
41                      DBDA(J)=-A*DBDA(J-1)-B(J-1)
                DA=-B(I)/DBDA(I)
                A=A+DA
                IF(ABS(DA)-ERROR) 11,11,40
40              CONTINUE
11      DO 42 J1=1,IM1
```

```
42      C(J1+1)=B(J1)
                EIGENS(I-1)=-1./A
                IF(I.EQ.2) GO TO 12
                I=I-1
                GO TO 10
12      CONTINUE
        ENDIF
        RETURN
        END
C       S U B R O U T I N E   S O R T I N G
        SUBROUTINE SORT(A,B,N)
        DIMENSION A(3),B(3)
C               VARIABLES
C                       A   ORIGINAL SERIES OF VALUES (N)
C                       B   ASCENDINGLY SORTED SERIES OF VALUES (N)
                DO 10 I=1,N-1
                DO 10 J=I+1,N
                IF(A(I).LE.A(J)) THEN
                        BIG=A(J)
                        SMALL=A(I)
                        A(I)=BIG
                        A(J)=SMALL
                ELSE
                ENDIF
10              CONTINUE
        DO 20 K=1,N
20      B(K)=A(K)
        RETURN
        END
C       S U B R O U T I N E   E I G E N - V E C T O R
        SUBROUTINE EIVECTR(A,B,EI,N)
        DIMENSION A(3,3),B(3,3),EI(3),C(3,3),X(3)
C               VARIABLES
C                       A   ORIGINAL MATRIX (N,N)
C                       B   EIGENVECTORS N X (N)
C                      EI   EIGENVALUES (N)
C                       N   DIMENSION
C               REQUIRED SUBROUTINES
C                       1) HOMO
        DO 20 K=1,N
                DO 10 I=1,N
                DO 10 J=1,N
                IF(J.EQ.I) THEN
                        C(I,J)=A(I,J)-EI(K)
                ELSE
                        C(I,J)=A(I,J)
                ENDIF
10              CONTINUE
        IF(C(2,2).EQ.0.0) GO TO 55
        IF((C(1,3).EQ.0.0).AND.(C(2,3).EQ.0.0)) THEN
           X(3)=0.0
           X(1)=1.
           X(2)=-C(1,1)/C(1,2)
        ELSE
        CALL HOMO(C,X,N)
        ENDIF
         GO TO 77
55       CALL HOMO(C,X,N)
77        XX=0.
                DO 15 JJ=1,N
```

```
15              XX=XX+X(JJ)*X(JJ)
        XX=SQRT(XX)
                DO 30 KK=1,N
30              B(K,KK)=X(KK)/XX
20      CONTINUE
        RETURN
        END
C       S U B R O U T I N E   H O M O G E N E O U S
        SUBROUTINE HOMO(A,X,N)
        DIMENSION A(3,3),B(3,3),BINVS(3,3),X(3),Y(3)
C               VARIABLES
C                       A   COEFFICIENT MATRIX (N,N)
C                       X   SOLUTION VECTOR (N)
C                       N   DIMENSION
C               REQUIRED SUBROUTINES
C                       1) INVS
C                       2) MPLY
C                       3) SUBN
        X(N)=1.
        NM1=N-1
                DO 40 I=1,NM1
                Y(I)=-A(I,N)
                        DO 40 J=1,NM1
40              B(I,J)=A(I,J)
        IF(NM1.EQ.1) BINVS(1,1)=1./B(1,1)
        IF(NM1.EQ.1) GO TO 10
        CALL INVS(B,BINVS,NM1)
10              DO 41 I=1,NM1
                X(I)=0.
                        DO 41 J=1,NM1
41              X(I)=X(I)+BINVS(I,J)*Y(J)
        RETURN
        END
C       S U B R O U T I N E   O U T - D O T ( V E C T O R )
        SUBROUTINE OUTVEC(A,B)
        DIMENSION A(3),B(3,3)
C               VARIABLES
C                       A   VECTOR TO MAKE TENSOR (3)
C                       B   TENSOR (3,3)
                DO 10 I=1,3
                DO 10 J=1,3
10              B(I,J)=A(I)*A(J)
        RETURN
        END
C       S U B R O U T I N E   S T R E S S - S T A R
        SUBROUTINE STPNU
        REAL INEDAM,NU,M,KAPPA,LAMBDA
        COMMON /HOKY1/ALPHA,BETA,B,KAPPA,LAMBDA,ETA,SIGMA(3,3)
        COMMON /HOKY2/DAMAGE(3,3),DAMRATE(3,3),NU(3,3,3),SSTAR
        COMMON /HOKY3/INEDAM(3,3),FI(3,3)
        COMMON /HOKY4/SEI(3),SP(3),SIGBAR,SIFRIM(3,3)
        COMMON /HOKY5/EIVEC(3,3),TEN(3,3),VEC(3),M(3)
        COMMON /HOKY6/ERROR,MITER
        COMMON /HOKY7/STRAIN(3,3),STRATE(3,3),DKK
        COMMON /HOKY8/ACONST,CTIMES,POWERM,POWERN
        CALL EIGEN(SIGMA,SEI,ERROR,MITER,3)
        CALL SORT(SEI,SP,3)
        J1=SIGMA(1,1)+SIGMA(2,2)+SIGMA(3,3)
        S1=SP(1)-J1/3.
        T1=(SP(1)-SP(2))**2
```

```
      T2=(SP(2)-SP(3))**2
      T3=(SP(3)-SP(1))**2
      SIGBAR=SQRT((T1+T2+T3)/2.)
      SS=SQRT(SP(1)**2+SP(2)**2+SP(3)**2)
      DUM1=((2./3.)*(SIGBAR/S1))**ALPHA
      DUM2=BETA*(J1/SS -1.)
      SSTAR=1.5*S1*DUM1*EXP(DUM2)
C
C
C     !!! FIND NU TENSOR !!!
      CALL EIVECTR(SIGMA,EIVEC,SP,3)
      DO 10 I=1,3
      DO 20 J=1,3
20    VEC(J)=EIVEC(I,J)
      CALL OUTVEC(VEC,TEN)
      DO 10 K=1,3
      DO 10 L=1,3
10    NU(I,K,L)=TEN(K,L)
      RETURN
      END
C     S U B R O U T I N E   D A M A G E - R A T E ( 1 )
      SUBROUTINE DDOT2
      REAL LAMBDA,NU,KAPPA,INEDAM,M
      COMMON /HOKY1/ALPHA,BETA,B,KAPPA,LAMBDA,ETA,SIGMA(3,3)
      COMMON /HOKY2/DAMAGE(3,3),DAMRATE(3,3),NU(3,3,3),SSTAR
      COMMON /HOKY3/INEDAM(3,3),FI(3,3)
      COMMON /HOKY4/SEI(3),SP(3),SIGBAR,SIFRIM(3,3)
      COMMON /HOKY5/EIVEC(3,3),TEN(3,3),VEC(3),M(3)
      COMMON /HOKY6/ERROR,MITER
      COMMON /HOKY7/STRAIN(3,3),STRATE(3,3),DKK
      COMMON /HOKY8/ACONST,CTIMES,POWERM,POWERN
      CALL INEGAB(DAMAGE,INEDAM)
      CALL INVS(INEDAM,FI,3)
      CALL FIFI(FI,FISQ,LAMBDA)
C
      DUM1=B*((SSTAR)**KAPPA)*FISQ
      CALL HEAVY(SIGMA,SP(1),M,EIVEC)
      DO 10 I=1,3
      DO 10 J=1,3
      SUM2=0.0
       DO 5 K=1,3
5      SUM2=SUM2+NU(K,I,J)*M(K)
      IF(J.EQ.I) THEN
              DAMRATE(I,J)=DUM1*(ETA+(1.-ETA)*SUM2)
      ELSE
              DAMRATE(I,J)=DUM1*(1.-ETA)*SUM2
      ENDIF
10    CONTINUE
      RETURN
      END
      SUBROUTINE BIJAIAJ(A,B,P)
      DIMENSION A(3,3),B(3,3)
      P=0.0
      DO 10 J=1,3
      DO 10 K=1,3
10    P = P + B(J,K)*A(1,J)*A(1,K)
      RETURN
      END
C     S U B R O U T I N E   H E A V Y S I D E - F U N C T I O N
      SUBROUTINE HEAVY(SIGMA,STRESS,M,EIVEC)
```

```
      REAL M
      DIMENSION SIGMA(3,3),EIVEC(3,3),M(3)
      DO 10 I=1,3
      M(I)=0.0
       DO 5 J=1,3
       DO 5 K=1,3
5      M(I)=M(I)+EIVEC(I,J)*SIGMA(J,K)*EIVEC(I,K)
       M(I)=M(I)/STRESS
      IF(M(I).GE.0.) THEN
        M(I)=M(I)
       ELSE
        M(I)=0.
       ENDIF
10    CONTINUE
      RETURN
      END
```